Effects of sterilization on drug loaded ophthalmic lenses materials

Andreia Sofia Gonçalves de Oliveira

Thesis to obtain the Master of Science Degree in

Biomedical Engineering

Supervisors: Doctor Ana Paula Valagão Amadeu do Serro
Doctor Benilde de Jesus Vieira Saramago

Examination Committee

Chairperson: Doctor João Pedro Estrela Rodrigues Conde
Supervisor: Doctor Ana Paula Valagão Amadeu do Serro
Members of the Committee: Doctor Rogério Anacleto Cordeiro Colaço
Doctor Helena Maria Prior Santos Costa Filipe

September 2016

To my great-grandmother and Maria Carlos

ACKNOWLEDGEMENTS

My first and foremost gratitude goes to my research advisors Professor Ana Paula Serro and Professor Benilde Saramago who provided me with the opportunities, the guidance and the support that has allowed me to develop as a researcher and an individual over the past year. I am truly grateful for the unending mentorship, encouragement, and trust. Thank you for keeping me motivated and efficient on my work, giving me enough freedom to explore, fail and improve.

I would like to express my appreciation to Dr. Helena Filipe for the availability on the sharing of knowledge and insightful viewpoints and to Professor Rogério Colaço for the wisdom, the inspiration and for having the right words at the right time. I would also like to thank him and to my both supervisors for believing in me and giving the chance to continue my PhD in their group.

Many thanks to Professor José Mata, who has been an awesome group member. Thank for all the advices and for the help, dedication and commitment.

I would like to gratefully acknowledge to Engineer Paula Matos and Engineer Nuno Inácio for all the availability demonstrated during the irradiations, to Ricardo Pereira for all the assistance with the autoclave and the lyophilization processes, to Professor Guilhermina Moutinho and Professor Helena Barroso for all the help and guidance with the antimicrobial assays and to Engineer Luis Neves for being always available to help me with the HPLC.

I would also like to express my appreciation to Professor Teresa Nunes and Professor Anabela Fernandes for their gracious support in the NMR and DSC assays.

I have had an extremely friendly and understanding atmosphere in my lab and all that is attributed to my advisors and their research group members. I would like to thank to Raquel Galante, Diana Silva, Andreia Pimenta, Patrizia Paradiso, Bruno Nunes and José Restolho that helped me to get through some tough times in the initial stages of this research, advising me and sharing their knowledge and experience with me. To Ana Topete who has been an amazing friend and shared my best and worst time in this research, for which I am extremely grateful. To Magda Carrilho who was also a great support in the last stages of this research and to Prashneel Kumar. To both of them, thank you for the good vibes.

I am truly grateful to have so many wonderful friends in my life to stand by me through all the good times and bad on the way to what I am now. Thanks to my friends who closely accompanied me in this journey: Giselle Rivas, Renato Silva, André Tinoco, Rita Antunes, Mónica Araújo, Maryna Bondar, Susana Silva, Suzana da Gama and Mónica Loureiro. It would be impossible to accomplished this work without all of your support.

I am also extremely grateful to my dear friend, Isabel Marques for being always available for me. Thank you so much for all the care, love and friendship.

I would like to thank as well to my second mom, Maria Carlos, for being a huge inspiration and a great mentor who has helped me in all phases of my graduate and personal life. Thank you for taking care of me and encouraging me to continue.

Finally, words cannot describe my everlasting gratefulness to my sister and my great-grandmother, Filipa Oliveira and Filomena Santos, for their unconditionally love and trust on every single decision I made in my whole life, and I hope I have made you proud.

ABSTRACT

The use of ophthalmic lenses as drug carriers seems a promising option for the sustained ocular drug delivery. However, to solve the problem of incorporating sufficient amounts of drug and achieving a sustained release while ensuring sterility is still a challenge. Sterilization is mandatory to reduce the risk of infection but it is imperative to preserve the drugs and materials properties. This work presents an investigation of the effects of two methods of sterilization, steam heat (SH) and gamma radiation, on several ophthalmic drugs (diclofenac, ketorolac, moxifloxacin and a combination of the last two), on two polymeric materials used for the production of ophthalmic lenses (a contact lens and an intraocular lens material), and on the drug loaded materials. The role of different conditions of SH sterilization, loading (in particular, the loading temperature), release and storage, was evaluated using the intraocular lens material loaded with moxifloxacin. The impact of the sterilization procedures and of the loading, release and storage conditions on the stability and antimicrobial activity of the drugs as well as on the properties of lenses materials (before and after drug-loading) was assessed. For all studied systems, SH sterilization stood out as an excellent method: it did not affect the drugs/materials and even improved the release profiles of the intraocular lens material loaded with all the studied drugs. For the intraocular lens material loaded with moxifloxacin, higher loading temperatures and longer storage times also significantly improved the release profiles.

Keywords: ocular drug delivery, ophthalmic drugs, ophthalmic lenses materials, gamma radiation sterilization, steam heat sterilization, loading conditions.

RESUMO

A utilização de lentes oftálmicas como transportadoras de fármaco, parece ser uma opção promissora para a libertação controlada de fármacos a nível ocular. Porém, resolver o problema de incorporar quantidades suficientes de fármaco, alcançar uma libertação sustentada e simultaneamente garantir a esterilidade ainda constitui um desafio. A esterilização é obrigatória para reduzir o risco de infeção, mas é impreterível preservar as propriedades dos fármacos e dos materiais. Este trabalho apresenta uma investigação sobre efeito de dois métodos de esterilização, autoclave (AUT) e radiação gama, sobre vários fármacos oftálmicos (diclofenaco, cetorolaco, moxifloxacina e uma combinação dos últimos dois), sobre dois materiais poliméricos usados na produção de lentes oftálmicas (um material de lentes de contacto e outro de lentes intraoculares) e sobre os materiais carregados com fármaco. O papel das diferentes condições de esterilização por AUT, carregamento (em particular, a temperatura de carregamento), libertação e armazenamento, foi avaliado usando o material de lentes intraoculares carregado com moxifloxacina. O impacto dos procedimentos de esterilização, das condições de carregamento, libertação e armazenamento na estabilidade e atividade antimicrobiana dos fármacos, bem como nas propriedades dos materiais (antes e após o carregamento com fármaco) foi investigado. Para todas os sistemas estudados a esterilização por AUT destacou-se como um excelente método: não afetou os fármacos/materiais e melhorou os perfis de libertação das lentes intraoculares, carregadas com todos os fármacos estudados. Para o material de lentes intraoculares carregado com moxifloxacina, as temperaturas elevadas no carregamento e os longos períodos de armazenamento também melhoraram significativamente os perfis de libertação.

Palavras chave: entrega ocular de fármacos, fármacos oftálmicos, materiais de lentes oftálmicas, esterilização por radiação gama, esterilização por autoclave, condições de carregamento.

TABLE OF CONTENTS

LIST OF FIGURES

LIST OF TABLES

LIST OF ABBREVIATIONS

Abs	Absorbance
ADSA-P	Axisymmetric Drop Shape Analysis Profile
AH	Aqueous humor
ATCC	American Type Culture Collection
B26Y	BenzFlex 26% Natural Yellow
CECT	Colección Española de Cultivos Tipo
CFL58	Contaflex 58
CL	Contact lens
co	Copolymer
CP	Cross polarization
CTN	Campus Tecnológico e Nuclear
DD	Distilled and deionized
$\overline{\mathbf{DD}}$	Dipolar dephasing
DFN	Diclofenac
DSC	Differential scanning calorimetry
EMA	Ethyl methacrylate
EPR	Electron paramagnetic resonance
EWC	Equilibrium water content
FDA	Food and Drug Administration
FEG	Field Emission Gun
FTM	Fluid Thioglycollate Medium
GR	Gamma radiation
HBSS	Hank's balanced salt solution
HEMA	2-Hydroxyethyl methacrylate
HPLC	High performance liquid chromatography
IOL	Intraocular lens
ISCSEM	Instituto Superior de Ciências da Saúde Egas Moniz
ISO	International Organization for Standardization
IST	Instituto Superior Técnico
KTL	Ketorolac
LASIK	Laser assisted in situ keratomileusis
LEBB	Laboratório de Engenharia Biomolecular e de Bioprocessos
LMAEM	Laboratório de Microbiologia Aplicada Egas Moniz
MAS	Magic angle spinning
MH	Mueller-Hinton
MIC	Minimum inhibitory concentration
MMA	Methyl methacrylate
MXF	Moxifloxacin
MXF+KTL	Moxifloxacin combined with Ketorolac

NMR	Nuclear Magnetic Resonance
NP-HPLC	Normal phase chromatography
NSAIDs	Nonsteroidal anti-inflammatory drugs
NVP	N-vinyl-2-pyrrolidone
PCO	Posterior capsule opacification
PDA	Photodiode Array
PEVA	Poly(ethylene vinyl acetate)
PHEMA	Poly(2-Hydroxyethyl methacrylate)
PMMA	Poly(methyl methacrylate)
PVA	Polyvinyl alcohol
RF	Radio frequency
RPE	Retinal pigment epithelium
RP-HPLC	Reversed phase chromatography
SA	Staphylococcus aureus
SAL	Sterility assurance level
SD	Standard deviation
SE	Staphylococcus epidermidis
SELTICS	Sideband elimination by temporary interruption of chemical shift
SEM	Scanning electron microscopy
SH	Steam heat
SR	Swelling ratio
SSB	Spinning sidebands
ssNMR	Solid state Nuclear Magnetic Resonance
T	Transmittance
TOSS	Total suppression of spinning sidebands
TSA	Tryptone soy agar
TSB	Tryptone soya broth
USP	United States Pharmacopeial Convention
UTR	Unidade Tecnológica de Radioesterilização
UV	Ultraviolet
UV−A	Ultraviolet light A
VGMX	Vigamox®
Vis	Visible

LIST OF SYMBOLS

$\mathbf{A}$	Area of the lens
$\mathbf{Al}$	Aluminium
$\mathbf{Au}$	Gold
$\mathbf{C}$	Concentration
$^{13}\mathbf{C}$	Carbon isotope-13
$\mathbf{Cap}$	Capacity
$\mathbf{CH}$	Methine group
$\mathbf{CH_2}$	Methylene group
$\mathbf{CH_3}$	Methyl group
$\mathbf{CO}$	Carbon monoxide isotope
$^{60}\mathbf{Co}$	Radioisotope cobalt-60
$\mathbf{CO_2}$	Carbon dioxide
$\mathbf{CONH}$	Secondary amide group
$\mathbf{CONH_2}$	Amide group
$\mathbf{COOH}$	Carboxyl group
$\mathbf{Cr}$	Chromium
$\mathbf{d}$	Optical path
$\mathbf{dC}$	Initial concentration gradient of NaCl
$\mathbf{D_{Cl^-}}$	Ion diffusivity of chloride
$\mathbf{D_{ion}}$	Ion diffusion coefficient
$\mathbf{D_{Na^+}}$	Ion diffusivity of sodium
$\mathbf{D-value}$	Decimal reduction time
$\mathbf{dx}$	Thickness of the hydrogel
$\mathbf{F}$	Rate of ion transport
$^{19}\mathbf{F}$	Fluorine isotope-13
$\mathbf{H}$	Halo
$^{1}\mathbf{H}$	Hydrogen isotope-1
$\mathbf{HCl}$	Hydrochloric acid
$\mathbf{H_2O_2}$	Hydrogen peroxide
$\mathbf{I}$	Transmitted light intensity
$\mathbf{I_o}$	Incident light intensity
$\mathbf{k}$	Korsmeyer–Peppas release rate constant
$\mathbf{L}$	Length
$\mathbf{m_l}$	Dry mass of the lens
$\mathbf{M_t}$	Amount of mass released at time t
$\mathbf{M_\infty}$	Total amount of mass released
$\mathbf{n}$	Diffusional exponent
$\mathbf{NaCl}$	Sodium chloride

Ø	Diameter
$\mathbf{O_3}$	Ozone
$\mathbf{OCH_3}$	Methoxy group
$\mathbf{OH}$	Hydroxyl group
$\dot{\mathbf{q}}$	Fraction of drug released at time t
$\mathbf{R^2}$	Correlation coefficient
$\mathbf{R_r}$	Aqueous humour fraction renovated at each minute
$\mathbf{SO_3H}$	Sulfonic acid group
$\mathbf{t}$	Time
$\mathbf{T}$	Temperature
$\mathbf{T_g}$	Glass Transition Temperature
$\mathbf{V}$	Volume
$\mathbf{V_r}$	Volume of the receiving chamber solution
$\mathbf{V_t}$	Total volume of the aqueous humor
$\mathbf{W_0}$	Weight of the dry hydrogel
$\mathbf{W_t}$	Weight of the swollen hydrogel at time t
$\mathbf{W_\infty}$	Weight of the swollen hydrogel at the equilibrium
$\boldsymbol{\gamma_{LV}}$	Interfacial tension between liquid and vapour
$\boldsymbol{\gamma_{SL}}$	Interfacial tension between liquid and solid
$\boldsymbol{\gamma_{SV}}$	Interfacial tension between solid and vapour
$\boldsymbol{\delta}$	Chemical shift
$\boldsymbol{\Delta P}$	Difference of pressure in the interface gas/liquid
$\Delta\mathbf{t}$	Time interval
$\boldsymbol{\varepsilon}$	Molar absorptivity
$\boldsymbol{\theta}$	Angle
$\boldsymbol{\lambda}$	Wavelength

I. INTRODUCTION

I-1. Motivation

Over the last years, several strategies for ocular drug delivery have been considered towards the development of novel and safe drug delivery systems capable of surpass the ocular barriers and maintain adequate drug levels in the ocular tissues. Though, until today none of the new methods became as important as eye drops. In fact, they are the most common form of ocular treatment, representing 90% of the marketed ophthalmic formulations. However, they have a low ocular bioavailability: less than 5% of the applied dose reaches the deeper ocular tissues. Thus, more investigation is needed in order to provide an improved system capable of deliver adequate amounts of drug to the target tissues during an appropriate time, avoiding the side effects associated with the current existing drug delivery methods.

Contact lenses (CL) and intraocular lenses (IOL) have arisen as promising options for the sustained release of drug into the ocular tissues from both segments of the eye. To turn these new drug carriers in safe and efficient options, besides the incorporation of sufficient amounts of drug into the lens matrix and the achievement of a sustaining drug release for a desired time, some issues concerning sterilization and storage, need also to be explored to ensure that all the restrict criteria are fulfilled, such as, therapeutic effectiveness, comfort, safety, biocompatibility and sterility. Sterilization is mandatory for the ophthalmic products/lenses due to the potential risk of infection. Moreover, every method of sterilization needs to be validated with respect to the assurance of sterility and should warrant that no adverse effects occur within the product/material. For drug loaded lenses, this issue becomes even more complex, since despite the maintenance of the lenses proprieties it is necessary to ensure that loaded drugs remain stable and active after the sterilization.

I-2. Objectives

The main objective of this research is to determine the effect of two different methods of sterilization, steam heat (SH) and gamma radiation (GR), on several ophthalmic drugs, on two polymeric materials currently used for the production of ophthalmic lenses and on the drug loaded lenses materials. Focusing in one drug loaded IOL material, it will be investigated the role of different conditions of SH sterilization, loading and release. Special attention will be given to the effect of loading temperature. Furthermore, the effect of storage of the drug loaded IOL in the drug solution will also be investigated.

Thus, to assess the impact of the different sterilization procedures, methodologies of loading, release and storage conditions, the drugs, lenses materials and drug loaded materials were subjected to many analytical assays to characterize the materials properties, to study the stability and antimicrobial activity of the drugs and to evaluate eventual changes in the drug release behaviour of the loaded materials.

I-3. Thesis outline

This thesis is divided in four main sections: literature review, materials and methods, results and discussion, and conclusions and future work.

In the literature review it is presented the current state of the art and the theoretical fundaments over the main subjects that will be addressed throughout this work. It begins with an elucidation of the necessity of developing new ocular drug delivery systems. Then it describes the main complications and disorders affecting both anterior and posterior segments of the eye, that can be treated with the studied drugs. The main characteristics and properties of the tested drugs and lenses materials is presented, as well as an overview of the current sterilization procedures and a detailed explanation of the sterilization methods chosen to be used in this work. Finally, the main forms of evaluating the sterility, stability and activity of the tested samples will be discussed.

Materials and methods introduces the materials used and describes the analytical methods and the characterization techniques applied. It details the preparation of all the samples (drugs, materials, and drug loaded materials) as well as the sterilization, loading, release and storage conditions used during all the research. The information regarding the procedures of drug analysis and material characterization are also referred.

Results and discussion is divided in three principal sub-sections. The first sub-section compares two sterilization methods (SH and GR) and discusses their suitability, regarding the effects on the studied drugs, on the CLs and IOLs materials, and on the drug loaded lenses materials. The main purpose of this section is to evaluate the drugs stability and the antimicrobial activity, the most important properties of the materials (transmittance, swelling, wettability, ionic permeability and morphology) and the drugs release behaviour, before and after sterilization.

In the second sub-section, the effect of different loading/release and SH sterilization conditions in the release profiles is discussed. Regarding the effect of loading temperature, besides the drug release studies, the materials properties (swelling, thermotropic behaviour and structural evaluation) and stability of the drugs are also presented.

Lastly, on the third sub-section the results about the effect of storage on sterilized loaded IOLs in terms of drug release behaviour and on the activity of the released drugs are shown and evaluated. This subsection also presents an estimation of the *in vivo* efficacy of the drug loaded lenses based on the application of a simple mathematical model to the experimental results of drug release.

In conclusions and future work, the main conclusions of this work are stated and some suggestions of future work following this project are also referred.

Furthermore, an appendix section is presented at the end of the thesis with supplementary information and additional results.

II. LITERATURE REVIEW

Over the last years, various strategies for ocular drug delivery have been considered by the researchers. However, the simple goal of getting the right pharmacologic agent in the appropriate therapeutic dose to a target ocular tissue, by a method that doesn't damage healthy tissues, remains a challenge.

II-1. Ophthalmic lenses as a new carrier for controlled drug release

The eye is one of the most important and complex sensory organ. It presents several barriers that constitute the main obstacles for ocular drug delivery (see Figure 1). It can be broadly divided into two major segments, the anterior segment (cornea, conjunctiva, aqueous humour, iris, ciliary body, pupil, zonules and crystalline lens) and posterior segment (sclera, choroid, retinal pigment epithelium (RPE), neural retina, macula, fovea, optic nerve and vitreous humour) [1], [2].

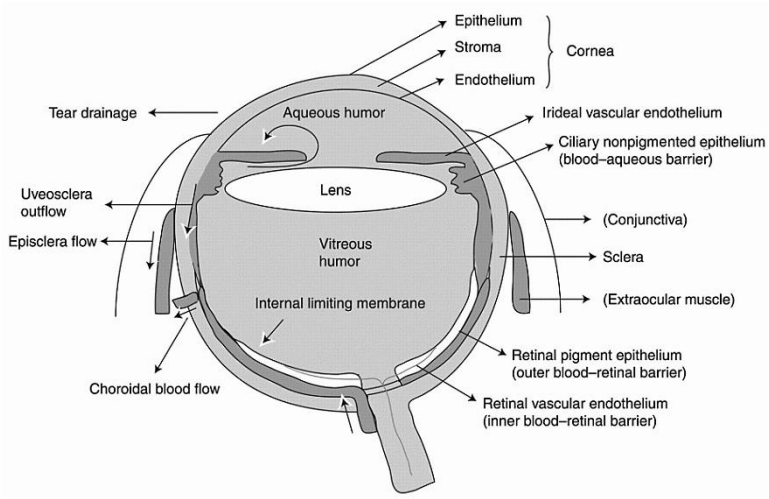

Figure 1. Main ocular barriers in ocular drug delivery. Adapted [3].

When considering drug delivery in ocular therapeutics, there are four important aspects, (1) the duration of delivery, (2) the targeting tissue, (3) the amount of drug (4) and the patient compliance. The duration of drug delivery can vary from minutes to years depending on the route of administration. The route of drug delivery will also determine whether, or not, the drug will be able to reach the targeted tissue in an appropriate concentration. Generally, infections or inflammations affecting the tissues from anterior segment of the eye are more easily to treat than diseases that affect the tissues from posterior segment of the eye, wish are more difficult to reach and treat. [4]. Lastly, the issue of compliance must be considered, especially when treating patients with chronic diseases [4].

Topical administration of drugs is the most common form of treatment of ocular diseases. It constitutes a challenge for formulators and scientists, mostly due to the eye barriers, that reduce drug permeability and contact time in the ocular cavity. An ideal topical system for ocular drug delivery shall include the following characteristics: ease of manufacturing, allow patient self-administration, reach the target site at desired concentrations in required periods of time interval, have a reduced systemic exposure, and henceforth systemic side effects, allow patient safety, comfort and compliance [5]. The

conventional ophthalmic dosage forms for topical delivery are drug solutions, suspensions and ointments [6]. Topical instillation, is the most widely preferred non-invasive route of drug administration, especially to treat diseases that affect the anterior segment of the eye. Eye drops, represent 90% of the marketed ophthalmic formulations. They are easy to apply, but must be administered frequently and their ocular bioavailability is low (less than 5% of topically applied dose reaches the deeper ocular tissues). Also, therapeutic drug levels are difficult to achieve and maintain for long periods into posterior segment tissues, due to the nasolacrimal drainage, tear turnover and tear evaporation [7], [8].

Over the past two decades, ocular drug delivery research advanced towards developing novel and safe drug delivery devices or techniques and patient compliant formulations in order to surpass these ocular barriers and maintain adequate drug levels in tissues, reducing the dosing frequency and associated side effects. Figure 2 shows the manly sites and methods for ocular drug delivery, that are currently being used or under investigation.

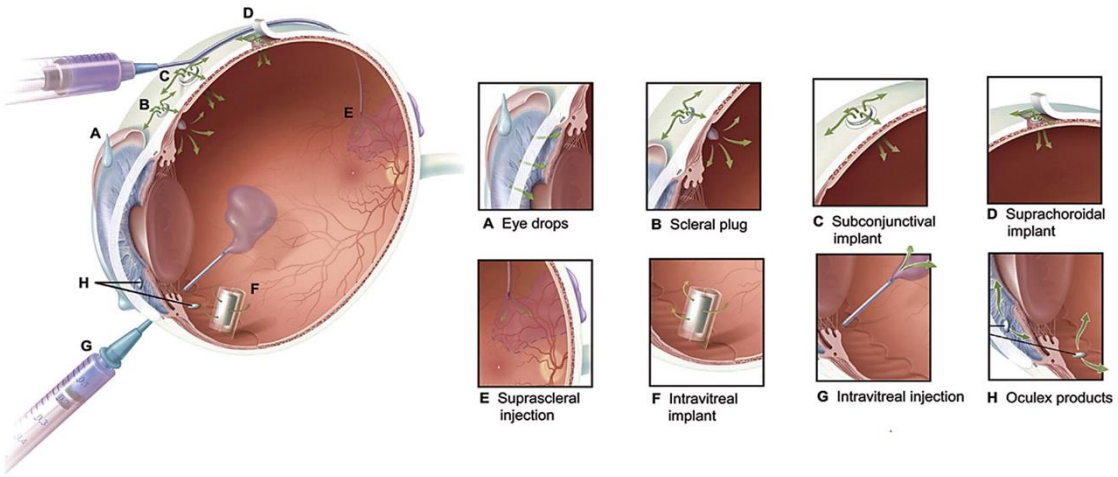

Figure 2. Schematic representation of the main routes of drug administration to the anterior and posterior chambers of the eye. Adapted [3].

The advances for the drug delivery into the anterior segment are manly the level of the formulation of topical solutions (suspensions, emulsions, gels and ointments), through the inclusion of permeation and viscosity enhancers. Various nano-formulations and biodegradable or non-biodegradable implants have also been introduced for the ocular drug delivery in the anterior portion of the eye [5], [9], [10]. For the ocular drug delivery into posterior segment, research has been widely focused towards development of drug releasing devices, injectable therapies and nano-formulations [5]. Different drug delivery approaches like, iontophoresis, sonophoresis, nano-carriers, micro-emulsions and stimuli-responsive smart polymers have also been investigated to address the limitations related to eye drops. However, some of these proposed approaches are expensive or use invasive routes of administration, bringing other clinical concerns to the research community [5], [11], [12]. Besides that, none of the currently used methods proved to be as patient friendly, as eye drops. Therefore, more investigation is needed, in order to provide a system with improved bioavailability, capable of deliver adequate quantities of drug to the target ocular tissues for the required time and which allows to avoid the side effects associated with the existing drug delivery approaches [5].

Within this context CLs and IOLs have emerged as a promising option for sustained release of drug into ocular tissues of both segments of the eye. The concept of delivering drugs through polymeric materials was introduced in the 1960s [13]. Since then, significant developments have been made in terms of the design and material chemistry to greatly improve these vision correction systems and explore their capability as drug carriers [14], [15].

There are still many considerations that need to be done when using drug loaded materials in ocular drug delivery, in order to meet all the restrict criteria, such us therapeutic effectiveness, comfort, safety, compatibility and sterility. The main present challenges in developing ophthalmic lenses as an ocular drug delivery system, are: the incorporation of sufficient amounts of drug into the lens matrix, the achievement of a sustaining drug release for a desired time, the maintenance of a good transparency, the capability of providing patient comfort and biocompatibility (in the sense of "exist in harmony with tissues without causing deleterious changes'') [14], [15].

CLs and IOLs can offer a higher drug bioavailability to the eye tissues and provide a better controlled release of pharmacological agents than conventional forms of treatment, e.g. preventing or treating inflammation, infection or other complications. The ideal performance of a drug eluting CL is compared to the eye drops therapy in Figure 3.

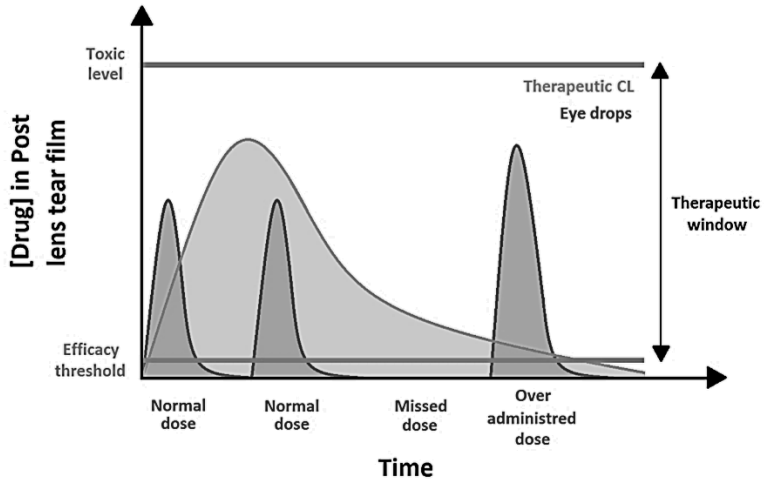

Figure 3. Graphical representation of the drug concentration in post lens tear film, after different therapeutic applications: eye drops instillation or a drug loaded CL.

Ophthalmic lenses can be loaded with drugs by soaking. Although this is a simple and inexpensive method, it may be ineffective, since drug is generally quickly released, with an initial burst. Several strategies have been attempted in order to extend drug residence time and improve bioavailability. Some examples are: incorporation of diffusion barriers (e.g. vitamin E), incorporation of ligands or functional monomers, incorporation of nanoparticles or other colloidal nanostructured systems, molecular imprinting, and surface multi layering [16], [17].

Despite the incredible potential of ophthalmic lenses in the therapeutic field, they are still not available in the market. Optimization is needed and other issues concerning e.g. sterilization, production and storage need to be explored, to ensure the stability of drugs and lenses till the use of the devices and fulfil the commercialization restrictions, turning these new drug carriers in safe and efficient options.

II-2. Ocular pathologies that may be treated/prevented with the studied drugs

Eye is one of the most sensitive organs: it can be affected by several infections or inflammations. The information available on the physiopathology of the eye is extensive, therefore in this section only the relevant diseases affecting both anterior or posterior segments, that are currently treated with the studied drugs (Moxifloxacin (MXF), Diclofenac (DFN) and Ketorolac (KTL)), will be discussed.

In the normal human eye, light rays travel into the eye through the pupil and are focused through the lens into the retina. The natural lens is made mostly of water and crystallins (lens proteins). Ageing leads to lens hardening due to the continuous grow of layers of fibers on the lens surface. Proteins may clump together and become cloudy in some areas, blocking light from passing clearly through the eye. The cloudiness of the lens is called cataract. Besides ageing, cataracts can also have other origins: congenital (occur in infants or children), developmental (caused by other eye diseases, such diabetes or from a previous eye surgery) or traumatic (due to an injury). Concerning cataract's treatment, if vision is only slightly blurry, a change in eyeglass prescription is a possible solution, however, in more severe cases, patients need to undergo surgery. In cataract surgery, the natural lens will be removed and replaced with a clear artificial lens implant (an IOL). Cataract surgery is often performed as an ambulatory procedure and does not require an overnight hospital stay [18]. Usually before and after the procedure, antibiotics (e.g. MXF) and anti-inflammatory eye drops (e.g., KTL and DFN) are prescribed to avoid illness and prevent ocular infections that may cause serious complications [19]–[21].

The most dramatic complication of IOLs implantation is endophthalmitis. Endophthalmitis is a purulent inflammation inside the eye, involving the vitreous and/or aqueous humor (AH), usually provoked by bacterial or fungal infection. Endophthalmitis may present acute symptoms for hours to a few days. These cases are medical emergencies, as a delay in the treatment may represent a permanent vision loss. The most common symptoms of endophthalmitis are eye pain, red eye, ocular discharge, blurred vision, lid swelling, conjunctival and corneal edema, vitreous inflammation, retinitis and blunting of red reflex. Most types of exogenous endophthalmitis are acute post-cataract surgery (the most common), chronic post-cataract surgery, post-injection (from intravitreal or intracameral injections), post-traumatic (after a penetrating trauma) and mould (as a result, for example, of keratomycosis (a fungal corneal infection)). In turn, most endogenous endophthalmitis are due to bacteraemic seeding via bloodstream, usually occurring as a complication of other infection, such us endocarditis (caused by S. aureus) or candidaemia (caused by Candida). Early diagnosis and treatment with antimicrobial therapy (e.g., MXF) is critical. Sometimes systemic antibiotics are not enough, thus intravitreal antibiotics and a vitrectomy may be necessary [21]–[23].

Posterior capsule opacification (PCO) and postoperative ocular inflammation are other concerns of the IOL implantation. Epithelial cell adhesion, growth and proliferation on the posterior side of the lens capsule and also on the IOL may cause loss of vision in months or years, after IOL implantation (called secondary cataract). Retained cortical fibres (elongated lens epithelial cells), bladder cells, myoepithelial cells and fibrocyte-like cells (derived from metaplasia) can also contribute to the PCO [15], [24]. The growth of the epithelial cell will depend on the IOL material and the monocytes/macrophages reaction. Usually, hydrophilic IOLs are less biocompatible than hydrophobic ones, mainly because the surfaces

hinder the adsorption of proteins (fibronectin, laminin, vitronectin, collagen, hyaluronan) that precedes the extracellular matrix formation and serves as receptor of the cells [15]. Nevertheless, even the most biocompatible IOL material induces a certain degree of inflammatory cell adhesion. The high incidence of the PCO and the relatively high cost of a laser capsulotomy, makes the treatment of PCO quite expensive [15]. Therefore, prevention of PCO has a great medical and economical relevance. Some prophylactic strategies are focused on physical structure/properties of the materials, such as the design of IOLs with a sharp edge, less roughness and low water contact angle, or coated with protein/cell repellent substances to avoid these complications [15], [24].

Severe cases of refractive errors like myopia, hyperopia, astigmatism or presbyopia, may also need surgery, to correct or improve vision. There are various refractive surgical procedures for correcting or adjusting the eye, for example, reshaping the cornea, round dome at the front of the eye or implanting a lens inside the eye. The most widely performed type of refractive surgery is LASIK (laser assisted in situ keratomileusis), that is used to reshape the cornea. For patients with myopia, certain refractive surgery techniques will reduce the curvature of the cornea that is too steep. For patients with hyperopia, some refractive surgery procedures will achieve a steeper cornea to increase the eye's focusing power. Astigmatism can be corrected with refractive surgery techniques that selectively reshape portions of an irregular cornea to make it smooth and symmetrical [25]. Anti-inflammatory eye drops (e.g. KTL and DFN) are usually recommended after these procedures to prevent infections and temporarily relieve eye pain, reduce redness or burning/stinging [19], [20].

Conjunctivitis (also called “pink eye”) is the term used to describe swelling (inflammation) of the conjunctiva. Conjunctiva contains tiny blood vessels that produce mucus to keep the surface of the eye moist and protected, but if it becomes irritated or swollen, the blood vessels will become larger and more prominent, making the eye appear red. There are three types of conjunctivitis: bacterial conjunctivitis (caused by bacterial infections and highly contagious); viral conjunctivitis (caused by virus infections, also highly contagious); and allergic conjunctivitis (caused by the body's reaction to an allergen or to an irritant and not contagious). Some of the most common ways to get the contagious forms of conjunctivitis are: forgetting to wash hands often and keep touching the eyes, reuse towels when wiping face or eyes, not cleaning CLs properly or use infected eye makeup. Children are usually more susceptible to get this type of conjunctivitis. “Pink eye” is typically a short-lived condition, commonly treated with eye drops. However, if symptoms continue, it may indicate a more serious problem. The treatment of conjunctivitis usually depends on the type of the infection. Viral conjunctivitis, symptoms can last 1-2 weeks and then will typically disappear on their own, but severe cases will need anti-inflammatory drops (e.g. KTL and DFN). For bacterial conjunctivitis, it will be necessary antibiotic eye drops (e.g. MXF) to treat the infection. For allergic conjunctivitis, treatment often includes the use of allergy eye drops and artificial tears [19]–[21], [26].

Keratitis or corneal ulcer is a condition where the cornea becomes swollen or inflamed, making the eye red and affecting vision. Some forms of keratitis may involve an infection (bacterial, viral, fungal or parasitic). The non-infectious form of keratitis can be caused by a simple fingernail scratch, wearing CLs for too long, improper cleaning and/or care or due to a deficiency in vitamin A (rare). Keratitis can lead to serious complications, including blindness if not treated. The common symptoms are red eye,

eye pain, tearing, irritation, burning, itchy or gritty, swelling around the eye, blurry vision and sensitivity to light. Keratitis treatment depends on the type and severity of the corneal problem. Antibacterial (e.g. MXF) or antifungal eye drops may be used to treat corneal infections and steroid eye drops may also be necessary to reduce the inflammation (swelling). If cornea is severely scarred or if thinning has occurred, it may be necessary a corneal transplant to restore vision. So, it is important to treat keratitis early to reduce the risk of complications [21], [27].

II-3. Ophthalmic drugs used in the present study

In the present work, the drugs that were chosen to incorporate in the lenses materials were DFN, KTL, MXF (and its ophthalmic commercial form, Vigamox® (VGMX)), and a combination of MXF with KTL.

Diclofenac sodium ophthalmic solution was approved by FDA in 1998 (from Alcon, Inc.), and indicated for the treatment of postoperative inflammation in patients who have undergone cataract extraction [19]. Diclofenac (DFN) is a nonsteroidal anti-inflammatory drug (NSAID) [19]. Ophthalmic solution of DFN is indicated in the treatment of eye pain, redness and swelling in patients who are recovering from cataract surgery. It is also used to temporarily relieve eye pain and sensitivity to light in patients recovering from corneal refractive surgery [28].

Ketorolac tromethamine ophthalmic solution was approved by FDA in 2003, (Acular LS® from Allergan, Inc.), and indicated for the reduction of ocular pain and burning/stinging following corneal refractive surgery [20], [29]. Similarly, to DFN, KTL is a NSAID. KTL ophthalmic solution is used to treat itchy eyes caused by allergies, and eye pain, swelling and redness that can occur after cataract surgery [20], [30].

Moxifloxacin hydrochloride ophthalmic solution was approved by the FDA in 2003, introduced as VIGAMOX® by Alcon, Inc., for the treatment of bacterial conjunctivitis caused by designated susceptible organisms, including, among others, *Staphylococcus aureus* and *Staphylococcus epidermidis* [21], [31]. MXF is a fourth-generation fluoroquinolone with antimicrobial activity [15]. Ophthalmic solution of MXF is used more frequently off label to treat keratitis and endophthalmitis, and as a prophylaxis agent in cataract and refractive surgeries [32], [33].

Some of the characteristics and proprieties of the studied drugs are presented in Table 1.

Table 1. Main characteristics and proprieties of the studied drugs [28], [29], [34]–[38] .

Drugs	Diclofenac sodium salt	Ketorolac tromethamine (Ketorolac tris salt)	Moxifloxacin hydrochloride
Pharmacologic action	Anti-inflammatory Analgesic Anti-pyretic	Anti-inflammatory Analgesic Anti-pyretic	Antibiotic
Empirical formula	$C_{14}H_{10}Cl_2NNaO_2$	$C_{15}H_{13}NO_3 \cdot C_4H_{11}NO_3$	$C_{21}H_{25}ClFN_3O_4$
Structural formula	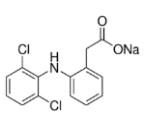	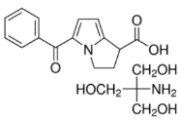	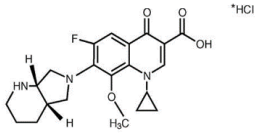
Molecular weight (g/mol)	318.13	376.40	437.89
Solubility in water (mg/mL)	50	25	19.6 (20°C)

The use of topical formulations that are a combination of an antibiotic and an anti-inflammatory drug (e.g. MXF+KTL) to treat inflammations such as conjunctivitis, to reduce post-operative inflammation or to prevent endophthalmitis, has been found to be more useful in some cases. These formulations are already commercialized in a few countries such as India, Pakistan or Swiss as 4 Quin KT eye drops from Entod Pharmaceuticals Ltd, Moxicip KT eye drops from Cipla Ltd or Megacom™ eye drops from Sentiss Pharma [39], [40]. However, as reported on the website of the mentioned producers drug-drug interaction studies have not been conducted yet for these ophthalmic solutions. However, considering the widely utilization of the combined dosage forms of MXF and KTL in the ophthalmic medical field, in this work both drugs were chosen to be combined in the same solution. DFN+MXF was not considered since it was not possible to separate and quantify by HPLC the drugs together.

II-4. Ophthalmic lenses materials: main characteristics and properties

During the past four decades, several polymers have been used to produce ophthalmic lenses. Some of the most commonly used are poly(ethylene vinyl acetate) (PEVA), silicones, acrylic polymers and copolymers, polyvinyl alcohol (PVA) and polyvinyl pyrrolidone (PVP) [41].

The most frequently used acrylates in ocular lenses are poly(methyl methacrylate) (PMMA), which give rise to hard lens and poly(2-hydroxymethyl methacrylate) (PHEMA) which is used in the production of soft lens.

PMMA is a thermoplastic material, with excellent optical properties: it transmits more light (up to 93% of visible light) than glass. It is also very hydrophobic and presents a good degree of biocompatibility [41], [42]. Hydrophobic materials are less likely to evolve into a PCO, what makes them very attractive for ophthalmic applications such as IOLs. However, PMMA has been associated with Glistening's formation (fluid-filled microvacuoles that form within the IOL) and because of its rigidity, the insertion requires large incisions, being frequently associated to endothelial damage and post-operative adhesion of inflammatory cells [15], [24], [43]. Hard lenses made of PMMA are commercially known as Perspex® or Plexiglas® and were the first to be introduced in the market, by Dr. Harold Ridley [41], [44].

PHEMA lenses have a hydrophilic structure which renders them capable of holding large amounts of water in their three-dimensional networks: these materials are therefore known as hydrogels. This characteristic is responsible for the softness of the hydrated material, which makes these lenses more comfortable for the patients. The first soft CLs made with PHEMA were obtained in the 1960s by Wichterle and Lim. Nowadays PHEMA is the main component of the modern soft CLs [13], [24].

Another compound that is used in the production of CLs is N-Vinyl-2-pyrrolidinone (NVP), an organic liquid that is usually polymerized together with MMA. NVP is widely used in the world for its film-forming and adhesive properties. As a monomer, it has mainly applications, being one of them in CL manufacturing, not only for increasing their water content, due to its hydrophilicity, but also to act as a crosslinker [42].

In this work two commercial synthetic copolymers will be used:

- CFL58, a hydrogel of poly(methyl methacrylate-co-N-vinyl-2-pyrrolidone) (p(MMA-co-NVP)) validated as CL material, and

- B26Y, a hydrogel of poly(2-hydroxyethyl methacrylate-co-methyl methacrylate) (p(HEMA-co-MMA)), an amphiphilic copolymer validated as IOL material.

Other components may be also present in the material's composition, however, there is no available information in the website of the suppliers. Anyway, they should not represent more than 1%.

The meaning of the attributed designation in these materials is due to their water content, 58% and 26% respectively. The "Y" letter of B26Y means "Natural Yellow™", and is related with the fact that this particular material is yellow because of the presence of a covalently incorporated UV-A blocking and a violet light filtering (not blocking) chromophore (identical to the chromophore present in the human crystalline lens) that helps to filtrate the harmful energetic UV-A light (315 nm ≤ λ < 400 nm) and part of the violet light (360 nm ≤ λ < 450 nm) to protect retina of the patient eyes [45], [46].

The structural formulas and the main characteristics of the monomers that form the matrix of the materials used in this study are shown in Table 2.

Table 2. Major constituents of the lens materials used in this work [47]–[52].

Monomers	MMA	HEMA	NVP
Empirical formula	$C_5H_8O_2$	$C_6H_{10}O_3$	C_6H_9NO
Structural formula	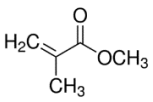	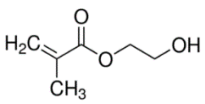	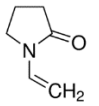
Chemical name	Methyl methacrylate	2-hydroxyethyl methacrylate	N-vinyl-2-pyrrolidone
Molecular weight (g/mol)	100.12	130.14	111.14
Water affinity	Hydrophobic	Hydrophilic	-
Refractive index	1.41 (20°C)	1.45 (20°C)	-

Acrylate-based CLs and IOLs, are currently seen as a vehicle with great potential for the delivery of ophthalmic drugs. A great number of studies have appeared in the literature, reporting the use of these materials as drug delivery devices. However, one of the limitations that have been commonly referred is the fast release rate of the drugs, making researchers focus on the development of new strategies in order to prolong the drug release [41], [53].

Ophthalmic lenses materials shall present several characteristics that allow its use in that specific application. The monomers commonly employed in lens materials will determine their physical, chemical and biological properties. Below are referred the main properties that shall be taken into account to evaluate the performance and characterize an ophthalmic lens material.

II-4.1. Optical transparency

Hydrogels to be used as CLs or IOLs need to be transparent in order to achieve maximal visual performance. The optical clarity of a lens material is defined as the percentage of transmission of visible light, that crosses the lens. The transmissibility of a lens may be obtained using an UV-Vis spectrophotometer. The lens is placed on one side of the cuvette (see Figure 4), and the transmittance/absorbance of the light through the lens is read in a defined wavelength range. In Figure

4, I_0 and I represent the intensity of incident light and transmitted light, respectively, and d is the optical path in the lens [54], [55].

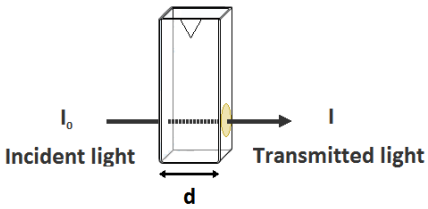

Figure 4. Schematic representation of light transmission determination through a lens.

The absorbance of the light (Abs) may be related with the transmittance (T) through the follow expression:

$$\mathrm{Abs} = \log_{10}\frac{I_0}{I} = -\log_{10}(T) \qquad \textbf{Equation 1}$$

According to the international standard for spectrum classification, ISO $21348:2007$, the visible light is situated in the wavelength range of $380\ \mathrm{nm} \leq \lambda < 760\ \mathrm{nm}$. Hydrogels used as lens materials should transmit over 90% of light in the visible part of the spectrum and preferably block the near ultraviolet light ($300\ \mathrm{nm} \leq \lambda < 400\ \mathrm{nm}$), in particular the ultraviolet A (UVA) rays ($315\ \mathrm{nm} \leq \lambda < 400\ \mathrm{nm}$), in order to avoid ocular problems and protect retina [46], [54].

II-4.2. Swelling kinetics

As referred previously, hydrogels are three-dimensional matrices with the ability to absorb considerable amounts of water, maintaining their dimensional stability. The integrity of a hydrogel in its swollen state is preserved either by physical or chemical crosslinking's. In chemically crosslinked hydrogels, known also as thermosetting hydrogels or permanent gels, like lenses materials, polymer chains are covalently bonded with each other and the polymer is not soluble in solvents. In this materials, swelling is counter balanced by the retraction force of elasticity, induced by the crosslinking points of the network, during the swelling process [56], [57].

The amount of water absorbed in a hydrogel is related with the presence of some functional groups, such as $-\mathrm{COOH}$, $-\mathrm{OH}$, $-\mathrm{CONH_2}$, $-\mathrm{CONH}$, and $-\mathrm{SO_3H}$. Also, porosity of the matrix, capillary effect, osmotic pressure, electrostatic charge and crystallinity of a polymer may influence the equilibrium water uptake [58], [59], [60]. Some hydrogels, called smart hydrogels, stimuli responsive hydrogels or environmentally sensitive hydrogels also swell in response to stimuli that can be either physical (temperature, pressure, light, ultrasound, electric field and magnetic field) or chemical (pH, ionic strength or by the influence of other molecular species) [12], [56], [57], [61].

The water content of a hydrogel depends on kinetics and thermodynamics parameters. During the swelling process, the first water molecules hydrate the most polar, hydrophilic groups (primary bound water), then the network swells and exposes hydrophobic groups (secondary bound water), which together represent the total bound water. After interactions of water with both hydrophilic and hydrophobic sites, the osmotic driving force of the network chains will allow the matrix to absorb more

water (free water), due to the presence of crosslinking junctions (covalent or physical) in the network. The balance between the retraction force of elasticity (from covalent junctions) and the infinite dilution force (from physical junctions) will establish an equilibrium swelling level [56], [62]. The swelling ratio, $\%\mathrm{SR}$ (percent swelling ratio) and the amount of water a hydrogel can hold at equilibrium, $\%\mathrm{EWC}$ (percent equilibrium water content) can be determined experimentally. The expressions used for that propose will be present hereinafter.

In the context of drug delivery, for swellable hydrogel-based systems, when the polymeric material is in contact with water (or biological fluids mainly composed of water), it will give origin to a swollen hydrogel, within which the drug can diffuse and be released. The diffusion from the hydrogel networks can be driven by concentration gradient (Fickian diffusion) or by polymer relaxation (non-Fickian, or viscoelastic diffusion). The non-Fickian diffusion is also known as anomalous transport [63].

II-4.3. Wettability

The surface characteristics of the lens will directly affect its interactions with the tear film and AH, and consequently its biocompatibility [54]. Usually, CLs are preferred to be more hydrophilic (good stability on the tear film and therefore more comfort for the patient). Concerning IOLs, hydrophilic acrylic materials usually have a good uveal biocompatibility but worse capsular biocompatibility, contrarily to hydrophobic acrylic materials [15], [64], [65].

Wettability measurement is used to predict the tendency of a liquid to spread onto a solid surface. It is assessed by measuring the contact angle, which is the angle formed by the tangent to the liquid/vapour interface with the solid/liquid interface at the three-phase boundary [54]. In 1805, Thomas Young [66] stated that a contact angle (θ) of a liquid drop on an ideal solid surface (flat and no deformable) is related with the mechanical equilibrium of three interfacial tensions (solid/vapour (γ_{SV}), solid/liquid (γ_{SL}) and liquid/vapour (γ_{LV}), through the Young's equation [54], [67]:

$$\gamma_{\mathrm{LV}} \cos\theta = \gamma_{\mathrm{SV}} - \gamma_{\mathrm{SL}} \qquad \textbf{Equation 2}$$

The wettability can be measured by several techniques. The most common used for lenses is direct contact angle measurement by sessile drop or captive bubble methods (Figure 5).

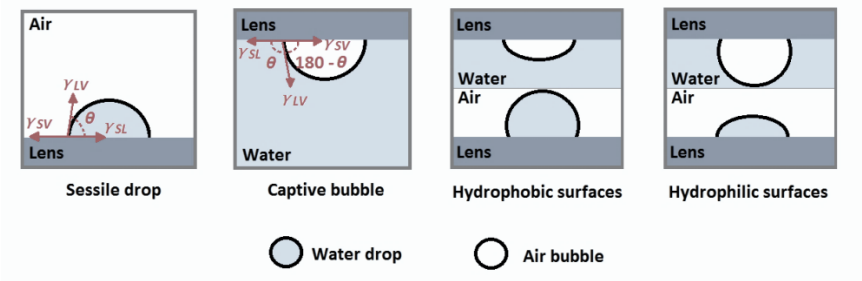

Figure 5. Schematic representation of sessile drop and captive bubble methods and their behaviour when in contact with hydrophobic or hydrophilic surfaces.

In the sessile drop technique, usually performed inside an ambient chamber saturated with water vapour to avoid evaporation, a liquid drop is deposited on the substrate surface using a syringe, while

in the captive bubble method, the lens is fixed on a stand in a reverse position, against gravity, and immersed in a liquid, inside a liquid cell (with quartz windows), and a gas bubble from a syringe is inserted on the bottom of the surface [54], [67], [68]. In both approaches, the contact angles are determined with the help of a goniometer and a software data analysis (Figure 6).

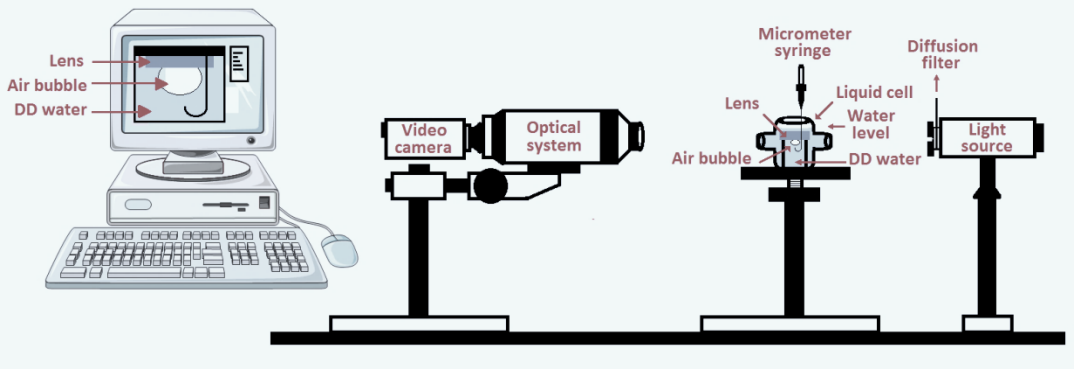

Figure 6. Schematic representation of the apparatus for the determination of contact angles using captive bubble method.

The contact angle is used to predict the affinity of lenses with water/aqueous solutions. Higher contact angles mean a lower wettability (hydrophobic surfaces) while lower contact angles correspond to a higher wettability (hydrophilic surfaces). In CLs, the higher the wettability of a lens surface, the greater the stability of the tear film over the surface lens [54], [68].

II-4.4. Ion permeability

The transport of water and ions through CLs is crucial for the provision of essential nutrients to the eye, removal of waste products and debris, and adequate lens movement. Diffusion of ions is a fundamental process needed to ensure an adequate post-lens tear film, reducing the likelihood of lenses from binding to the cornea [69], [70]. Water is able to move through a hydrogel in a way quite different from the movement of ions. It is more difficult for ions to travel through a matrix and usually, its transport is impeded in lenses with a water content below of 20% [54]. The minimal value required of ion permeability for an appropriate movement of a lens in the eye is $1.5 \times 10^{-5}\ \mathrm{mm^2/min}$ [71].

IOLs must also exhibit a relatively high ion permeability [72]. However, the permeability is most relevant for IOLs with UV chromophores (high concentrations of UV chromophores can reduce ion permeability) and for Phakic-IOLs, to avoid disturbing the metabolism of the crystalline lens [72], [73]. Phakic-IOLs are a special kind of IOLs that are implanted surgically into the eye to correct refractive errors: they supplement or correct the vision without replacing the natural crystalline lens [73].

The ion diffusion coefficient ($\mathrm{D_{ion}}$) is an indicative of the ion permeability or salt permeability. A common methodology for determining ion permeability is through the use of a diffusion cell (see Figure 7) containing the lens in the middle of two chambers, the donor chamber (with a saline solution) and the receiving chamber (with DD water).

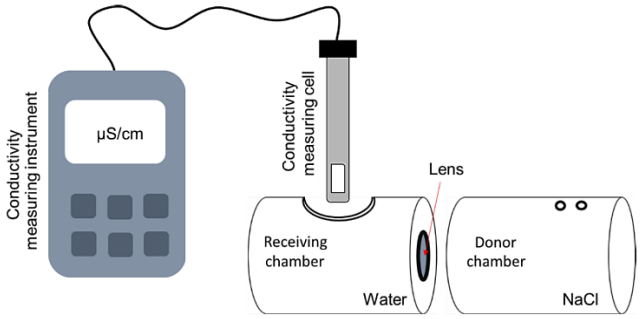

Figure 7. Schematic representation of the apparatus for determination of ion permeability. Adapted [74].

As time passes, the ions cross the lens matrix towards the receiver compartment and D_{ion} can be estimated by measuring the conductivity of the fluid on the receiving chamber and subsequently converting into salt concentrations. Then the Fick's law is applied.

II-4.5. Morphology

Scanning electron microscopy (SEM) is a powerful tool for microstructural analyses. It is widely used to observe the surface morphology of lenses materials, producing images with a resolution of nanometres [75].

SEM is a type of electron microscope that produces scanning images of a sample, using a focused beam of electrons. These electrons interact with the atoms of the sample, producing various signals (secondary electrons are the most widely used in the analysis) that contain information about the morphology and topography of the sample in the form of a grey scale image [75].

The polymeric surface of a lens usually has no electrical conductance and for that reason a $10 - 15\ nm$ layer of a conductive material, such as gold (Au) or chromium (Cr) is usually applied by sputter coating. Since the acquisitions of SEM images are performed under vacuum conditions, samples need to be previously dried before making the sputter coating [75], [76].

II-4.6. Thermotropic behaviour

Differential scanning calorimetry (DSC) is a procedure used to investigate the response of polymers to temperature variations. It can be used in a wide range of studies, being a valuable method in the determination of the glass transition temperatures. Thermal analysis of samples by DSC measures the heat flow related to phase transitions of materials as a function of time. The heat capacity of samples is linearly correlated to a reference standard and measured as radiated or adsorbed energy [77], [78].

If a polymer in its solid state is heated it will, at some point, reach its glass transition temperature (T_g). At this point the mechanical properties of the polymer change from those of a brittle material to an elastic one due to changes in chain mobility. The heat capacity of the polymer is different before and after the T_g, being usually higher above T_g (see Figure 8). The transition does not occur suddenly at one unique temperature but rather over a range of temperatures. The temperature in the middle of the inclined region of the thermogram (midpoint of the transition) is often taken as the T_g value [77], [78].

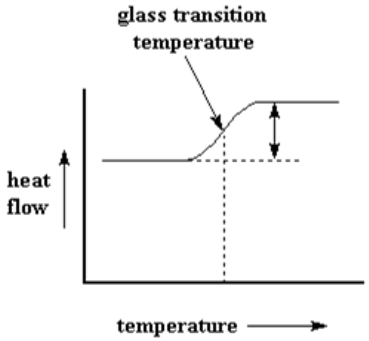

Figure 8. Schematic representation of a DSC curve for the determination of T_g [79].

The DSC set-up is composed by a measurement chamber with two pans (crucibles) that are heated/cooled in its interior (see Figure 9), and a computer to program the heating/cooling cycles and process data. One of the crucibles contains the material being investigated and the other is typically empty, being used as reference. The rate of temperature change, for a given amount of heat, will differ between the crucibles. This difference will depend on the composition of the sample as well as on physical changes, such as phase changes or chain mobility changes form the atoms in the polymer. In a heat-flux DSC, the system varies the heat provided to one of the pans in order to keep the temperature of both pans the same. The difference in heat output of the two heaters (sample and reference) is recorded and the result is plotted as the difference in heat versus temperature or time, after a suitable calorimetric calibration [77], [78].

Figure 9. DSC equipment and its heating/cooling chamber with the crucibles inside.

II-4.7. Structural proprieties

Solid state Nuclear Magnetic Resonance (ssNMR) spectroscopy, a particular type of NMR spectroscopy, is a powerful method for the characterization of solid materials or products in the solid form. It is particularly useful in the determination of molecular structures, in interaction studies and for polymorphic characterizations [80].

The basic principle behind ssNMR is that, nuclei are electrically charged and many have spin that leads them to behave like a magnet. When an external magnetic field is applied, it can occur an energy transfer from the base level to a higher energy level. This energy transfer takes place at a wavelength that corresponds to a certain radio frequency and when the spin returns to its base level, energy will be

emitted at the same frequency. The signal of this energy transfer is measured and processed in order to yield an NMR spectrum [80].

Usually ssNMR spectra are very broad, due to the effects of anisotropic interactions (orientation dependent) that are observed in the spectrum. Anisotropic interactions have a considerable influence on the behaviour of a system of nuclear spins. Some of those interactions in ssNMR are: direct dipolar interactions, chemical shift anisotropy, Zeeman interactions, quadrupole interactions, J-coupling (indirect dipolar interactions) and spin-spin coupling. In order to minimize these anisotropic interactions between nuclei and to increase signal to noise ratio in rare spin, such as ^{13}C NMR spectra, several methods have been developed [80]–[82]. Usually to obtain a high-resolution NMR spectra of rare nuclei in solid samples, three techniques are combined: (i) cross-polarization (CP), (ii) magic angle spinning (MAS), and (iii) high-power proton decoupling. Actually, the most common probe-head used in ssNMR is a double-resonance probe capable of CP and MAS experiments in conjunction with high-power proton decoupling [83].

Cross polarization (CP) pulse sequences is mainly used to transfer magnetic polarization from abundant nuclei (e.g., $^{1}\mathrm{H}$ or $^{19}\mathrm{F}$) to rare nuclei (e.g., $^{13}\mathrm{C}$, with a natural isotopic abundance of 1.1%). The result is an enhancement of the NMR signal of the rare nucleus [81], [83].

MAS technique, introduces an artificial motion (sample spinning) by placing the axis of the sample rotor at the magic angle (54.7356^{o}), relative to the external applied magnetic field. That means, when $\theta = 54.7356^{\mathrm{o}}$ the expression $1 - 3 \times \cos^2\theta = 0$ (θ is the angle between the spinning axis and the external magnetic field) and the interactions are averaged to zero or reduced to the isotropic values, which allows for chemical shift resolution. The rate of MAS must be equal or greater than the magnitude of the anisotropic interaction, otherwise if the sample is spun at a rate less than the magnitude of the anisotropic interaction, a manifold of spinning sidebands (SSB) becomes visible, which is a series of peaks, spaced at integer multiples of the MAS rate from the isotropic peak. For some cases, there are pulse sequences available to eliminate these SSB, for example the TOSS sequence (total suppression of spinning sidebands) or SELTICS sequence (Sideband Elimination by Temporary Interruption of Chemical Shift) [80], [81], [83].

High-Power proton decoupling, in the solid state, consists in applying decoupling fields on the order of at least $60 - 100\ \mathrm{kHz}$ for $^{1}\mathrm{H}$ decoupling. Typically, higher decoupling fields provide better signal-to-noise. Usually, decoupling of abundant spins such as protons, requires much more power for solids than for solutions. Decoupler can only be switched off for a relatively short time, otherwise the RF coil will become very hot, leading to arcing and sample heating. Switch off the decoupler is also a routine technique used to distinguish between protonated and non-protonated carbon nuclei, i.e., it is a method which allows the discrimination of quaternary carbon atoms from those with one or two directly bonded protons and is known as Dipolar dephasing ($\overline{\mathrm{DD}}$). It is based on dipolar coupling between the directly bonded protons and the carbon atoms, and uses a time period on the order of $30 - 40\ \mu\mathrm{s}$ before the acquisition, were the signals due to the functional groups of methine $(=\mathrm{CH}-)$ and methylene $(=\mathrm{CH_2}-)$ carbon nuclei are suppressed. Methyl carbons $(=\mathrm{CH_3}-)$ are usually not significantly suppressed during the $30 - 40\ \mu\mathrm{s}$ dephasing period [83].

II-5. Sterilization

Due to the potential risk of infection, ophthalmic lenses are mandatory to be put on the market in a sterile state. The level of sterility required is governed by European Standard EN 556 and also by U.S. Food and Drug Administration (FDA) guidelines [84].

Sterilization is defined as the process needed for the complete destruction/removal of all microorganisms, including spore-forming/non-spore-forming bacteria, viruses, fungi and protozoa, that could contaminate pharmaceuticals or other medical devices and thereby, constitute a health hazard. Reaching an absolute state of sterility cannot be demonstrated, thus the sterility of a pharmaceutical preparation or a medical implantation device is only defined in terms of probability and is referred as the sterility assurance level (SAL). SAL is described as the probability of an item being non sterile, after being exposed to a validated sterilization process. Any sterile medical device that may be commercialized in Europe, must be sterilized with a SAL of 10^{-6}, which means that it shall present a probability of one or less than one in a million of being non sterile [85], [86].

According to of the International Pharmacopoeia of 2015, the classical sterilization techniques, like SH or hot air are the most reliable methods and should be used whenever possible [85]. FDA divides the sterilization techniques currently used to sterilize medical devices in two categories, the established and the novel systems. The established sterilization procedures (with a long history of safety and effectiveness and with satisfactory quality system inspections) include dry heat, ethylene oxide, saturated heat or steam, ionizing radiation (gamma and electron beam), hydrogen peroxide (H_2O_2) and Ozone (O_3). The novel sterilization methods (those that FDA has not reviewed and determined to be adequate and effectively sterilize for an intended use) are vaporized peracetic acid, high intensity light or pulse light, ultraviolet light, sound waves and microwave radiation [87].

Every method of sterilization should be validated for each type of product/material, with respect to the assurance of sterility and to warrant that no adverse alterations occur within the product/material. Also, validation programmes and biological indicators should be used periodically to validate the sterilization procedures and as routine control of individual cycles, during manufacture [85].

If products could not be sterilized in final containers by the referred procedures, the implementation of an aseptic process of manufacturing is crucial.

II-5.1. Ophthalmic drugs sterilization

Every ophthalmic dosage form has to be manufactured under conditions validated to render it sterile in its final container [88]. The sterilization procedure to be used will strongly depend on the nature of the drug [89]. The most common methods of achieving sterility of ophthalmic formulations are SH sterilization, dry heat sterilization, ionizing radiation sterilization (gamma and electron beam), gas sterilization (ethylene oxide and ozone), filtration and aseptic processing. For ophthalmic formulations packaged in plastic containers, the combination of two or more of these methodologies is also frequently applied, since the most suitable method for sterilizing a product may not be the best to sterilize the package and therefore, the products and packages may be sterilized separately by different methods and, in the end, joined under aseptic conditions [87]–[89]. The preferable method to sterilize ophthalmic

drugs in their final container is SH sterilization, although this method is sometimes not recommended because it may cause thermal instability on some active ingredients and in these cases, an alternative sterilization procedure is operated. Some of those alternative procedures are irradiation, bacterial filtration and manipulation under aseptic conditions. For the last two, the final containers shall be sterile at the time of filling and closing [88], [89].

II-5.2. Ophthalmic lenses sterilization

Most commercial lenses are sold in a final shipping package or a dispenser, containing a storage saline solution, that is submitted to terminal sterilization. This means that the set lens + solution is sterilized only at the end of the manufacturing and packaging process [84].

A considerable number of sterilizing techniques are currently employed in the production of sterilized ophthalmic lenses. Each method offers certain advantages and disadvantages. The most typical methods are SH sterilization, ionizing radiation sterilization (gamma and electron beam), and gas sterilization (ethylene oxide and ozone). Alternative sterilization methods are permitted if appropriately validated for the intended [90], [91].

SH is also the most preferable sterilization procedure used in the lenses manufacture. This method presents great advantages over the others, it uses a simple procedure, being one of the most cost-effective techniques. Its main disadvantages are related with the potential effects of high temperature and pressure on the lens packaging than often results in a slightly wrinkled foil. Also, in the saline additives, such as hyaluronic acid in CL, hydrolysis at elevated temperatures is a concern when using SH sterilization [84].

Sterilization of lenses is a mandatory step to prevent the risk of infection. Nevertheless, it is imperative to ensure that the sterilization procedure does not compromise the biomaterials properties. The issue becomes even more complex if we talk about drug loaded lenses. In this case, besides the material properties, it is necessary to ensure that the loaded drugs keep active.

II-5.3. Sterilization methods used in this study

II-5.3.1. Steam heat

When heat and pressure are used as a sterilizing agents, denaturation of enzymes and structural proteins of the microorganism occur, creating an accumulation of irreversible damage to their metabolic functions and thus, killing them [85], [92].

SH, also called saturated steam, moist steam under pressure or autoclaving is the sterilizing method of choice whenever it can be used. In SH sterilizers, the central parameters governing the efficiency of the sterilization process are temperature, pressure and exposure time. Generally, a cycle comprises three phases: heating, sterilizing, and cooling. The choice of the cycle parameters depends on the heat sensitivity of the material and on the knowledge of the heat penetration rate into the item or substance. For SH sterilization, the common range of sterilizing temperatures is $121–138$ ºC and time exposures is $5-15$ min. The typical cycle is 15 min at 121 °C and 1 bar, but alternative conditions using different combinations of time and temperature are also recommended. In certain cases, the sterilization

may be carried out at temperatures below $121\ ℃$, using combinations of time and temperature that have been also validated. Usually, lower temperatures imply higher times. However if the microbial burden of a certain substance/material before the sterilization is known, the times may be adjusted offering a satisfactory level of sterilization [85], [92].

The indicator strain proposed in the international norms for the validation of the SH sterilization process is spores of *Bacillus stearothermophilus* (e.g., ATCC 7953) for which the D−value (i.e., interval of time required to provide one decimal logarithm ($1 - \log_{10}$) or 90% reduction in the initial microbial population (bioburden)) is $1.5 - 2$ min at $121\ ℃$, using approximately 10^6 spores per indicator [85], [93].

Figure 10 presents schematically a typical autoclave: besides the heating elements it includes a system of valves that allows to control pressure [94].

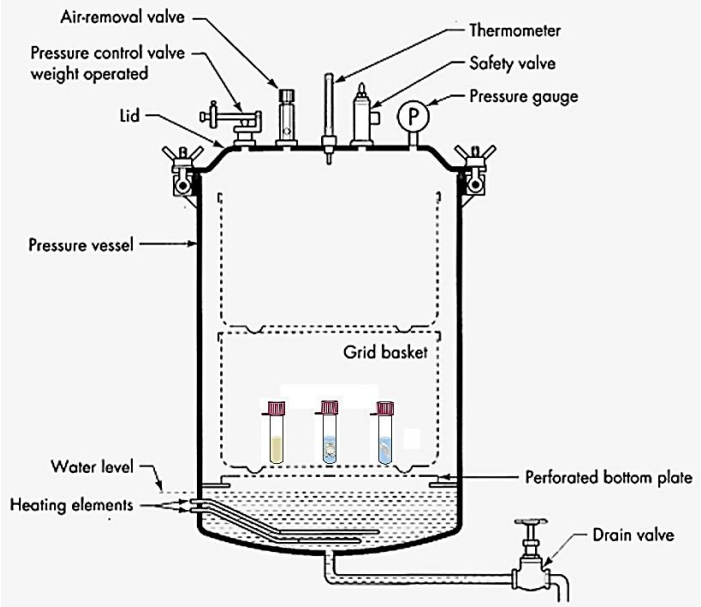

Figure 10. Schematically representation of a typical autoclave. Adapted [94].

II-5.3.2. Gamma radiation

Gamma radiation (GR) also called gamma irradiation is used to incite ionization of the molecules in microorganisms, through direct penetration of high energy photons or indirectly through the generation of free radicals, causing DNA destruction and leading them to death [85].

Terminal sterilization of drugs and medical devices can be achieved by exposure to gamma rays produced by an appropriate radioactive source, that usually is $^{60}\mathrm{Co}$ (cobalt−60) [85]. GR represents a reliable alternative for the sterilization of thermosensitive drugs and medical devices. Some of the advantages of GR include high penetration power, isothermal character (small temperature rise) and no residues, providing a great assurance of product sterility [95].

It is usual to select an absorbed radiation level of $25\ \mathrm{kGy}$, since this is the reference value to guarantee an appropriate SAL. However, other levels may be employed if they have been validated for the intend [85]. For certain cases, substances/materials may need more or less dose to ensure an effective sterilization, nevertheless, and as referred previously, it is important to ensure that the sterilization procedure does not destroy the materials or significantly reduces the activity of

pharmaceutical formulations. As reported in literature, in order to minimise the effects of ionization in drug formulations in the form of aqueous solutions, a radio-protecting excipient such as mannitol, pyridoxine or nicotinamide may be added to the solution, to scavenge some of the reactive species formed during hydrolysis [96].

GR processes implies specific cautions, whereby only expertise and well trained staff should monitor the processes to ensure their safety. Radiation doses must be monitored with specific calibrated dosimeters during all the process. The entire system should also be controlled and validated every time the source material is changed and, for precaution, at least once a year [85].

The indicator strain proposed by the international norms for the validation of GR sterilization with 25 kGy is spores of *Bacillus pumilus* (e.g., ATCC 27142) for which the D−value is 3 kGy using $10^7 - 10^8$ spores per indicator. Also, spores of *Bacillus cereus* and *Bacillus sphaericus* (e.g., $\mathrm{SSI\ C}\ 1/1$ and $\mathrm{SSl\ C_1A}$ respectively) are used but for higher implemented doses [85].

In the present work, samples were sterilized in the Portuguese facility, at CTN-IST. This facility was specifically designed for the sterilization of medical devices. The irradiation facility is a semi-industrial installation of continuous irradiation of $^{60}\mathrm{Co}$ and comprehends five principal zones: the irradiation cell (with a nominal activity of $1.5\ \mathrm{x}\ 10^{16}$ Bq); the control room of the irradiator; the labyrinth and transport conveyor system; the reception storage area for non-sterile products; and the storage area for sterile products [97].

The most important component of this unit is the irradiation cell (see Figure 11). Its walls are made of high-density concrete ($2.23\ \mathrm{g/cm^3}$) with a thickness of $1.8 - 2\ \mathrm{m}$, working as a biological shield. The access to the irradiation chamber is through a labyrinth of $23.3\ \mathrm{m}$ long inside that shield. In the middle of the irradiation cell is the irradiator, that consists of 30 stainless steel tubes arranged in a planar geometry. The power source, a radioisotope $^{60}\mathrm{Co}$ is doubly encapsulated in stainless steel tubes enclosed into those 30 tubes. When the radiator is not in the irradiation position, it is collected into a shell consisting of a concrete pit coated with iron blocks and with a dedicated cooling system for circulating cooled water. To be in the working position, an electromechanical system rises the irradiator placing it into the irradiation position [97].

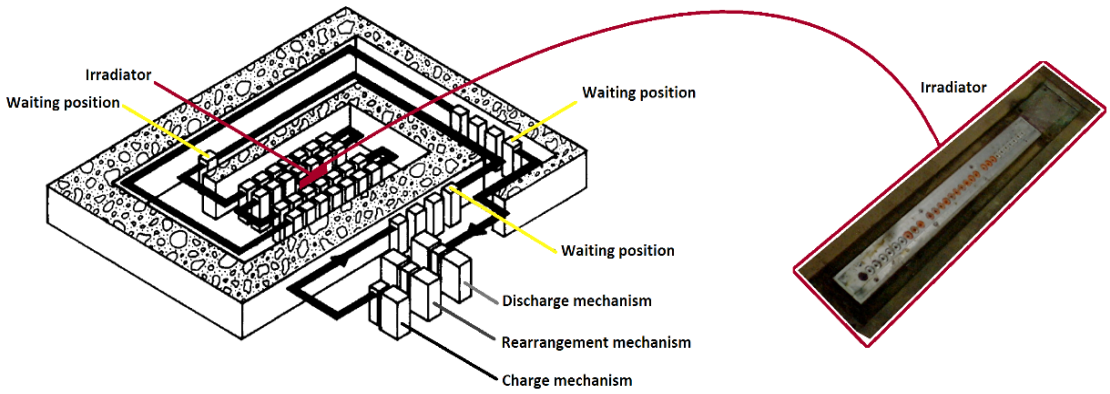

Figure 11. Schematic diagram of the irradiation cell, the labyrinth and the conveyor system. Adapted [97].

II-5.4. Sterility tests

To verify the sterility of the materials, there are two approved techniques by FDA, USP 71 and Portuguese Pharmacopeia 9: direct inoculation and membrane filtration. To meet the official requirements, two different growth media are used. Usually, fluid thioglycollate medium (FTM) for aerobic and anaerobic bacteria and a soyabean-casein digest medium or tryptone soya broth (TSB) for aerobic bacteria fungi and yeasts. In the present work, direct inoculation method was chosen to verify the sterility of lenses materials and membrane filtration to verify the sterility of drug solutions [98]–[100].

In direct inoculation method, samples are added directly into the growth medium in aseptic conditions and then incubated at least for 14 days. Positive controls (samples intentionally contaminated with known microorganisms) and negative controls (sterilized solvents) are both incubated together with the testing samples. After the incubation period the mediums are analysed in terms of turbidity. A turbid medium indicates contamination. This method have some drawbacks because it is very depended on the type of sample, volume or microorganisms concentration, to provide a statistically valid assay [98]–[101].

The membrane filter technique (see Figure 12) is more suitable for solutions then direct inoculation. In this method a sample solution is filtered through a sterile membrane usually a $0.45\ \mu$ filter. The membrane captures all microorganisms and removes other components that can cause turbidity and can inhibit the microorganism's growth. Then the membrane is washed by filtering a sterile fluid to remove any compound that can cause a bacteriostatic effect, and is aseptically divided and placed into the grown media and incubated. Positive and negative controls are incubated together with the testing samples to be analysed in terms of turbidity [98]–[101].

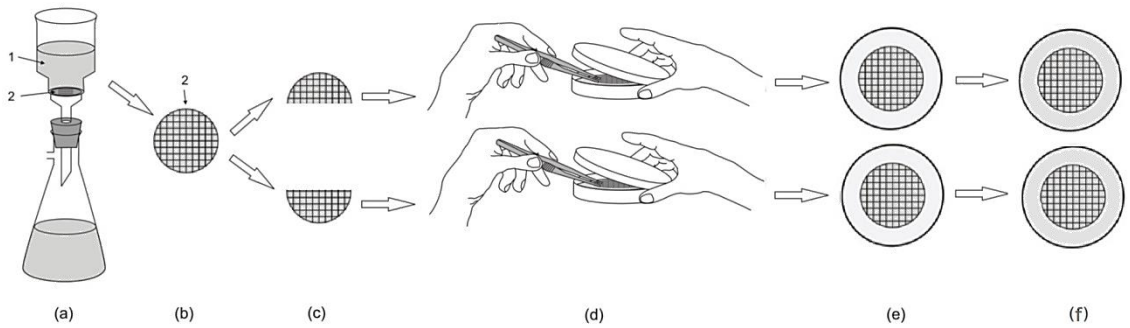

Figure 12. Schematic representation of membrane filter technique. (a) A known quantity of sample solution (1) is filtered through a membrane (2). (b) Then, the membrane is removed, (c) divided in aseptic conditions (d) and placed into a petri plate, containing an appropriate culture medium. (e) Plates are incubated at a defined temperature for 14 days (f) and then analysed for turbidity. Adapted [102].

II-6. Stability of drug formulations

In the manufacturing industry of ophthalmic formulations it is critical to ensure not only the sterility, but also an optimal biological activity and physical stability [12].

To evaluate the eventual degradation of drugs that are subjected to invasive procedures, high performance liquid chromatography (HPLC) is frequently used. Variations in spectra shape or retention time of the molecules may indicate changes in the molecules structure. Furthermore, HPLC is very

useful to assess the purity and/or determine the content of many chemical and pharmaceutical substances in solution [103].

HPLC is a separation technique used for the analysis of organic molecules or ions. It is based on mechanisms of adsorption, partition or ion exchange, depending on the type of stationary phase used. HPLC involves a solid stationary phase, which normally is contained in a stainless steel column, and a liquid mobile phase which moves through the stationary phase. The separation of the components of the solution results from the difference in the relative distribution ratios of the solutes between the two phases [103].

The apparatus is represented in a schematic way in Figure 13, and it consists of a pumping system (to deliver controlled amounts of mobile phase), an injector (used to introduce the sample into the mobile phase at/or near the head of the column), a chromatographic column (filled with a stationary phase), a detector (generally an UV-vis, although others may be used, as photodiode, fluorescence, electrochemical, evaporative light-scattering, etc.) and a data collection device (a computer, an integrator or a recorder) [103].

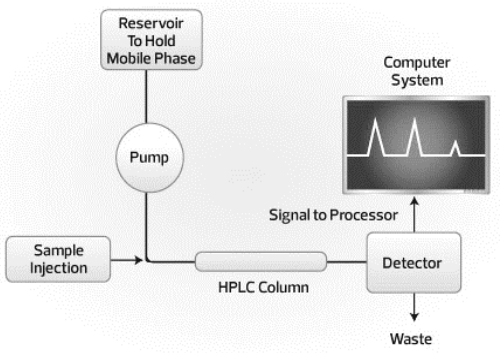

Figure 13. Schematic representation of a HPLC system. Adapted [104].

HPLC mobile phases may be non-polar (normal phase chromatography (NP-HPLC)) or polar (reversed-phase chromatography (RP-HPLC)). Concerning stationary phases, there are many types: unmodified silica, alumina or porous graphite are used in NP-HPLC, being separation based on differences in the adsorption of the solutes; chemically modified supports prepared from polymers, silica or porous graphite are used in RP-HPLC, being separation based principally on partition of the molecules between the mobile and the stationary phases [103].

The choice of mobile phase is based on the desired retention behaviour, on the physicochemical properties of samples as well as on the type of detector used. Usually, for NP-HPLC lipophilic solvents should be employed while for RP-HPLC aqueous mobile phases are more adequate. The mobile phase should be filtered before the assay through suitable membrane, of Nylon or cellulose acetate, to remove particles or undissolved material [103].

In the case of antibiotics, microbiological assays may be also used to evaluate drugs stability, since they allow to determine the eventual loss of activity. Because of the convenience and the cost-effectiveness, disk diffusion, also called agar diffusion technique is probably the most widely used method for determining antimicrobial activity. In this method, a growth medium, usually Mueller-Hinton (MH) agar is prepared and sterilized. The microorganism of interest (obtain from a previously prepared

bacterial culture) is diluted in a saline solution at a pre-defined concentration. These suspensions are then seeded in the growth medium and let to solidify in petri dishes. Filter paper discs are placed equally spaced on the surface of the infected agar plate. The antibiotic solutions with a pre-determined concentration are then released on the top of each disc. Negative controls (sterilized discs impregnated with solvent) are placed in the same plate and sometimes positive controls too (commercialized pre-impregnated disks with a standard concentration of drug with the respective known inhibition halo). The diffusion of the drug immediately begins when the drug is placed on the disks, creating a concentration gradient in the agar, that decreases with the distance from the discs. After an incubation period, the bacterial growth around each disc and sensitivity may be determined measuring the size of the inhibition halo. If there was no growth around the disk it means the bacteria used are resistant to that antibiotic or to the applied concentration [105], [106]. The establishment of a correlation between the concentration of an antimicrobial agent with the size of the inhibition halo (calibration curve) allows to predict the activity of the same antimicrobial agent as a response to any experimental condition [107].

The same procedure may also be used for the determination of the minimum inhibitory concentration (MIC) which refers to the minimum concentration of antibiotic necessary to prevent growth of a determined microorganism. In this case, it is called agar dilution method and uses a serial of two fold dilutions that also allow to estimate the concentration of an antimicrobial agent in the agar [107].

It is also important to mention that the choice of the appropriate strains to make the antimicrobial assays should always be framed in the intended application. In 2008 B. Sherwal and A. Verma [108] presented the prevalence of the microorganisms evolved in a total of 400 cases of eye infection (250 of conjunctivitis, 120 of keratitis, 15 of endophthalmitis and 15 of other infections). *Staphylococcus aureus* and *Staphylococcus epidermidis* were the most commonly isolated microorganisms, found as bacterial cause of eye infection, each of them representing 19,13% of the initial 400 cases, totalizing about 153 cases. This has also been recently reported by other investigators [109], [110].

III. MATERIALS AND METHODS

III-1. Materials

III-1.1. Ophthalmic drugs

The drugs used in this work were Moxifloxacin hydrochloride $\geq 98\%$ from Carbosynth Ltd., VIGAMOX® $5\ \mathrm{mg/mL}$ ophthalmic solution from Alcon, Diclofenac sodium salt $\geq 99\%$ and Ketorolac tris salt $\geq 99\%$, both obtained from Sigma-Aldrich.

III-1.2. Ophthalmic lenses materials

Contaflex 58 (CFL58), and BenzFlex 26% Natural Yellow™ (B26Y) were kindly provided by PhysIOL SA (Liège - Belgium).

Some of the main characteristics of these materials are listed in Table 3.

Table 3. Main characteristics and properties of ophthalmic lenses materials [111]–[113].

Ophthalmic lenses materials	B26Y	CFL58
UV−blocker	Natural Yellow™	No
Classification (ISO $18369-1:2006/\mathrm{Amd.}\,1:2009$)	–	Filcon II 2
Monomers	HEMA/MMA	MMA/NVP
Diameter (mm)	14.5 – 16.0	12.7
Thickness (mm)	1	1.1 – 1.2
Colour	Yellow	Colourless
Light transmission	–	$> 94\%$
Refractive index (at 20°C)	1.461 (Wet) 1.508 (Dry)	1.40 (Wet) 1.54 (Dry)
EWC (%) (at 20°C)	26	58
Oxygen permeability (Dk) $\left((\mathrm{cm}^2/\mathrm{sec}) \times (\mathrm{mL\ O^2/mL} \times \mathrm{mmHg})\right)$	–	21×10^{-11}
Ionicity	–	Non-ionic

Before utilization, the raw materials were submitted to impurity extraction in order to remove eventual residual monomers or foreign substances, resulting from the manufacturing process. The extraction was carried out using a soxhlet extractor, schematically represented in Figure 14.

The system operating principle consists in placing the extracting solvent (DD water) in the lower reservoir (a glass evaporating flask) and heat it (with a heating mantle) to its boiling point. DD water in the vapour phase will move upwards through the soxhlet distillation arm and drip into its chamber. The condenser, with circulating water at $12^{o}\mathrm{C}$, will ensure that the vapour cools and gets back to the liquid state dripping into the soxhlet compartment, where the lenses materials (disks) are placed. When the soxhlet is almost full, the chamber will be emptied by the siphon arm, where the DD water and the extracted impurities will drain back to the lower reservoir. For each material approximately 60 cycles were completed, respecting a ratio of 20 mg of material / 1 mL of DD water. At the end of the extraction, the disks were rinsed with freshly DD water and cut into smaller disks using a hollow punch tool with $5\ \mathrm{mm}$ of inner diameter to approach the average weight of real lenses [114]. In some cases, disks with

different dimensions were used as well, as specified in the description of the characterization techniques. Then, all lenses materials were dried at $36^{o}C$ for 7 days and stored in a sealed flask until their utilization.

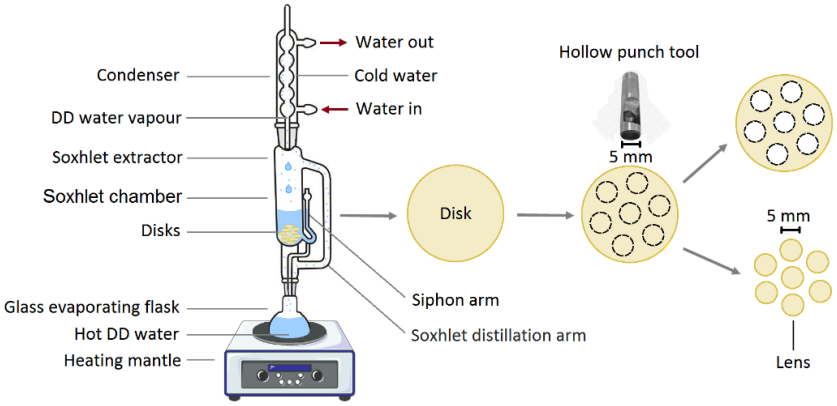

Figure 14. Schematic representation of a soxhlet extractor to wash lenses materials (disks) and lens cutting procedure.

III-1.3. Others

Staphylococcus aureus ATCC 25923, *Pseudomonas aeruginosa* ATCC 15442, *Escherichia coli* ATTC 10536, *Candida albicans* ATCC 10231 and *Aspergillus niger* ATCC 16404 were all obtained from American Type Culture Collection (ATCC) and *Staphylococcus epidermidis* CECT 231 (equivalent to ATCC 12228) from Colección Española de Cultivos Tipo (CECT). Blank antimicrobial susceptibility disks (Oxoid), Tryptone soya agar (TSA) (Oxoid) and Mueller-Hinton agar (Oxoid) were all purchased in Thermo Fisher Scientific. Orto-phosphoric acid (Technical grade) 85%, Calcium chloride and Sodium chloride 99.5% were obtain from Panreac. Methanol (HPLC grade) $\geq 99.8\%$ was obtained from Fisher Scientific and Acetonitrile (HPLC Plus gradient) $\geq 99.95\%$ from Carlo Erba Reagents. Triethylamine $\geq 99\%$, Potassium phosphate monobasic $\geq 99\%$, Potassium chloride $\geq 99\%$, Disodium hydrogen phosphate, Magnesium sulfate heptahydrate, Sodium bicarbonate and D-Mannitol $\geq 98.0\%$ were all purchased from Sigma-Aldrich. Distilled and deionized (DD) water was obtained using a Millipore Milli−Q water purification system.

III-2. Methods

III-2.1. Sterilization methods

In the present work two methods of sterilization were applied to drugs, ophthalmic lenses materials and drug loaded disks: SH and GR. The SH sterilization was accomplished in a vertical steam sterilizer, an UNICLAVE $88/75L$ from Laboratório de Engenharia Biomolecular e de Bioprocessos (LEBB) of IST. The parameters used for the SH sterilization were $60\ min$ at $121^{0}C$ and $1\ bar$. In some cases, drug loaded materials were also sterilized for $30\ min$ or $90\ min$. GR sterilization was done in Unidade Tecnológica de Radioesterilização (UTR) at Campus Tecnológico e Nuclear (CTN), from Instituto Superior Técnico (IST), using ^{60}Co as a source of gamma rays. GR was performed in atmospheric air at room temperature, using

three different doses: 5, 15 and 25 kGy. As the dosing rate was approximately 5 kGy/h, the time used for each dose was 1, 3 and 5 hours respectively. Depending on the studied propose, sometimes only one or two of the radiation doses were applied. Radiation doses were monitored with specific calibrated dosimeters (PMMA dosimeters - Red Perspex 4034) during all the process.

III-2.1.1. Sterilization of drugs

To prepare drug solutions two solvents were used, NaCl at 130 mM and Hank's balanced salt solution (HBSS) with a pH of 7.3 (buffer solution). NaCl constitutes more than 75% of the human blood plasma ion and was prepared by dissolution of 7.5972 g in 1 L of DD water [115]. HBSS is a buffer solution with ion concentrations nearly equal to those of human blood plasma and was prepared in 1 L of DD water by dissolving 8 g of NaCl, 0.4 g of potassium chloride, 0.0358 g of disodium hydrogen phosphate, 0.060 g of potassium phosphate monobasic, 0.144 g of calcium chloride, 0.246 g of magnesium sulfate heptahydrate and lastly 0.350 g of sodium bicarbonate, with a gentle stirring [116].

The drugs were sterilized in solution by SH (60 min) and by GR (5, 15 and 25 kGy), which concentrations are different depending on the studied propose. Drug solutions of DFN, KTL, MXF and a combination of MXF with KTL were prepared in NaCl solution with a [drug] of 2 mg/mL. For GR sterilization, solutions with 5% of mannitol and in powder were also tested. MXF solutions were prepared as well with a [drug] of 2 and 5 mg/mL and sterilized by SH (60 min). Additionally, MXF and VGMX solutions were prepared in HBSS solution with a [drug] of 5 mg/mL and sterilized by SH (30 min).

III-2.1.2. Sterilization of lenses materials

To evaluate the material proprieties, CLs and IOLs were sterilized by SH (60 min) and by GR (5, 15 or 25 kGy) in NaCl solution (henceforward, also called just NaCl or aqueous solution). IOLs were also sterilized by SH (60 min) and by GR (5 kGy) in drug solutions with a concentration of 2 mg/mL of DFN (only for SH), KTL, MXF or MXF+KTL.

III-2.2. Drug loading and drug release

For the drug loading/release assays disks were cut in 5 mm of diameter. Before the loading/release experiments all lenses materials were properly dried and their height was measured for further calculations. In all the experiments, loading was accomplished using drug soaking method, where disks were immersed in a drug solution for 4 days at a defined temperature. After drug incorporation, loaded disks were removed from the drug solution, rinsed with DD water and blotted with dry absorbent paper to remove the excess of drug on the surfaces. For the drug release experiments, carried out in static sink conditions, lenses materials were immersed in 3 mL of drug solvent solution (NaCl 130 mM or HBSS) and placed in a shaker (Incubating Mini Shaker from VWR), to mimic the eye conditions, at 36°C and 180 rpm. To determine the amount of drug release (methodology of quantification will be described hereinafter in section III-2.3.1), aliquots of a defined volume were collected and replaced with the same volume of fresh solvent solution. The aliquots were taken over time, until the plateau was reach, point at which no more

drug was released. All the release experiments were done at least in triplicate. Regarding the release studies, several conditions of loading, sterilization, storage and release were tested. Tables 4, 5, 6 and 7 summarizes all the conditions used throughout this investigation in the drug release assays.

Table 4. Summary of the experimental conditions (loading, sterilization and release) for the study of the effects of SH and GR sterilization on the release profiles of loaded CLs and IOLs materials.

Drug solution	Loading conditions (during 4 days)		Sterilization conditions				Release conditions (during 9 days)	
	C (mg/mL)	T (°C)	Method	Solution	Duration (min)	Moment	Periodicity of aliquots collection	Aliquot V (mL)
DFN	2	4	No sterilization				Between 1 to 8 hours of the 1st day of release: 1 / h. Between day 1 to 9 of release (days): 1; 2; 3; 4; 5,5; 7.	0.3
			SH	Drug sol.	60	*3rd day of loading **Before loading		
				Aq. sol.				
KTL			No sterilization					
			SH	Drug sol.	60	*3rd day of loading **Before loading		
				Aq. sol.				
			GR	Drug sol.				
				Aq. sol.				
MXF			No sterilization					
			SH	Drug sol.	60	*3rd day of loading **Before loading		
				Aq. sol.				
			GR	Drug sol.				
				Aq. sol.				
KTL (From MOX+KTL solution)			No sterilization					
			SH	Drug sol.	60	*3rd day of loading **Before loading		
				Aq. sol.				
			GR	Drug sol.				
				Aq. sol.				
MXF (From MOX+KTL solution)			No sterilization					
			SH	Drug sol.	60	*3rd day of loading **Before loading		
				Aq. sol.				
			GR	Drug sol.				
				Aq. sol.				

* For samples sterilized in drug solution. ** For samples sterilized in aqueous solution.

Table 5. Summary of the experimental conditions (loading, sterilization and release) for the studies of the effects of SH sterilization and loading temperature on the release profiles of loaded IOLs materials.

Drug solution	Loading conditions (during 4 days)		Sterilization conditions			Release conditions (during 103 days)	
	C (mg/mL)	T (°C)	Method	Duration (min)	Moment	Periodicity of aliquots collection	Aliquot V (mL)
MXF	2	4	No sterilization			Between 1 to 8 hours of the 1st day of release: 1 / h. Between day 1 to 13 of release (days): 1; 2; 3; 4; 5.5; 7; 9; 11; 13. Between day 13 to 103 of release: Every 5 days.	0.3
		36					
		60					
		80					
		4	SH	30	*3rd day of loading		
				60			
				90			
				60	*1st day of loading		
	5		No sterilization				
			SH	60	*3rd day of loading		

Table 6. Summary of the experimental conditions (loading and release) for the study of the effect of the release conditions and reversibility of the drug release profiles of loaded IOLs materials.

Drug solution	Loading conditions (during 4 days)		Release conditions (during 78 days)	
	C (mg/mL)	T (°C)	Periodicity of aliquots collection	Aliquot V (mL)
MXF	2	60	Between 1 to 8 hours of the 1st day of release: 1 / h. Between day 1 to 13 of release (days): 1; 2; 3; 4; 5.5; 7; 9; 11; 13. Between day 13 to 78 of release: Every 5 days.	0.3
			Between day 1 to 10 of release: 1 / day. Between day 10 to 78 of release: Every 2 days.	3 (total volume)
		4	Between 1 to 8 hours of the 1st day of release: 1 / h. Between day 1 to 13 of release (days): 1; 2; 3; 4; 5.5; 7; 9; 11; 13. Between day 13 to 78 of release: Every 5 days.	0.3

Table 7. Summary of the experimental conditions (loading, sterilization, storage and release) for the study of the effect of storage on the release profiles of loaded IOLs materials.

Drug solution	Loading conditions (during 4 days)		Sterilization conditions			Storage* (months)	Release conditions (during 103 days)	
	C (mg/mL)	T (°C)	Method	Duration (min)	Moment		Periodicity of aliquots collection	Aliquot V (mL)
MXF	5	60	No sterilization			No storage	Between 1 to 8 hours of the 1st day of release: 1 / h. Between day 1 to 13 of release (days): 1; 2; 3; 4; 5.5; 7; 9; 11; 13. Between day 13 to 103 of release: Every 5 days.	0.3
			SH	30	After loading	1		
						2		
						3		
		80	No sterilization			No storage		
			SH	30	After loading	3		
VGMX		60	No sterilization			No storage		
			SH	30	After loading	1		
						2		
						3		
		80	No sterilization			No storage		
			SH	30	After loading	3		

* At room temperature and protected from light.

III-2.3. Drugs analysis

III-2.3.1. Quantification of released drugs and determination of drugs degradation

The amount of drug released was determined with both, an UV−Vis spectrophotometer (Multiskan™ GO Microplate Spectrophotometer from Thermo Scientific) using several Microplates (UV−Star Microplates 96 wells, from Greiner Bio-One) and a HPLC (Waters Alliance 2695) incorporated with a Nova-Pak C18 RP column (60 Å, 4 µm, 3.9 mm × 150 mm) and a Photodiode Array (PDA) detector (Waters 2996). The data collected from the HPLC were processed with the Empower PDA Software (from Waters).

For both methodologies the concentration of the released drugs was determined based on the principles of Beer-Lambert law. This law defines the relationship between the concentration of the solution and the amount of light absorbed by the solution:

$$\mathrm{Abs} = \varepsilon \times \mathrm{d} \times \mathrm{C} \qquad \textbf{Equation 3}$$

where Abs is the absorbance, ε is the molar absorptivity ($\mathrm{L} \times \mathrm{mol}^{-1} \times \mathrm{cm}^{-1}$), C is the concentration of the drug in the solution ($\mathrm{mol} \times \mathrm{L}^{-1}$) and d is the optical path length. The absorbance of light is directly related to the number of molecules present in the solution (concentration) [55].

The drug quantifications were performed by reading the absorbance of each aliquot collected, selecting an appropriated wavelength for each drug ($276\ \mathrm{nm}$ for DFN, $315\ \mathrm{nm}$ for KTL and $290\ \mathrm{nm}$ for MXF and VGMX [117]–[122]). For each aliquot, at least, two measurements were done and for each drug, several calibration curves were produced during all the experiences and all the quantifications were made in the linear range of the calibration curves.

Apart from quantifying the released drugs, HPLC was also used to analyse the eventual degradation of the drugs after being submitted to the treatments, such as sterilization, heating or storage. For HPLC assays, two mobile phases were prepared considering the studied drug. The mobile phase for DFN was produced by using orto-phosphoric acid (at $0.05\ \mathrm{M}$), acetonitrile and methanol in the ratio of $40/48/12\ \mathrm{v/v/v}$, respectively, according to the method described by R. Shaalan and T. Belal [117]. The mobile phase for KTL, MXF, MXF+KTL and VGMX was prepared using phosphate buffer ($2.72\ \mathrm{g}$ of potassium phosphate monobasic per $1\ \mathrm{L}$ of DD water and $1\ \mathrm{mL}$ of triethylamine at pH 3.0 – adjusted with orto-phosphoric acid) and methanol in the ratio of $45/55\ \mathrm{v/v}$ respectively as described by M. Ashfaq and I. Mariam [119]. All mobile phases were introduced into the column at a flow rate of $1\ \mathrm{mL/min}$. The injection volume was $20\ \mu\mathrm{L}$, the monitoring by the detector was in the range of $210 - 395\ \mathrm{nm}$ and all the quantifications were run at $25 \pm 5^{\mathrm{o}}\mathrm{C}$.

To analyse the drugs degradation, DFN and KTL formulations were diluted in NaCl solution until reaching the concentration of $100\ \mu\mathrm{g/mL}$ (in section IV-1), MXF and MXF+KTL were diluted in NaCl solution (in section IV-1 and IV-2) until achieving the concentration of $35\ \mu\mathrm{g/mL}$ and MXF and VGMX were diluted in HBSS solution (in section IV-3) until the concentration of $35\ \mu\mathrm{g/mL}$. All samples were prepared, at least in triplicate, and for each sample two measurements were performed. The relative concentration of drug solutions was determined using the follow equation:

$$\%\ \text{Relative concentration} = \frac{[\mathrm{drug}]_{\text{after the experiments}}}{[\mathrm{drug}]_{\text{before the experiments}}} \mathrm{x}100 \qquad \textbf{Equation 4}$$

where the experiments refer to the procedures of sterilization, heating or storage.

III-2.3.2. Determination of MICs and drugs activity

The microbiological assays were performed in Instituto Superior de Ciências da Saúde Egas Moniz (ISCSEM).

The antimicrobial agents used were MXF, MXF+KTL and VGMX against two strains of gram-positive bacteria: *Staphylococcus aureus* (SA) and *Staphylococcus epidermidis* (SE). Before starting the microbiological assays, both strains were previously cultured in TSA medium for $24\ \mathrm{h}$ at $37 \pm 2\ ^{\mathrm{o}}\mathrm{C}$.

The agar diffusion method was used to determine the activity of the studied drugs and the agar dilution method was used to determine the MIC values and the calibration curves necessary to estimate the drugs concentration. In the latter case, drug solutions were prepared with the concentrations of 0.25, 0.5, 1, 2, 4, 8, 16 and $32\ \mu g/mL$. For both proposals of study, all the inoculated mediums were prepared in quadrangular petri plates ($120 \times 120\ mm$) by adding $350\ \mu L$ of the bacterial suspension (with a concentration of 0.5 McFarland in DD water) and $50\ mL$ of MH agar ($38\ g$ of MH agar / $1\ L$ of DD water), previously sterilized by SH at 121^0C for $15\ min$ and kept in a water bath at 50^0C until stabilize the temperature. Filter paper discs with $6\ mm$ diameter were placed on the agar plates with $15\ \mu L$ of each sample solution and, at least, one negative control per plate ($15\ \mu L$ of a sterilized solvent solution). Then, all petri plates were turned upside down and incubated for $24\ h$ at $37 \pm 2\ ^oC$. After the incubation period, the inhibition halos were measured (in mm) using a digital calliper ($0 - 150mm/0.01mm \pm 0.02$).

To determine the [drug] of sample solutions in agar diffusion method, for each drug and microorganism, the values obtained from the inhibition halos (H) of the calibration curves in the agar dilution method, were plotted as $Log(C)$ vs H (because microbial activity does not growth linearly with the concentration of an antimicrobial agent), and by adding a tendency line, m and b were determined, since the linear equation was given in the form of:

$$Log_{10}(C) = m \times H + b \qquad \textbf{Equation 5}$$

Then, for a given m and b (in each bacteria and for each drug) the concentration (C) from the tested samples was predicted, using the halos of inhibition obtained in agar diffusion method.

The antimicrobial activity (%) was determined in to different ways. To evaluate the activity of drugs after the sterilization procedures, MXF and MXF+KTL solutions were prepared with a concentration of $10\ \mu g/mL$ for all the experimental conditions. Therefore, the activity, before and after sterilization, was determined by the following expression:

$$\%\ \text{Antimicrobial activity} = \frac{[drug]_{\text{after sterilization}}}{[drug]_{\text{before sterilization}}} x100 \qquad \textbf{Equation 6}$$

where both [drug] were obtained by applying Equation 5. These microbiological assays were done at least three times in duplicate.

To determine the activity of the released drugs (MXF and VGMX from day 3 and 7 of release), the total concentration of the release solution was previously quantified by HPLC. Then, the activity was determined with the following expression:

$$\%\ \text{Antimicrobial activity} = \frac{[drug]_{\text{determined by microbiological assay}}}{[drug]_{\text{determined by HPLC}}} x100 \qquad \textbf{Equation 7}$$

where only the $[drug]_{\text{determined by microbiological assay}}$ was obtained from Equation 5. These microbiological assays were accomplished only once in duplicate.

III-2.3.3. Sterility tests

The sterility tests were provided by Laboratório de Microbiologia Aplicada Egas Moniz (LMAEM), from ISCSEM.

The membrane filtration technique was chosen to verify the sterility of drug solutions. Sterilized drug solutions by SH ($15\ \mathrm{mL}$ of DFN, KTL, MXF and MXF+KTL) and by GR (5kGy) ($15\ \mathrm{mL}$ of KTL, MXF and MXF+KTL) were totally filtered through a sterile membrane ($0{,}45 - \mathrm{micron}$). The membrane was aseptically divided and placed in two culture media, FTM and TSB, and both were incubated for $30^{\circ}\mathrm{C}$ and $25^{\circ}\mathrm{C}$, respectively, for 14 days. Positive controls and negative controls were also prepared and incubated together with the testing samples. The positive controls consist in 4 infected membranes (2 per medium) by the passage of $15\ \mathrm{mL}$ of suspensions (1 per membrane) previously prepared with sterilized DD water and 4 different microorganisms at 10^3 (qualitatively). The microorganisms used as positive controls for FTM medium were *Pseudomonas aeruginosa* and *Escherichia coli* and for TSB medium were *Candida albicans* and *Aspergillus niger.* The negative controls consist in 2 membranes (1 per medium) used to filter $15\ \mathrm{mL}$ of sterilized DD water. After the incubation period, cultures were analysed in terms of turbidity.

III-2.3. Materials characterization

III-2.3.1. Transmittance

Optical clarity studies were carried out by measuring the absorbance of visible light through samples (disks cut in a half) in their hydrated state. The study was performed for both types of materials that were sterilized in NaCl solution, and also for loaded samples sterilized in drug solution with a concentration of $2\ \mathrm{mg/mL}$. The absorbance was measured in the wavelength range of $200 \leq \lambda(\mathrm{nm}) < 760$ (for non-loaded lenses) and $360 \leq \lambda(\mathrm{nm}) < 760$ (for loaded lenses) and at room temperature, using a quartz cuvette ($\mathrm{Cap} = 3.5\ \mathrm{ml},\ \mathrm{d} = 10\ \mathrm{mm}$, from LABBOX) and an UV−Vis spectrometer (Multiskan™ GO Microplate Spectrophotometer, from Thermo Scientific). Before the measurements, zeroing was defined with an empty cuvette, then disks were properly blotted with cleanroom paper (from VWR) and placed on the lateral surface of the cuvette, covering the entire area of the optical path. For each type of lens material and experimental condition, the procedure was held, at least once, using both sides of each sample and in three different regions, with a total of 6 measurements per sample. The percentage of transmittance was calculated using the follow relation:

$$\%\mathrm{T} = 10^{-\mathrm{Abs}} \times 100 \qquad \textbf{Equation 8}$$

where T is the transmittance and Abs is the absorbance [54], [55].

III-2.3.2. Swelling kinetics

Both materials were cut in small lenses with 5 mm of diameter to performed the selling assays. The swelling kinetics was determined in water and, in some cases, in MXF solution ($2\ \mathrm{mg/mL}$), at different temperatures. Lenses materials were firstly dried and their dry weigh was measured. Then, each disk was immersed in $1\ \mathrm{mL}$ of DD water or MXF solution at $2\ \mathrm{mg/mL}$ and incubated at the respective temperature. During the assays sample disks were taken out of the solution, gently blotted with absorbent paper and weighed, until achieving the equilibrium. The procedure was done at 2, 4, 6,

9, 24 and 48 hours. The swelling ratio, $\%\mathrm{SR}$, and the equilibrium water content, $\%\mathrm{EWC}$, were estimated, respectively, using the following expressions:

$$\%\mathrm{SR} = \frac{W_t - W_0}{W_0} \times 100 \qquad \textbf{Equation 9}$$

$$\%\mathrm{EWC} = \frac{W_\infty - W_0}{W_\infty} \times 100 \qquad \textbf{Equation 10}$$

where W_t is the weight of the swollen hydrogel at time t, W_∞ is the weight of the swollen hydrogel at the equilibrium and W_0 is the weight of the dry hydrogel [123], [124].

III-2.3.3. Wettability

For the wettability studies, the water contact angle was measured using the captive bubble method at room temperature in disks cut in a half. CLs and IOLs materials, non-sterilized and sterilized in NaCl solution, were previously hydrated in DD water for $24\ \mathrm{h}$ and then fixed to a porcelain support and placed downwards inside a liquid cell (with quartz windows), which was full of DD water. Then, with an inverted needle from a micrometric syringe, an air bubble of approximately $3 - 6\ \mu\mathrm{L}$ was placed on the lens surface. For each type of lens, at least 13 bubbles in both sides of a lens were monitored for 1 minute, being recorded 14 images along the time, for each bubble. A video camera (JAI CV-A50) connected to a microscope (Wild M3Z) was used to acquire the images and the video signal was transmitted to a frame grabber (Data Translation DT3155).

The image analysis was performed with ADSA-P software (Axisymmetric Drop Shape Analysis Profile) which uses Laplace's capillarity equation, that relates the surface tension of the liquid with the profile of the bubble, and is given by the follow equation:

$$\Delta P = \gamma_{LV} \times \left(\frac{1}{R_1} + \frac{1}{R_2}\right) \qquad \textbf{Equation 11}$$

where ΔP represents the difference of pressure in the interface gas/liquid, γ_{LV} is the surface tension of the liquid and R_1 and R_2 are the two curvature radius of the bubble, which are then related with the contact angle by geometrical relations [125] .

III-2.3.4. Ion permeability

The ion permeability of the lenses materials was measured using a PMMA horizontal diffusion cell with two compartments, the donor and receiver chambers. The samples (entire disks) fully hydrated in DD water were mounted between the two compartments. The donor chamber was filled with $24\ \mathrm{mL}$ of NaCl solution and the receiver chamber with $32\ \mathrm{mL}$ of DD water. After a suitable calibration, the conductivity was measured at each hour for at least sixteen hours using a conductivity measuring cell (TetraCon 325 from WTW, with 4 graphite electrodes and a temperature sensor) inserted in the receiver chamber and connected to a conductivity meter (Cond 340i from WTW) to set the measurements and record the values. Two calibration curves were prepared to convert conductivity data (in $\mu\mathrm{S/cm}$) into NaCl concentrations (in $\mu\mathrm{g/mL}$). One, with a higher range, to process data obtained from CLs materials

(14 points with concentrations in the range of 6.25 and 500 μg/mL) and another one, with a smaller range, to process data collected from IOLs materials (12 points with concentrations between 0.32 and 22.6 μg/mL). The NaCl concentrations were then plotted as a function of time and the rate of ion transport (F) was given from the slope of the linear regression. The ion permeability was then calculated applying the Fick's law (Equation 12).

$$\frac{F \times V_r}{A} = D_{ion} \times \frac{dC}{dx} \qquad \textbf{Equation 12}$$

Where F is the rate of ion transport, V_r is the volume of the solution in the receiving chamber, A is the area of the lens and $\frac{dC}{dx}$ is the initial concentration gradient of NaCl that across the hydrogel with a defined thickness, dx [60]. The experiments were done at 36°C and in triplicate. Note that the ion diffusion occurred under electroneutrality conditions, thus the diffusivity was a combination of diffusivities of sodium ions (D_{Na^+}) and chloride ions (D_{Cl^-}) [69], [70].

III-2.3.5. Morphology

The morphology of the samples was observed in the MicroLab – Electron Microscopy Laboratory of IST.

To access the surface morphology, disks of CLs and IOLs materials (5 mm of diameter) were previously hydrated in DD water for 24h, carefully cleaned with an absorbent paper and then placed in a −80°C freezer for 3 h and lyophilized overnight. Then, the samples were coated with a 15 nm layer of Cr by sputtering, using a turbo-pumped sputter coater (Q150T ES, from Quorum Technologies) and analysed in vacuum conditions with a Field Emission Gun-Scanning Electron Microscope (FEG−SEM) (JEOL JSM−7001F model, from JEOL).

III-2.3.6. Thermotropic behaviour

Thermotropic behaviour assays were performed with a differential scanning calorimeter (DSC) (200 F3 Maia model, from NETZSCH). After a suitable calibration, the measurements were run under a nitrogen atmosphere. The Proteus Software was used to acquire data and evaluate the results.

IOLs materials (3 mm of diameter) were characterized both unloaded and loaded with [MXF] 2mg/mL at 4°C and 60°C. For each experimental condition, three DSC runs were taken, one per sample, to determine the average T_g value. Before the experiments, the samples were taken out of DD water or the loading solution, properly cleaned and dried in a vacuum oven at 36°C for 7 days to remove as much as possible the free and loosely bound water. Then, samples were weighted before and after being placed inside a concavus pan (Al crucible with a lid – Ø: 5 mm, C = 30/40 μl – from NETZSCH), sealed with a sealing press (from NETZSCH) and placed together with an empty sealed reference pan in the heating block of the equipment. The DSC thermograms were recorded during two successive heating cycles using the following experimental conditions: (i) isothermal scan for 10 min at 20°C; (ii) heating scan from 20 to 140°C (10°C/min); (iii) isothermal scan for 10 min at 140°C; (iv) cooling scan from 140 to 20°C (10°C/min). (v) isothermal scan for 10 min at 20°C; (vi) and, finally, a heating scan from 20 to

$140^{o}C$ ($10^{o}C/min$). After processing the data, the glass transition temperatures were considered as the midpoints of the steps in the baseline.

III-2.3.7. Structural proprieties

ssNMR experiments for structural characterization were carried out at Centro de Química Estrutural of IST by Dr. Teresa G. Nunes

Powdered samples of MXF ($\sim 200\ mg$) or swollen IOLs materials (8 discs of $5\ mm$ diameter per experiment) were packed into a cylindrical zirconia rotor (Ø: $7\ mm$; L: $18\ mm$). Before the experiments, the IOLs materials were hydrated in saline solution or loaded with MFX in different experimental conditions (different times, temperatures and solution concentrations) were rinsed and cleaned properly with absorbent paper to remove the excess of solution from their surfaces. ^{13}C CP/MAS – TOSS spectra without and with $30\ \mu s$ of Dipolar dephasing ($\overline{DD}$) were obtained at $75.49\ MHz$ on a Tecmag (Redstone)/Bruker 300 WB spectrometer, at a MAS rate of $3.3 - 3.7\ kHz$ with 90^{o} RF pulses of about $4{,}5\ \mu s$, contact time of $2\ ms$ and a relaxation delay of $10\ s$. ^{13}C CP/MAS spectra with suppression of ^{13}C non-quaternary signals were achieved by interrupting proton decoupling during $30\ \mu s$ before the acquisition period. ^{13}C chemical shifts were referenced with respect to an external glycine sample (^{13}CO observed at $176.03\ ppm$). The number of scans accumulated for each spectrum was: 1008 and 8480 for MXF without and with $\overline{DD}$ respectively; more than 7000 for the IOLs materials loaded with MXF solution; and 1256 for swelled IOLs materials in NaCl solution.

As a first move towards peaks identification, it was used a program available at http://www.nmrdb.org/simulator [126] which is based on an algorithm that only considers intramolecular interactions. Then, available chemical shift tables were used for the identification of almost all peaks.

III-2.3.8. Sterility tests

The sterility tests were provided by LMAEM, from ISCSEM.

The direct inoculation method was chosen to verify the sterility of lenses materials. Both types of lenses materials (with $5\ mm$ of diameter) were sterilized by SH and by GR ($5\ kGy$) in NaCl solution, and then placed directly in two culture media (FTM and TSB) where they were incubated, respectively, at $30^{o}C$ and $25^{o}C$ for 14 days. Positive controls and negative controls were also prepared and incubated together with the testing samples. The positive controls consist in four inoculated culture mediums (1 per microorganism) with microorganism's suspensions of 10^{3} (qualitatively): two FTM inoculated with *Pseudomonas aeruginosa* and *Escherichia coli*; and two TSB inoculated with *Candida albicans* and *Aspergillus niger*. The negative controls consist in two non-inoculated culture media, one of FTM and another of TSB. After the incubation period, cultures were analysed in terms of turbidity.

IV. RESULTS AND DISCUSSION

IV-1. Effects of sterilization

This section aims to contribute for the clarification of the effects of two different methods of sterilization, SH and GR, on several ophthalmic drugs, on two polymeric materials currently used for the production of ophthalmic lenses and on drug loaded lenses including changes on the intrinsic properties of the materials and on the drug release behaviour.

IV-1.1. Effects of sterilization on drugs

The ophthalmic drugs used in the present section (DFN, KTL, MXF and MXF+KTL) were sterilized by SH in aqueous solution and by GR with three different doses, 5, 15 and 25 kGy. For each dose of radiation, samples were sterilized in different forms of preparation, in aqueous solution with and without mannitol and in powder.

IV-1.1.1. Quantification of drugs degradation

To evaluate the degradation of the studied drugs, as a consequence of having undergone sterilization, HPLC was used to analyse the samples before and after the sterilization. The quantification of drugs degradation is presented in Figure 15 and Figure 16 as the relative concentration (%) calculated with Equation 4.

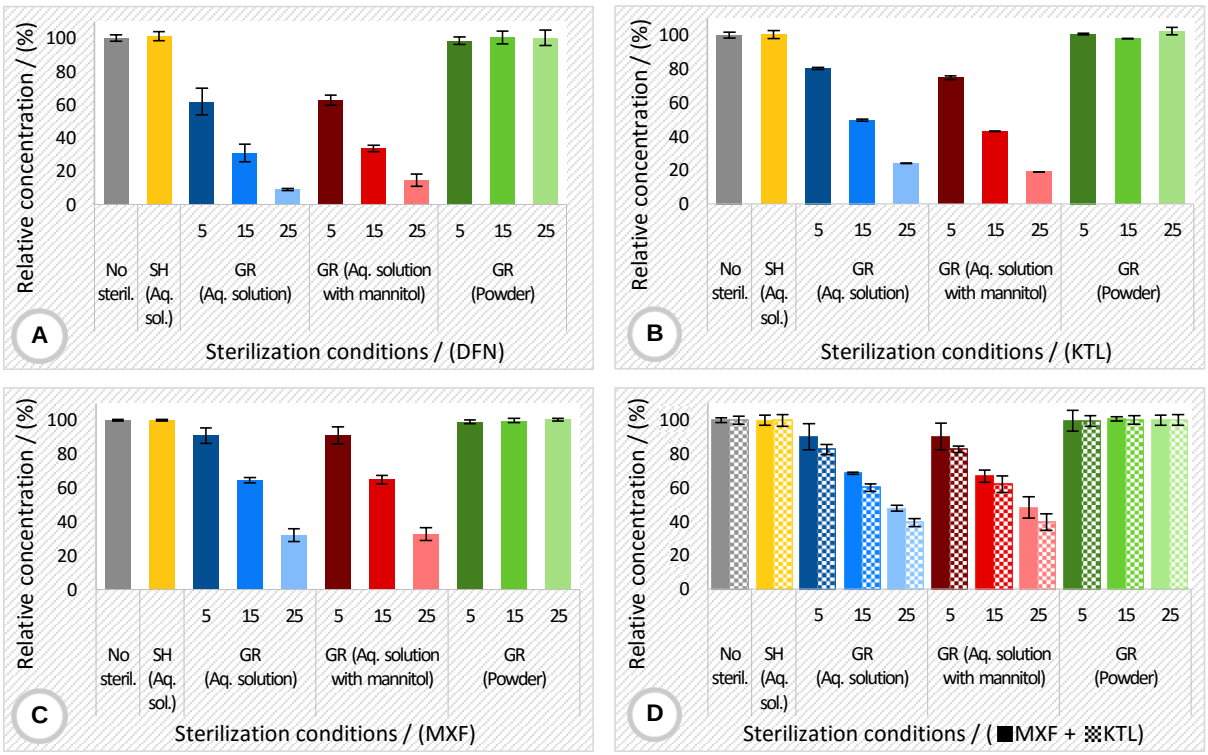

Figure 15. Relative concentration (%) of DFN (A), KTL (B), MXF (C) and MXF+KTL (D) determined by HPLC, for all experimental sterilization conditions. The error bars correspond to ± SD.

Figure 16 compares the effect of sterilization on MXF and KTL preparations when sterilized separately or combined in MXF+KTL.

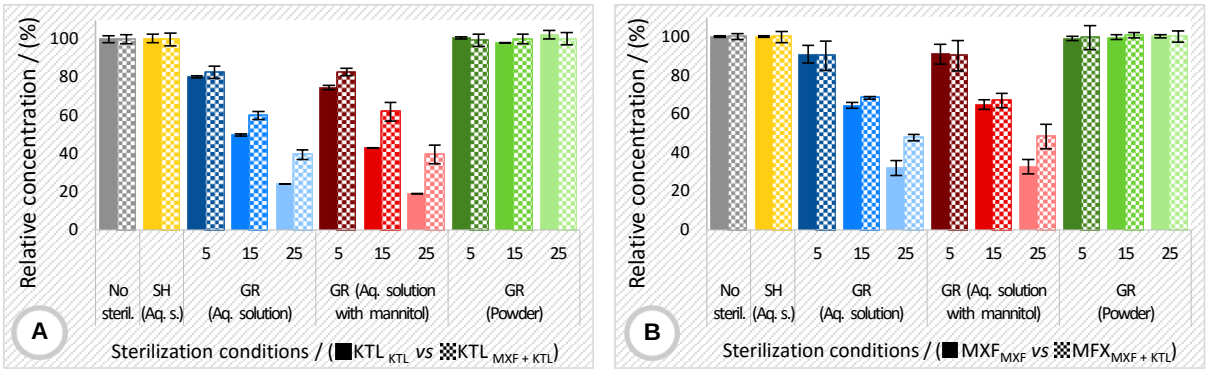

Figure 16. Relative concentration (%) of MXF and KTL, when sterilized together or separately, determined by HPLC, for all experimental sterilization conditions. (A) – Comparison of the relative concentration (%) of KTL when sterilized alone or mixed with MXF. (B) – Comparison of the relative concentration (%) of MXF when sterilized alone or mixed with KTL. The error bars correspond to ± SD.

Figure 15 shows that sterilization produces different effects depending on the method and on the preparation form of the drugs. For all studied drugs there was no degradation when they were sterilized by SH (in solution) or with 5, 15 or 25 kGy of GR (in powder). However, all drugs degraded with higher doses of GR (15 and 25 kGy) when they were sterilized in solution. Nonetheless, when sterilized with 5 kGy of GR in solution, there was a minimal degradation of MXF and MXF+KTL (less than 10% for both) and some degradation of KTL and DFN, being DFN the most affected (approximately 20% and 38% of degradation, for both respectively). Generally, anti-inflammatories were more degraded by GR than antibiotics, when in solution. For all drugs, it seems also mannitol had no visible effect on the drug degradation prevention as was previous reported by literature [96], [127].

In Annexes I, II, III and IV in Figures A1, A3, A5 and A7, the corresponding HPLC chromatograms for each drug and experimental conditions are available. In each chromatogram the non-sterilized solution was compared with all sterilized preparations. The chromatograms show the degradation peaks resulting from GR sterilization of the drugs in solution with an intensification of the absorbance (increase in the concentration) of the degradation peaks (unknown formed radiolytic compounds) with the increase of the radiation dose.

The results in Figure 16 demonstrate that KTL and MXF are better resistant to GR when combined, especially for higher doses of GR; for example, at 25 kGy, degradation of both drugs was reduced in more than 15% when the drugs were sterilized together. This was probably due to the fact that MXF+KTL solution was prepared with 2 mg/mL of each drug, meaning that the final solution was more concentrated. Thus, considering that the irradiated volume was constant, which means same number of water molecules, the ratio between the number of radicals formed (related to the number of water molecules) and the number of drug molecules in each preparation was definitely higher when solutions where separated, with less drug molecules competing during radiolysis, so the proportion of particles affected was clearly higher. This suggests that GR in super saturated solutions may be a viable

option when drugs need to be sterilized in the solution form. In fact, some studies already report a decrease in degradation with the increase of the concentration of the solutions [128].

It was mentioned before, in literature, that many pharmaceuticals are more stable to GR in the dry state than in aqueous form which is consistent with these results. Actually, minimal degradation (<1%) of several antibiotics has been reported, when irradiated in the solid form [95]. Radiolysis species produced by radiation can react with the active ingredients or other excipients, causing decomposition [129]. Reducing the temperature of irradiation (cryo-irradiation) and/or minimizing water content in the samples may be also better option to limited the activity of the free radicals and reduce the degradation of the drugs [95], [130].

The most common form of sterilization of the studied drugs is SH applied to aqueous solutions [131]–[133]. GR has been more used in formulated systems which incorporate the drugs. In agreement with the present results, DFN solution was already reported as highly degradable by GR, however other studies have presented different results [128]. A. Özer et al., investigated the effect of GR on DFN loaded liposomes–niosomes and lipogelosomes–niogelosomes to treat rheumatoid arthritis and concluded that sterilization with GR at $25\ \mathrm{kGy}$ did not affect the efficacy of the treatment [134]. Other study [132] showed the presence of an impurity in some brands of a commercial DFN injection, terminally sterilized by SH, which is not in agreement with the obtained results. This study also revealed that the formation of the impurity depended on the initial pH of the formulation (less degradation for formulations with a higher pH). In fact, in the present work, the pH of the formulations was not controlled. S. Mathew, et al., loaded albumin microspheres with KTL and proved they were stable after GR. K. G. Parthiban et al., presented a study of a pH-triggered in situ gelling system for sustained delivery of KTL, sterilized by SH, with no adverse effects on the formulation [135]. B. Singh, et al. studied the effect of GR in two fluoroquinolones (norfloxacin and gatifloxacinin) in their solid state, irradiated with 25 and $100\ \mathrm{kGy}$, and presented degradation rates for irradiated samples with $25\ \mathrm{kGy}$ of less than 1% for norfloxacin, 2% for gatifloxacinin, and less than 3% for both drugs irradiated with $100\ \mathrm{kGy}$ [136]. P. Pawar et al. presented an ocular insert containing an aqueous dispersion of MXF and other components, sterilized by GR, that proved to be effective and safe in the *in vivo* drug release studies performed in albino rabbits [137]. These studies confirmed that, at least, antibiotics in the solid form resist very well to GR.

Summing up, the preferable sterilization methods for the studied drugs were SH followed by $5\ \mathrm{kGy}$ of GR (only for antibiotics) when drugs were in solution, without mannitol, and GR, at all doses, for drugs in the powder form.

IV-1.1.2. Determination of drugs activity

To evaluate the stability of the MXF and MXF+KTL after sterilization, microbiological assays were performed using the agar diffusion method, in order to evaluate their activity. Both pharmaceuticals were tested against two strains of bacteria, SA and SE, and for each assay two plates were used. Figure 17 displays a photograph as an example of one of the assays with the distribution of the discs over the plates used in the determination of the antimicrobial activity and Figure 18 presents the respective results of the activity for both drugs and strains determined using Equation 6.

Figure 17. Antimicrobial activity of MXF against SA. Numbers correspond to the sterilization conditions of drug solutions: [1] – No sterilization; [2] – SH; [3, 4 and 5] – 5, 15, and 25 kGy of GR (aq. solution with mannitol) respectively; [6, 7 and 8] – 5, 15, 25 kGy of GR (aq. solution) respectively; [9, 10 and 11] – 5, 15, 25 kGy of GR (powder) respectively; Letters correspond to negative controls: [a_1 and a_2] – Sterilized aqueous solution (drug solvent used in conditions 1, 2 and 7 to 11); [b] – Sterilized aqueous solution with mannitol (drug solvent used in conditions 3 to 5).

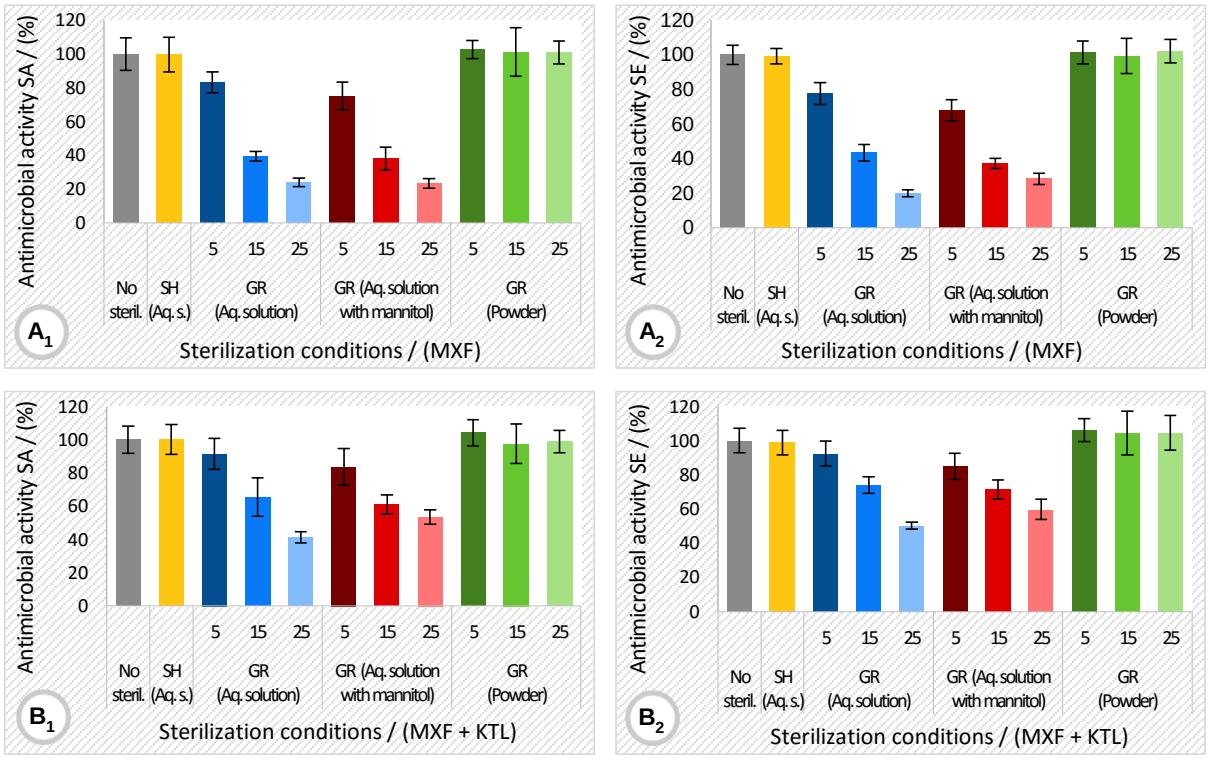

Figure 18. Antimicrobial activity (%) of MXF, against SA (A_1) and SE (A_2), and for MXF+KTL versus SA (B_1) and SE (B_2), for all experimental sterilization conditions. The error bars correspond to ± SD.

As expected, GR seems to have a deleterious effect on the activity of these drugs when they are in solution. The results are consistent with the ones obtained by HPLC and once again, for both strains, SH sterilization of solutions and GR sterilization of powders did not affect the drugs activity, and the increase in the radiation dose led to a decrease in the activity of drug solutions. More, mannitol did not prevent the activity losses and the activity of irradiated antibiotics in solution was higher for the combination MXF+KTL than for MXF, in both strains. For these reasons, the best sterilization methods

proposed before for the antibiotics continue to be SH followed by GR (5 kGy) for solutions without mannitol, and GR, at all doses, for powders.

At this stage, owing to degradation by GR in solution, the three radiation doses were abandoned for DFN in solution and the two higher doses, 15 and 25 kGy were abandoned for the other drugs in solution. Moreover, mannitol was discarded.

IV-1.1.3. MIC determination

For the MIC determination it was used the agar dilution method. Figure 19 shows a photograph as an example of one of the assays with the distribution of the samples over the plate and Table 8 summarizes the values of MIC, obtained for each drug and each bacterial strain.

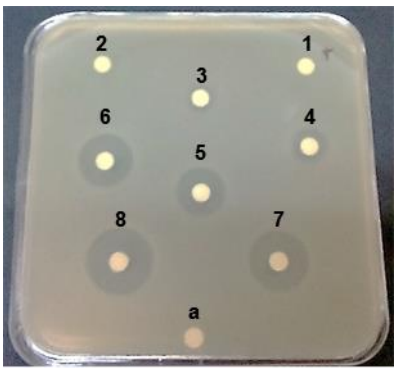

Figure 19. MIC determination of VGMX by agar dilution on SA. Numbers correspond to VGMX solutions with different concentrations: [1 to 9] – $0.25, 0.5, 1, 2, 4, 8, 16$ and 32 μg/mL respectively. [a] – Negative control: sterilized aqueous solution (drug solvent).

Table 8. MIC ranges determined experimentally and found in literature.

Bacteria	Data source	MIC (μg/mL)	
		MXF or VGMX	MXF+KTL
SA	Literature	0.06 – 2 [138]–[141]	2 [142]
SE		0.24 – 2 [138], [140], [141], [143]	
SA	Experimental	0.5 – 1	
SE			

Although VIGMX was not studied in this section, it was introduced here since it is the commercial form of MXF. From the values obtained experimentally the MICs were in the range of $0.5 - 1$ μg/mL for both strains of bacteria and all formulations, and are consistent with the values reported in literature. The differences between reported values of MICs are very common, because several factors such as, concentration of nutrients and agar, temperature, humidity, pH and colony density, influence the growth of bacterial colonies [144]. According to the experimental results, a minimal concentration of 1 μg/mL is recommended for an efficient treatment against these bacteria strains.

IV-1.1.4. Sterility tests

To determine the efficiency of the sterilization methods, the membrane filtration technique was used and the obtained results are presented in Table 9.

Table 9. Sterility test results of sterilized drug solutions by SH and with $5\ \mathrm{kGy}$ of GR.

Drugs	Sterilization conditions	
	SH	GR ($5\ \mathrm{kGy}$)
DFN	Sterile	-
KTL	Sterile	Sterile
MXF	Sterile	Non sterile
MXF+KTL	Sterile	Non sterile

As expected, since SH is a FDA approved methodology (that ensures a SAL of 10^{-6}) [85], all solutions were efficiently sterilized by this method. Concerning GR, only KTL was sterile. MXF and MXF+KTL present some bacterial growth, meaning that $5\ \mathrm{kGy}$ was not sufficient to sterilize the $15\ \mathrm{mL}$ of drug solution (the minimum required volume to preformed the test). This suggests GR by itself, at this dose, is not enough to sterilized this volumes of drug, however if combined with an aseptic process may be capable of achieving the desirable SAL of sterility. In this work, considering the planed volume of $0.5 - 1\ \mathrm{mL}$ to be used during drug loading assays, this result was not taken in consideration because the tested volume was 15 to 30 times more than the volume planned to be used during loadings. This characterises the worst of the scenarios and is not representative of the experimental one. For this reason, further tests are suggested to ensure if $5\ \mathrm{kGy}$ will be or not effective sterilizing smaller volumes of drug solutions.

IV-1.2. Effects of sterilization on lenses materials

To evaluate the effect of the sterilization on the IOLs and CLs materials which have been approved for the production of commercial lenses, several properties were studied, namely transmittance, swelling, wettability, ion permeability and morphology. In all studies non-sterilized lenses were always compared to the sterilized ones (in aqueous solution). Finally, the results of the sterility tests are presented.

IV-1.2.1. Transmittance

The transmittance was measured for both lenses in all the sterilization conditions in the wavelength range of $200 \leq \lambda\,(\mathrm{nm}) < 760$. This range was chosen due to the fact the IOLs material (B26Y) has a covalently incorporated UV−A blocking and a violet light filtering chromophore that helps to filtrate the harmful energetic UV−A light between $315 \leq \lambda\,(\mathrm{nm}) < 400$ and part of the violet light between $360 \leq \lambda\,(\mathrm{nm}) < 450$ [45]. The control lens material was hydrated in DD water and was not sterilized. The other samples were hydrated and sterilized in aqueous solution. The spectra obtained for both lenses are illustrated in Figure 20.

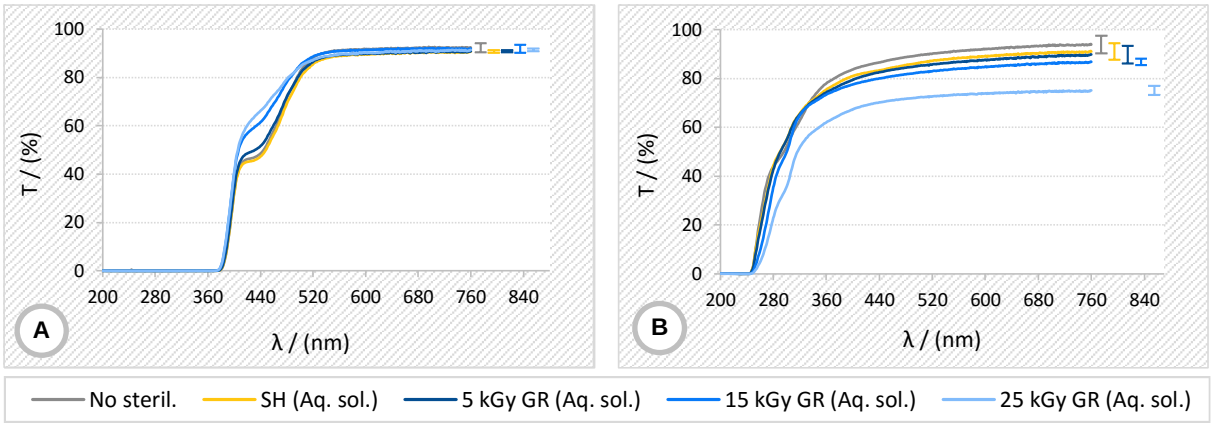

Figure 20. Transmittance (%) of ophthalmic lenses materials, non-sterilized and sterilized in aqueous solution in different sterilization conditions: (A) – B26Y; (B) – CFL58. The error bars correspond to ± mean SD of measurements obtained in range of $\lambda \in [200, 759]$.

The results obtained for B26Y did not present differences in the visible range, however between $400 - 500$ nm, the increase in the radiation dose leads to an increase in %T. In fact, in this range it seems to have occurred a partial degradation of the violet light filtering chromophore. Concerning CFL58, the increase in the radiation dose leads to a decrease in %T, placing the material sterilized with 15 and 25 kGy of GR below 90%, the threshold established for an appropriate optical transmissibility of visible light in a CL [54]. SH seems to be more appropriate for the sterilization of both materials, but GR with 5 kGy may be used. Furthermore, considering that B26Y is also commercialized without the UV–filter, GR may be too a suitable option for the sterilization of this material.

IV-1.2.2. Swelling kinetics

To characterize the water sorption of both materials, after being submitted to the sterilization procedures, the swelling profiles and EWC were determined in DD water at two temperatures (4 and 36ºC). The temperatures choice was based on the temperatures used in drug loading/release experiments, respectively 4 and 36ºC. Before the assay, all samples were properly dried for 7 days at 36ºC. %SR and %EWC are represented for B26Y in Figure 21 and Figure 22, and for CFL58 in Figure 23 and Figure 24, respectively.

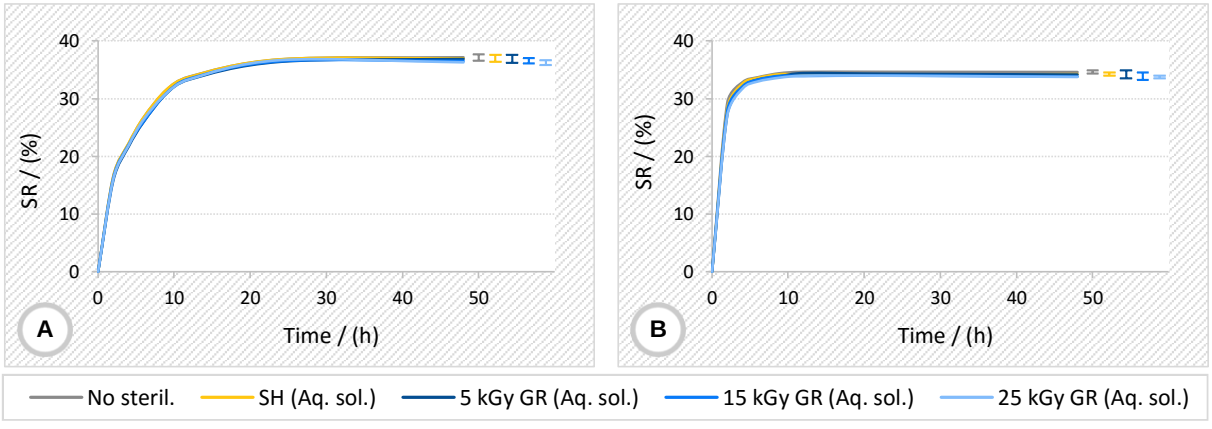

Figure 21. Swelling profiles (%) of B26Y, non-sterilized and sterilized in aqueous solution, in different sterilization conditions: (A) – at 4ºC; (B) – and at 36ºC. The error bars correspond to ± mean SD.

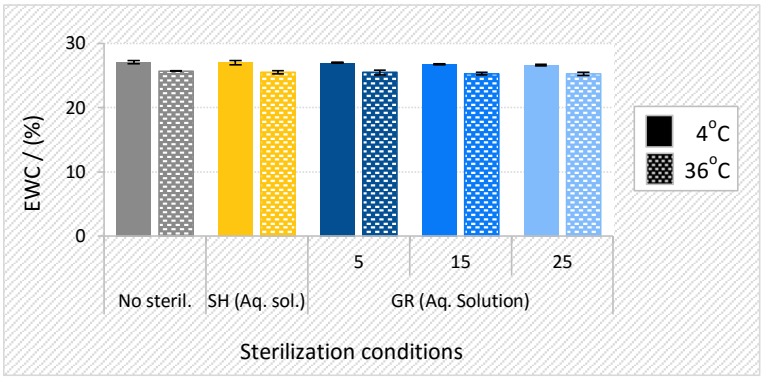

Figure 22. Equilibrium water content (%) of B26Y at $4^{o}C$ and $36^{o}C$, non-sterilized and sterilized in aqueous solution, in different sterilization conditions. The error bars correspond to $\pm$ SD.

The sterilization did not affect the swelling behaviour of B26Y, but curiously the swelling profiles demonstrate that the water uptake was faster at high temperatures and the EWC was slightly higher at low temperatures.

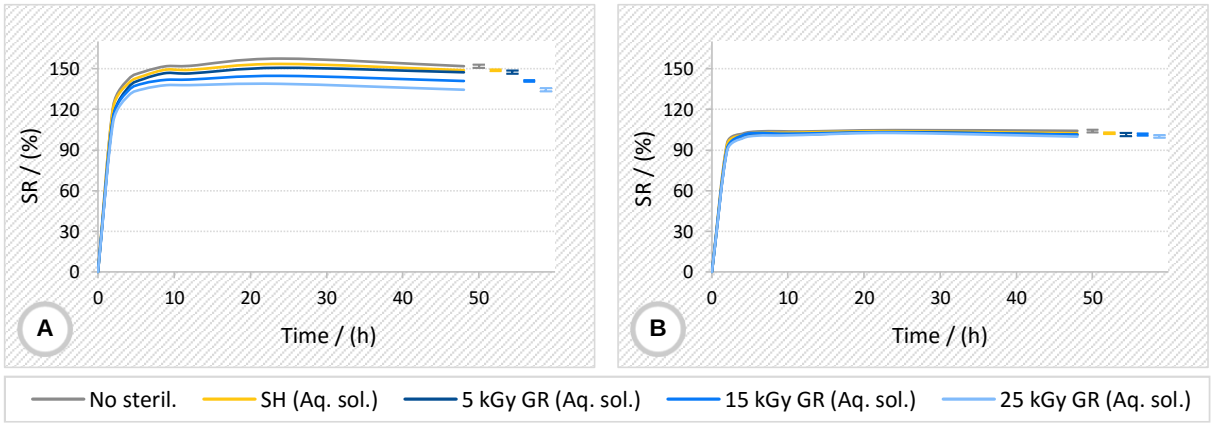

Figure 23. Swelling profiles (%) of CFL58, non-sterilized and sterilized in aqueous solution, in different sterilization conditions: (A) – at $4^{o}C$; (B) – and at $36^{o}C$. The error bars correspond to $\pm$ mean SD.

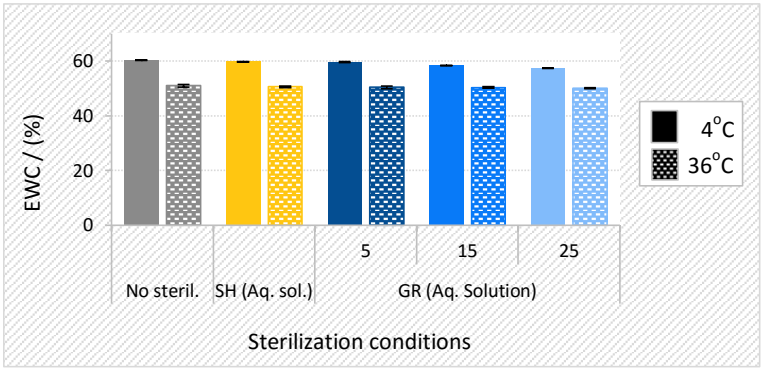

Figure 24. Equilibrium water content (%) of CFL58 at $4^{o}C$ and $36^{o}C$, non-sterilized and sterilized in aqueous solution, in different sterilization conditions. The error bars correspond to $\pm$ SD.

For CFL58 sterilization, GR affects the swelling behaviour decreasing the EWC with the increase of the radiation dose. Perhaps, gamma ray promotes a certain degree of crosslinking in the polymer

network, tightening the matrix. Once again the swelling profiles show that the water uptake was faster at $36^{o}C$ and the EWC increased at $4^{o}C$.

The absorption process involves the diffusion of water molecules into the free spaces, increasing the segmental mobility and leading to expansion of the chain segments between crosslinks, resulting in swelling [123]. A lot of factors influence the dynamics of the water sorption process, among them are the retraction force of elasticity, osmotic pressure, electrostatic charge, hydrophilic and hydrophobic interactions, nature and concentration of the crosslinker in the hydrogel or the presence of a physical or chemical stimuli (stimuli-sensitive hydrogels) [12], [56]–[59], [61], [62], [95], [123]. S. Cai and Z. Suo reported that, usually, temperature-sensitive hydrogels, absorb a large amount of water at low temperatures and become swollen, while, at high temperatures, they absorb a small amount of water and shrunk [145]. This behaviour is in agreement with the present results. However, other authors found a discontinuous behaviour or even an opposite behaviour of hydrogels in response to a temperature increase [145], [146]. For example, N. Vishal and H. Shivakumar showed that, when the temperature increased from 20 to 40°C, the polymer (a hydrogel containing poly(methacrylic acid-co-acrylamide)) swelled faster but the EWC was enhanced [147]. They justified this phenomena as a consequence of the disentanglement of the polymeric chains by destruction of the hydrogen bonding between polymer molecules, causing an increase in the chain mobility and facilitating the network expansion at higher temperatures [147]. It seems each hydrogel has its own properties, that are strictly related with its composition, and behaves differently in response to an environmental change.

IV-1.2.3. Wettability

To evaluate the surface wettability of sterilized and non-sterilized materials, contact angles were measured by the captive bubble method. The results are presented for both materials in Figure 25.

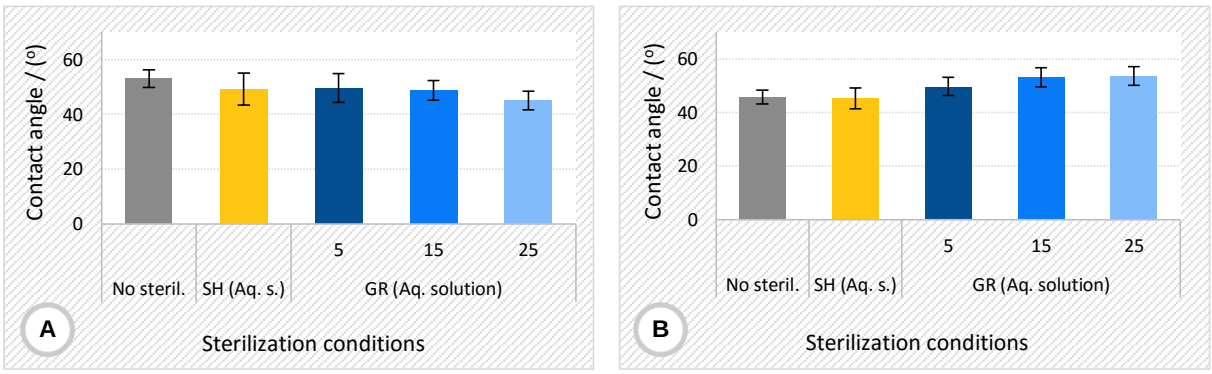

Figure 25. Water contact angles of lenses materials, non-sterilized and sterilized in aqueous solution, in different sterilization conditions: (A) – B26Y; (B) – CFL58. The error bars correspond to ± SD.

Figure 25 does not show significant differences among the contact angles for both materials after sterilization. The largest variation was approximately $\pm 8^{o}$ between a non-sterilized lens and a lens sterilized with $25\ kGy$ of GR. A slight increase is observed in the hydrophilicity of B26Y with the increase of the radiation dose, and, oppositely, a slight decrease in the hydrophilicity of CFL58 also with the

increase of the radiation dose. For CFL58 these results were expected since the WC decreased in the same manner for the same conditions.

IV-1.2.4. Ion permeability

The values of the ionoflux diffusion coefficients (D_{ion}) calculated from the measured conductivities using Equation 12, for both materials are shown in Table 10.

Table 10. Ionoflux diffusion coefficients obtained experimentally for the ophthalmic lenses materials, non-sterilized and sterilized in aqueous solution by SH and with 5 kGy of GR.

Sterilization conditions	Ionoflux diffusion coefficients (mm^2/min) ± SD	
	B26Y	CFL58
No sterilization	$2.0\times10^{-4} \pm 1.4\times10^{-5}$	$8.9\times10^{-3} \pm 5.3\times10^{-4}$
SH	$1.6\times10^{-4} \pm 1.5\times10^{-5}$	$8.9\times10^{-3} \pm 3.5\times10^{-4}$
5 kGy GR	$2.3\times10^{-4} \pm 1.6\times10^{-5}$	$1.0\times10^{-3} \pm 5.5\times10^{-4}$

As was mentioned before, the transport of ions through lenses is more important for CLs than for IOLs. The minimal required value is 1.5×10^{-5} mm^2/min [71]. Sterilization slightly affected the ion permeability and all the obtained D_{ion} coefficients, before and after sterilization, are above of the minimum required value, at least by one order of magnitude.

IV-1.2.5. Morphology

The surface analysis of the sterilized and non-sterilized CLs and IOLs materials was performed by scanning electron microscopy. For CLs, three images were collect using tree different magnifications, 1000x, 3000x, and 10000x and for IOLs only two images were recorded but with the magnifications of 1000x and 3000x. Figure 26 presents the morphology of a non-sterilized IOL sample and Figure 27 the morphology of a non-sterilized CL sample. After sterilization in different conditions (SH, 5 and 25 kGy of GR), the images did not reveal any alteration, and, for this reason, only non-sterilized materials are shown here. The rest of the imagens are available in Annex V (for B26Y) and Annex VI (for CFL58).

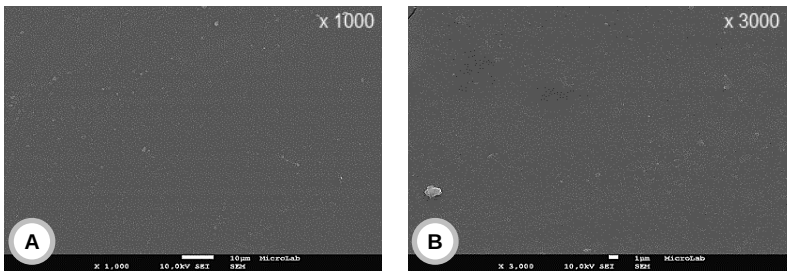

Figure 26. SEM images of the surface of a non-sterilized B26Y. (A) – Magnification of 1000x. (B) – Magnification of 3000x.

The surface of B26Y is very smooth when compared with that of CFL58. However, during the assay, B26Y displayed some fragility to the electron beam, being almost impossible to obtain the images for the magnification of 3000x without cracking the surface. An important point is that the roughness of

the provided CFL58 material is not adequate for CLs. For future commercial application, the finishing of this material should be greatly improved and further characterization studies will be needed.

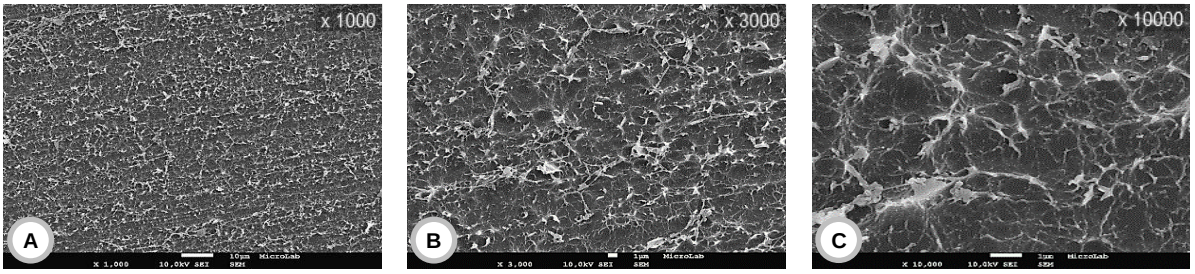

Figure 27. SEM images of the surface of a non-sterilized CFL58. (A) – Magnification of 1000x. (B) – Magnification of 3000x. (C) – Magnification of 10000x.

IV-1.2.6. Sterility tests

To determine the efficiency of the sterilization methods, direct inoculation method was chosen to verify the sterility of lenses materials. Table 11 presents the obtained results.

Table 11. Sterility test results of sterilized lenses materials by SH and with 5 kGy of GR, in aqueous solution.

Lenses materials	Sterilization conditions	
	SH	GR (5 kGy)
B26Y	Sterile	Sterile
CFL58	Sterile	Sterile

Both materials submitted to SH and 5 kGy of GR were sterile, leading to conclude that the chosen sterilization methods are effective sterilizing same lenses materials with an equivalent mass.

IV-1.3. Effects of sterilization on drug loaded materials

Drug release experiments were carried out in both materials to assess the effect of the sterilization methods on the drug release behaviour in terms of release kinetics and amount of drug released. Regarding the previous results obtained for the sterilization of drugs and materials, the sterilization methods that did not present negative effects in terms of degradation of the drugs and modification of the properties of the materials were SH and 5 kGy of GR. Despite the great response of the studied drugs to GR sterilization in the powder form, they weren't explored in terms of drug release, since the methodology used for loading was soaking and lenses would have to be dried before the release, being then in different conditions. Moreover, CLs are not sold in the dry state and both materials are being explored for comparative proposes. For these reasons only SH and 5 kGy of GR were explored in the release experiments for all tested drugs, except DFN-loaded materials which were not submitted to GR due to the high degradation exhibited by the GR-sterilized DFN solution.

IV-1.3.1. Drug release studies

For all system combinations, the polymeric samples were loaded for 4 days, at $4^{o}C$ in drug solution (0,5 mL - prepared in NaCl with a concentration of $2\ mg/mL$) and sterilized by SH or with $5\ kGy$ of GR in drug loading solution (on the 3^{rd} day of loading). Despite previous results have shown, that the materials were not affected by the SH or GR ($5\ kGy$) sterilization, to confirm this result, the materials were also sterilized before loading in NaCl solution. After sterilization, both materials were dried and then loaded in the same conditions. All the quantifications were done by HPLC. Release profiles from B26Y are presented in Figure 28 for DFN, KTL and MXF and in Figure 29 for MXF+KTL. In all cases the release profiles obtained with the correspondent non-sterilised samples are included for comparison purposes.

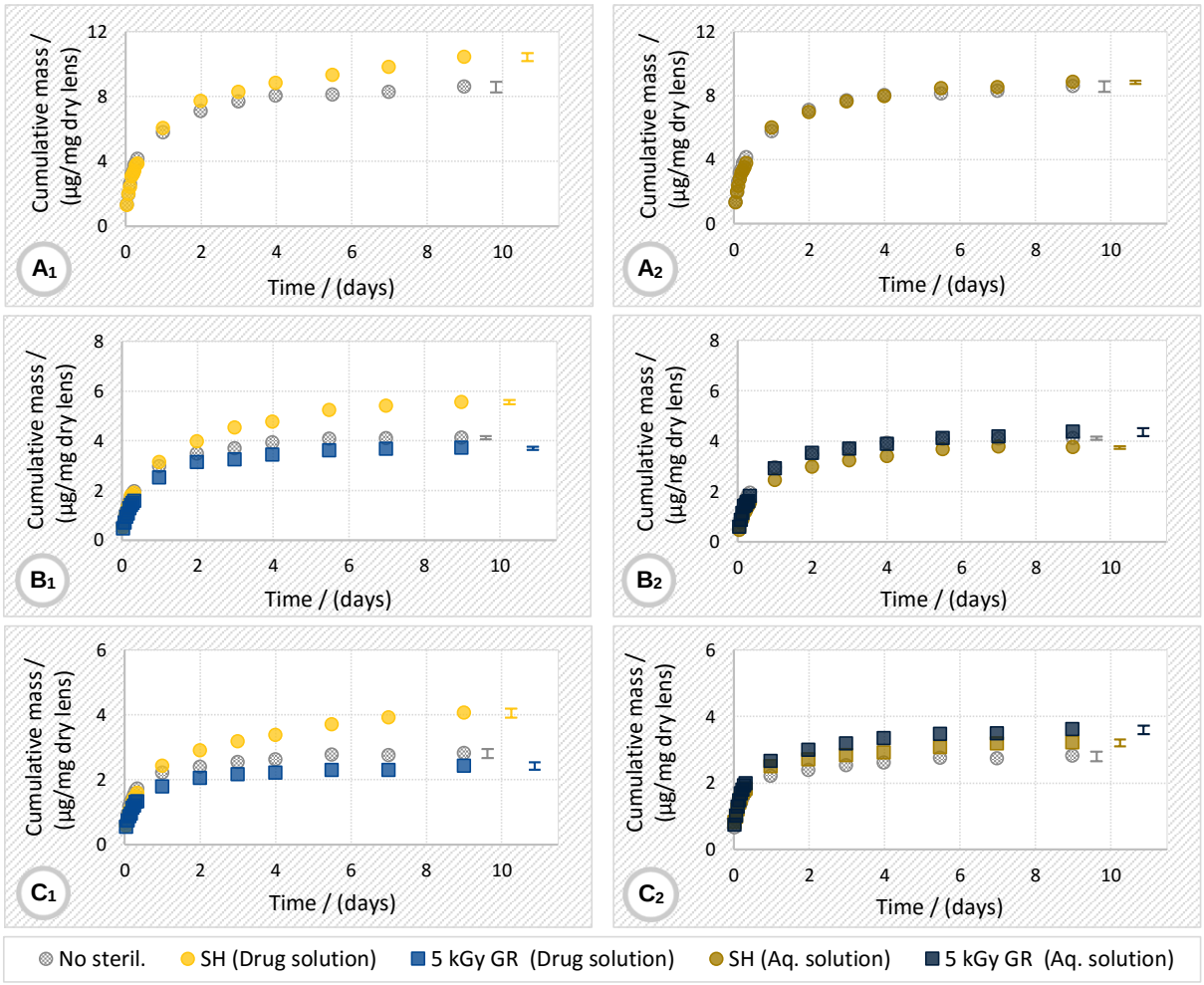

Figure 28. Cumulative release profiles of DFN (A_1 and A_2), KTL (B_1 and B_2) and MXF (C_1 and C_2) from B26Y, determined by HPLC. A_1, B_1 and C_1 correspond to sterilized samples on the 3^{rd} day of loading and A_2, B_2 and C_2 to sterilized samples before loading. The error bars correspond to $\pm$ mean SD.

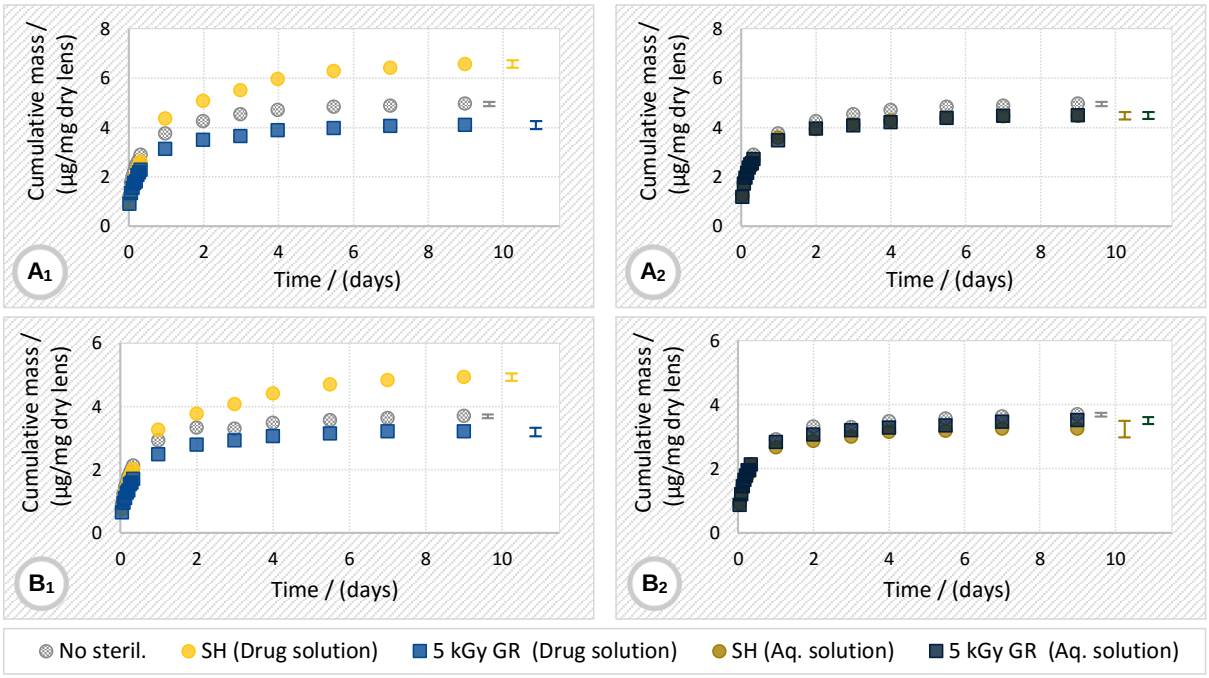

Figure 29. Cumulative release profiles of MXF+KTL from B26Y, determined by HPLC: [A_1 and A_2] – KTL release; [B_1 and B_2] – MXF release. A_1 and B_1 correspond to sterilized samples on the 3^{rd} day of loading and A_2 and B_2 to sterilized samples before loading. The error bars correspond to ± mean SD.

Overall, when performed on the 3^{rd} day of loading, GR slightly decreases the released amount, while SH improves all the release profiles, not only in the amount but also in the kinetics of release. In this material, DFN loaded more followed by KTL and then MXF. Between MXF and KTL and the combination of MXF+KTL the release was slightly increased for both drugs in the mixture.

In Annexes I, II, III and IV in Figures A2, A4, A6 and A8, the corresponding HPLC chromatograms of the release solutions of DFN, KTL, MXF and MXF+KTL, from both lenses materials, are presented. Each chromatogram contains all the sterilization conditions per drug and per material (between 3 to 5 release curves) for the release solutions from the 2^{nd} day of release. The chromatograms are consistent with these results and may explain the decrease in the amount released when IOLs were sterilized by GR in the loading solution. For the 3 irradiated systems in drug solution, the chromatograms reveal degradation peaks, which justify the decrease in the amount of released drug. These results suggest that for lenses immersed in drug solutions, GR is probably not a good option, at least for these drugs, since the degradation products formed after sterilization can be toxic for the eye and damage the healthy tissues. Contrarily, SH seems to be a promising method for the sterilization of any of the studied systems: it not only increased the amount released but also improved the release control (for at least, 9 days).

For CFL58 the release profiles are showed in Figure 30 for DFN, KTL and MXF and in Figure 31 for MXF+KTL.

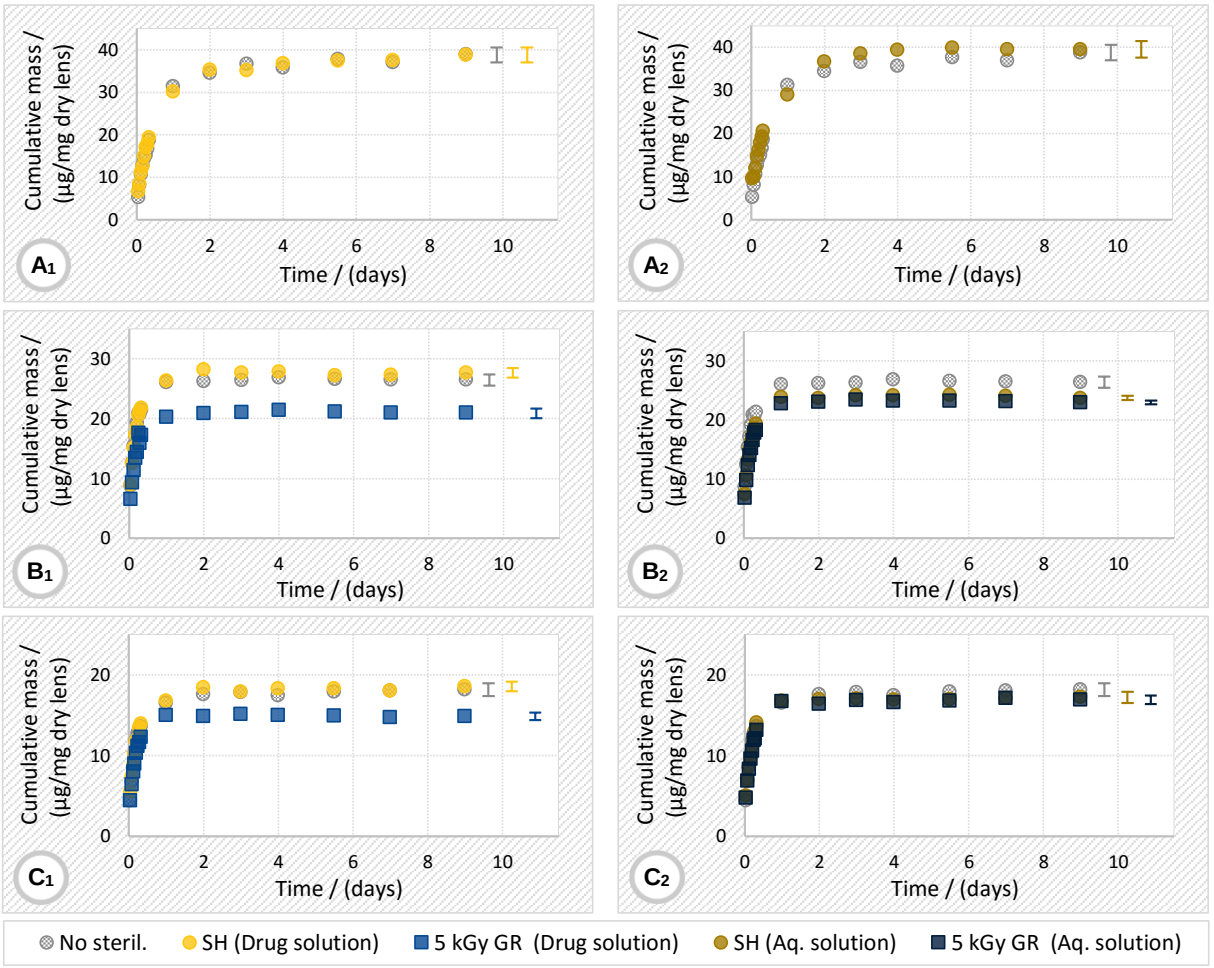

Figure 30. Cumulative release profiles of DFN (A_1 and A_2), KTL (B_1 and B_2) and MXF (C_1 and C_2) from CFL58, determined by HPLC. A_1, B_1 and C_1 correspond to sterilized samples on the 3^{rd} day of loading and A_2, B_2 and C_2 to sterilized samples before loading. The error bars correspond to $\pm$ mean SD.

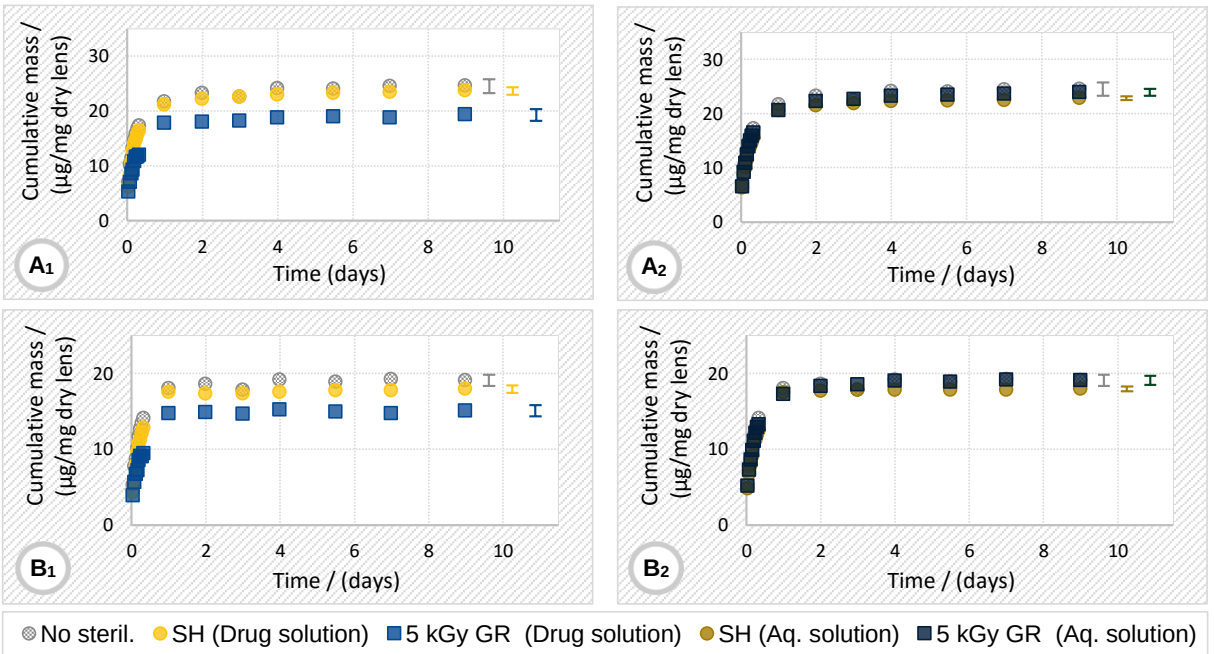

Figure 31. Cumulative release profiles of MXF+KTL from CFL58, determined by HPLC: [A_1 and A_2] – KTL release; [B_1 and B_2] – MXF release. A_1 and B_1 correspond to sterilized samples on the 3^{rd} day of loading and A_2 and B_2 to sterilized samples before loading. The error bars correspond to $\pm$ mean SD.

When compared with B26Y, the release from CFL58 was faster and yield higher amounts of drugs. It seems that polymeric matrices with higher EWC load more drug, but also lead to a rapid release. In all cases, there was an initial burst in the released drug and almost all drug was released in the first 24 h. In this material, DFN loaded more followed by KTL and then MXF. Between MXF and KTL and the combination of MXF+KTL the uptake/release was practically the same, however MXF loaded a little more when alone. The results demonstrated, once more, that GR leads to a lower release of the drug, while SH did not affect the drug release. Indeed, considering that the release profiles were practically not altered when soaking was done after sterilization, probably the observed decrease in the released amount (Part 1 of Figure 30 and Figure 31), was due to drug degradation during irradiation of the drug-loaded materials. HPLC chromatograms (in Annexes I, II, III and IV in Figures A2, A4, A6 and A8) illustrate the degradation peaks for all the released drugs (from 2^{nd} day of release) sterilized by GR in drug solution. In the chromatograms of MXF (in both lenses) a slight difference in the retention times is noticed, which may be due to small changes in the column along the time.

Thus, for CFL58 samples immersed in drug solutions, GR is not an option, at least for these drugs, but SH is a great solution since it did not cause any harmful effect. However, for this material, other strategies should be explored to improve the drug release profile.

At this point, it would be interesting to analyse in detail the shape of the drug release profiles in order to conclude about the drug transport mechanisms through hydrogels. Because the drugs and hydrogel materials vary significantly in charge and chemistry, drug uptake/release rates usually are highly dependent of drug-hydrogel combination [148]. Generally, solute uptake/release rates are governed by the solute diffusion coefficient in the hydrogel. Drugs diffuse primarily through the water-filled spaces of the polymer network and, depending on the hydrogel material, they can specifically interact or not with the polymer chains. These solute-specific interactions between drugs and polymers can fall within two classes: strong and irreversible binding or weak and reversible adsorption (characteristic in pharmaceutical drugs) [148]. D. Liu et al., reported drug diffusion coefficients of CLs materials made of HEMA and methacrylic acid, with weak specific drug adsorption to polymer chains [148]. These specific interactions between the solutes and the hydrogel matrices may be also affected by sterilization procedures, leading to favourable or unfavourable effects. However, sterilization can also eventually dictate the success in the control of the release if it does not damage the material or affects the drug activity.

With the aim of better understanding the effect of the sterilization on the cumulative release profiles, the experimental data of the release curves were fitted to the kinetic model of *Korsmeyer–Peppas*. This model was developed in 1983 by *Korsmeyer* and *Peppas* and it is a simple model which describes Fickian and non-Fickian drug releases, from swelled and non-swelled polymeric devices. The model is given by the following equation:

$$\dot{q} = \frac{M_t}{M_\infty} = k \times t^n \qquad \textbf{Equation 13}$$

where $\dot{q} = \frac{M_t}{M_\infty}$ is the fraction of drug released at time t, k is the release rate constant and n is the diffusional exponent [149]. This model equation fits the first 60% of drug release curve (cumulative

release vs time). Then, plotting $\mathrm{Log}(\dot{q})$ *vs* $\mathrm{Log}(t)$, it is possible to determine parameters n and k by linear regression:

$$\mathrm{Log}(\dot{q}) = n * \mathrm{Log}(t) + \log(k) \qquad \textbf{Equation 14}$$

Based on the diffusion exponent (n) obtained, the type of drug transport mechanism trough the polymer can be predicted. For the case of cylindrical shaped matrices, which is the one applicable to the polymeric samples, values of $n \leq 0.45$ correspond to a Fickian or a quasi-Fickian diffusion mechanism, values of $0.45 < n < 0.89$, to non-Fickian diffusion (known as well as anomalous transport), while $n = 0.89$ and $n > 0.89$ correspond to the case II transport and to the super case II transport, respectively [63], [149].

From the fit of the first 60% drug release data into the kinetic model of *Korsmeyer–Peppas*, the diffusional exponent values were determined for all the experimental releases. The kinetic parameters obtained (diffusional exponents and the respective coefficients of determination (R^2)) are reported in Annex VIII, Table A1. The values of n were found to be $0.45 < n < 0.89$ for all the drug releases from CFL58 and for DFN and KTL releases from B26Y, indicating processes typically controlled by non-Fickian drug diffusion or anomalous drug transport. For MXF and for MXF+KTL releases, n values were ≤ 0.45 characteristic of Fickian or quasi-Fickian drug diffusion. These results show that, despite the similar behaviour observed for different drugs in the same sterilization conditions, the interactions between drugs and polymeric matrices are specific for each particular system and are probably determinant of the shape of the release profiles.

IV-1.3.2. Characterization of loaded IOLs material

At this stage, the study of CFL58 material for CLs was abandoned, owing to the high roughness of the samples surface, the fast release of the loaded drugs and the material degradation by GR. Thus, the following sections and sub-sections will focus only on the material B26Y for IOLs.

To evaluate the effect of the sterilization on loaded B26Y, samples were pre-soaked with all drugs for 4 days at $4\,^{o}\mathrm{C}$ with [drug] $2\ \mathrm{mg/mL}$ and sterilized by SH or with $5\ \mathrm{kGy}$ of GR, in the 3^{rd} day of loading. Comparison with non-sterilized samples which were prepared exactly in the same way, was always done.

IV-1.3.2.1. Transmittance

The transmittance was measured for pre-soaked IOLs materials in the wavelength range of $360 \leq \lambda\,(\mathrm{nm}) < 760$. For the transmittance study and for each drug, the 1^{st} control lens material was only hydrated in DD water and the 2^{nd} control lens material was loaded with the drug but not sterilized. The other samples were all loaded and sterilized in the drug solution. The spectra obtained for all the samples are displayed in Figure 32. In order to better interpret the results, the UV−Vis absorbance spectra of all drugs were also obtained and are presented in Annex IX, Figure A15.

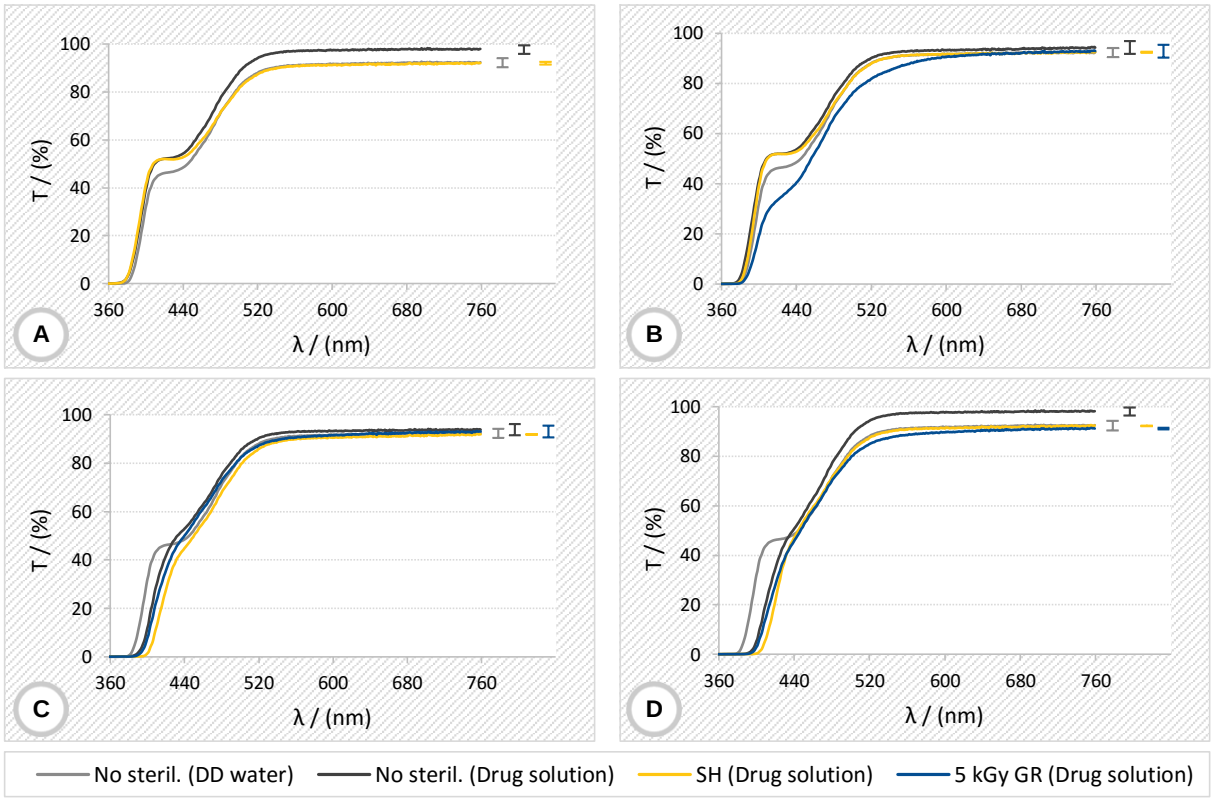

Figure 32. Transmittance (%) of B26Y, loaded with DFN (A), KTL (B), MXF (C) and MXF+KTL (D), non--sterilized and sterilized in different sterilization conditions. The error bars correspond to ± mean SD.

The results obtained for the %T of loaded IOLs materials only presents differences in the transmissibility of irradiated lenses loaded with KTL, where it appears some changes occurred within the polymer. The other systems weren't affected by the presence of the drug neither due sterilization during loading. The small attenuation noticed in the region of the violet light filter, between $380 - 400$ nm in the materials loaded with MXF and MXF+KTL is due to the fact that these drugs absorb light in this range (please see Figure A15). It is additionally perceived an unexplainable small increase in %T in the visible range, of non-sterilized loaded materials with DFN or MXF+KTL, which is reverted back after sterilization. These results were re-confirmed.

IV-1.3.2.2. Morphology

The surface analysis of the sterilized and non-sterilized loaded IOL sample was performed by SEM. The images revealed no alterations due to the presence of the drug and the different sterilization procedures, and for this reason, the imagens are depicted only in Annex VII in Figures A11, A12, A13 and A14, for loaded materials with DFN, KTL, MXF and MFX+KTL correspondingly.

IV-2. Effect of different experimental SH sterilization and loading/release conditions on the properties and release profiles of MXF loaded IOLs materials

In face of the promising results presented above for the release of drugs from the loaded IOL material sterilized by SH, it is pertinent to clarify which factors, during the de SH sterilization process, could have contribute for such results. In this context, the loading/release and sterilization conditions were varied with the objective of understanding their effect on the drug release behaviour and on the intrinsic properties of the material. For these studies only one drug was used. The chosen drug was MXF.

IV-2.1. Effect of SH sterilization conditions

Regarding the SH sterilization conditions, several parameters were tested: Table 12 summarizes those conditions and relates them to the respective purpose of study. All samples were loaded and sterilized in 0.5 mL of MXF solution prepared in NaCl. UV−Vis spectrophotometry was used to estimate the amount of MXF released.

Table 12. Summary of loading/sterilization conditions for the study of the effects of SH sterilization.

Drug solution	Loading conditions (during 4 days)		Sterilization conditions			Proposed studies
	C (mg/mL)	T (ºC)	Method	Duration (min)	Moment	
MXF	2	4	No sterilization			Effect of the moment of autoclaving
			SH	60	1st day of loading	
					3rd day of loading	
			No sterilization			Effect of the duration of sterilization
			SH	30	3rd day of loading	
				60		
				90		
			No sterilization			Effect of the concentration of loading/sterilization solution
			SH	60	3rd day of loading	
	5		No sterilization			
			SH	60	3rd day of loading	

IV-2.1.1. Drug release studies

In what concerns the effect of the moment of autoclaving, release curves (Figure 33 (A)) revealed that sterilizing in the 1st day or in the 3rd day of loading period does not affect neither the amount released or the release kinetics.

In turn, with respect to the effect of the duration of sterilizing during 30, 60 or 90 min did not change the release profiles: only an almost imperceptible increase was observed (Figure 33 (B)). This was probably due to the fact that the total time that each sample remained inside the autoclave was almost the same. Generally, a sterilizing cycle comprises three phases: heating, sterilizing, and cooling. Sterilizing time was defined and varied in the experiments, but the time it takes to heat (until achieve the 121ºC and a pressure of 1 bar) and cool (return to at least, 90ºC and 0 bar) is characteristic of each

equipment. In this case for the defined sterilizing times, 30, 60 and 90 min, the total time that the samples remained inside the autoclave were, 2.5, 2.67 and 2.83 h respectively, which are relatively close.

The comparison of the release curves obtained in both cases with the one obtained with non-sterilized samples shows that SH sterilization induces significant changes in the release of the drug: contrarily to what happens with the non-sterilized samples which release the most part of the drug in a few hours, SH sterilized samples present a sustained release over almost 60 days, which is an important finding in the field of drug release.

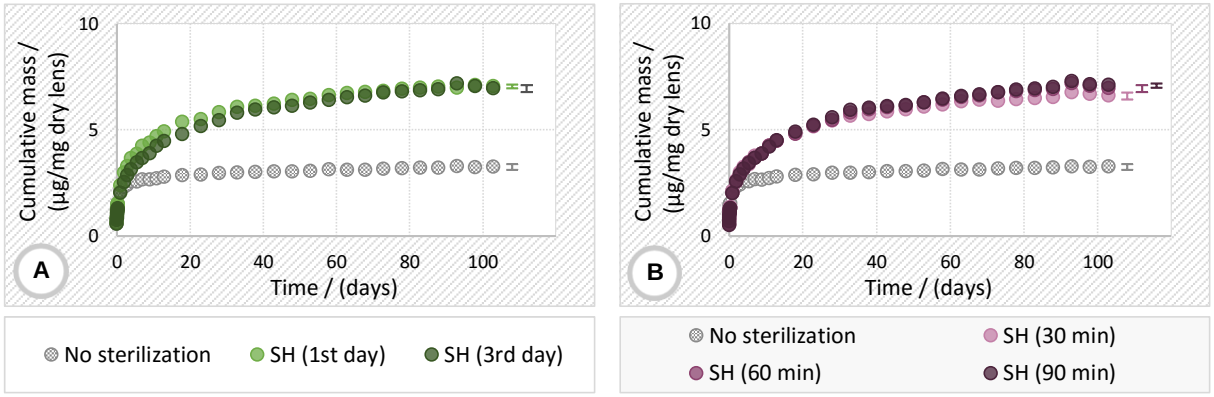

Figure 33. Cumulative release profiles of MXF from B26Y determined by UV–Vis spectrophotometry. A – Study of the effect of the moment of autoclaving. B – Study of the effect of the duration of sterilization. The error bars correspond to ± mean SD.

The results of the experiments carried out to investigate the effect of the drug concentration in the loading/sterilization solution are presented in Figure 34.

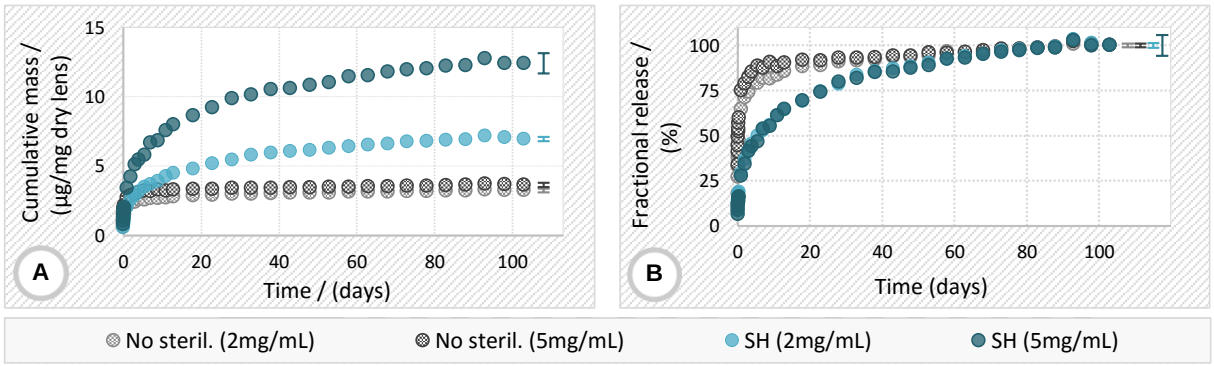

Figure 34. Cumulative release (A) and fractional release (B) profiles of MXF from B26Y, determined by UV–Vis spectrophotometry. Study of the effect of the drug concentration in the loading/sterilization solution. The error bars correspond to ± mean SD.

The increase in the concentration of the loading/sterilization solution did not affect the release when the materials were non-sterilized, but after sterilization the amount released clearly increased with concentration (Figure 34 (A)). After normalizing the release curves (Figure 34 (B)) (by dividing the cumulative mass released by the plateau value), it was possible to see that the increase in the concentration only affect the amount of drug released. The release rate in terms of percentage was exactly the same after the SH sterilization for both concentrations studied, evidencing that for this system

MXF-loaded IOL material the diffusivity is not concentration dependent. Once again a sustained release over almost 60 days is observed in opposition to the non-sterilized samples.

The kinetic model of Korsmeyer-Peppas was fitted to the release data till 60% of the release is achieved. The obtained values for the diffusional exponent, available in Annex VIII Table A2, were ≤ 0.45 which indicates that the mechanism of the release was mainly controlled by Fickian or quasi-Fickian diffusion. This is consistent with the previous obtained results (in section IV-1).

IV-2.2. Effect of loading temperature

IV-2.2.1. Drug release studies

Special attention has been devoted to the effect of temperature on a special class of hydrogels, the environmentally-sensitive hydrogels (which have the ability to respond to changes in their environment), where small variations in this parameter can significantly affect their network structure and influence their swelling or drug release behaviour. Despite B26Y does not belong to this class of polymers, it exhibited great improvements in the drugs release upon autoclaving (which involves high temperature). Thus, following the previous study and considering that SH sterilization was performed at $121^{o}C$, several temperatures were chosen to perform the loadings without autoclaving, in order to understand if the increase in the amount of drug released and the improvement in the release kinetic was related to the fact of the materials having been exposed at such higher temperature during the sterilization procedure.

As in the previous experiments, samples were loaded in 0.5 mL of MXF solution prepared in NaCl. The quantification of the drug released was done by UV−Vis spectrophotometry. Table 13 summarizes all the conditions used in this set of experiments.

Table 13. Summary of loading/sterilization conditions for the study of the effect of loading temperature.

Drug solution	Loading conditions (during 4 days)		Sterilization conditions			Proposed study
	C (mg/mL)	T (^{o}C)	Method	Duration (min)	Moment	
MXF	2	4	No sterilization			Effect of loading temperature
		36				
		60				
		80				

The release profiles (in Figure 35) confirm the suspicions. The higher the loading temperature, the greater the amount released and the longer the release time. The results suggest that, in SH sterilization procedure (which involves not only temperature but also pressure) temperature shall have an important role in the kinetic of release. This can be related, among other factors, with the fact that rising the temperature can cause an increase in the penetration rate of the fluid into the lens [146]. However, this behaviour may be different for other systems, meaning that other parameters, such as the diffusion and interaction of the drug with the polymeric matrix, may depend differently on the temperature [145], [146], [148]. Each system (material-drug) behaves differently under temperature variations, depending on the physical and chemical features of the materials and drugs.

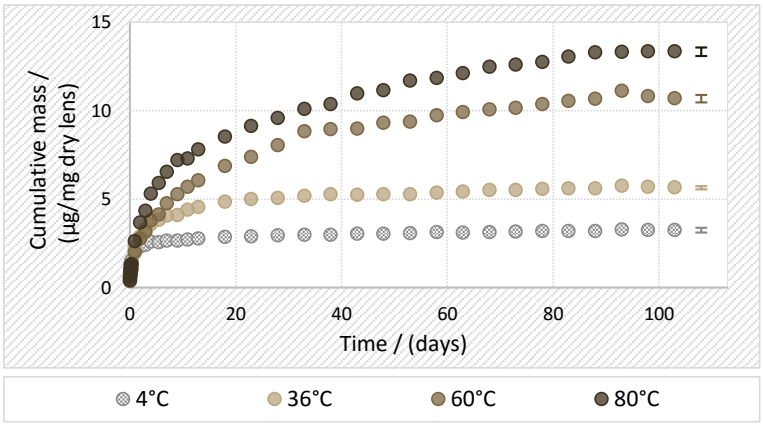

Figure 35. Cumulative release profiles of MXF from B26Y, determined by UV−Vis spectrophotometry. Study of the effect of loading temperature. The error bars correspond to ± mean SD.

To evaluate the possibility of degradation of MXF, as a consequence of having been exposed to such higher temperatures during 4 days, HPLC was also used to analyse the drug solutions before and after the procedure. The results (available in Annex X, Table A4) allow to conclude that no degradation occurs after 4 days of exposure to 60ºC and 80ºC.

The diffusional exponent values were also determined from the release data using the Korsmeyer–Peppas model (Annex VIII, Table A2). Values of n, were found to be between $0.45 < n < 0.89$ for loading temperatures equal or higher than 36ºC, denoting a non-Fickian drug diffusion or anomalous drug transport. For this system, MXF−B26Y, it appears that when lenses materials are soaked at 4ºC, and submitted (or not) to SH sterilization, the diffusion mechanism is mostly Fickian. However, when temperatures up from to 36ºC are used during loadings, the diffusion turns into a non-Fickian mechanism or anomalous transport.

Drug absorption and diffusion through the materials strongly depends on several matters: physical and chemical characteristics of the drug; nature of the interactions between the polymers and the drugs (related to the presence of some functional groups); affinity and size of solvent molecules; porosity of the matrix; degree of crystallinity of the polymer; capillary effect; osmotic pressure; and electrostatic charge [41], [44], [54], [58]–[60], [150]. All these dependencies can variate with temperature, ion concentrations and pH, turning the understanding of the phenomena a quite complex.

The increase in temperature, by itself, can cause considerable alterations in the pH even in pure water, altering the ion mobility and decreasing the viscosity [151], [152]. As mentioned before, in this work, unfortunately the pH values were not controlled. When considering that the solutions were prepared in NaCl (and this is not a buffer solution) and loading was performed at different temperatures, large variations in the pH probably occurred during the assays. Thus, if the pH can have an influence in the profile behaviour, it may be missing such values that could additionally help to explain these results. Usually, the pH of the pure water decreases with the increase in temperature, but depending on the type of solution it can behaves differently [151], [152]. Also the solubility of MXF is pH dependent, it increases with pH (above 6) due to the ionization of the carboxylate group [37].

IV-2.2.2. Characterization of loaded IOLs materials

With the intend of explaining why the hydrogels when subjected to high temperatures display a significant improvement in the drug release behaviour, several techniques were used to verify if the material suffers significant changes when exposed to high temperature.

IV-2.2.2.1. Swelling kinetics

The swelling profiles and EWC were determined in DD water and in $MXF_{2\ mg/mL}$ solution, at different temperatures (4, 36 and $60^{o}C$). The temperatures choice was related with the soaking temperatures used previously. The results are represented in Figure 36 and Figure 37 respectively.

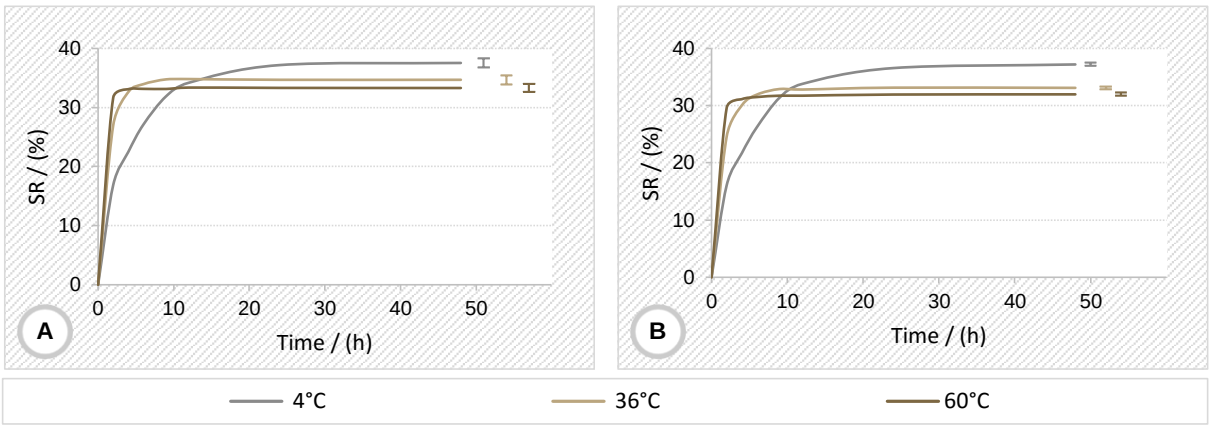

Figure 36. Swelling profiles (%) of B26Y at 4, 36 and $60^{o}C$. (A) – Performed in DD water; (B) - Performed in $MXF_{2\ mg/mL}$ solution. The error bars correspond to $\pm$ mean SD.

As was seen in section IV-I, the swelling profiles demonstrate that with the increase in temperature, the solution uptake becomes faster and the EWC slightly decreases.

The idea of performing the experiments in the loading solution was to understand if the swelling was affected by the presence of the drug, since it was found in the literature, that swelling can widely variate depending on the characteristics of the surrounding solution [54]. J. Wang and W. Wu studied the effect of the ionic strength, in a xerogel made of $EMA_{(25\%)}$ / $HEMA_{(75\%)}$. They swelled the hydrogel in aqueous solutions with various NaCl concentrations and the EWC decreased with the increase in the NaCl concentration [124]. Another study [147] confirmed that an increase in the ionic strength significantly decreased the swelling ratio of an anionic polymer, and attribute such behaviour to the change in the charge distribution on the surface of the matrix, referring that, as the concentration of Na^{+} in the swelling medium increased a stronger ‘‘charge screening effect’’ of additional cations was achieved, causing imperfect anion-anion electrostatic repulsions and a decrease in the osmotic pressure between the polymer and the surrounding solution, therefore, causing swelling to decrease. On the contrary, when the hydrogels were placed in pure water, the maximum osmotic pressure was developed and hence the maximum swelling was achieved [147]. This phenomenon can also help to explain the present results, since it is noted a slight decrease in the EWC when the assays are performed in MXF (comparatively to DD water). In fact, it has been mentioned in the literature that PMMA/PHEMA

copolymers are negatively charged. On the other hand, MXF in the form of hydrochloride is highly ionisable in water, leading to the formation of the ionic species, MoxifloxacinH^+ and Cl^-. Thus, a similar ‘‘charge screening effect’’ can be responsible for the interactions between the polymers and MoxifloxacinH^+ in solution [37], [153], [154].

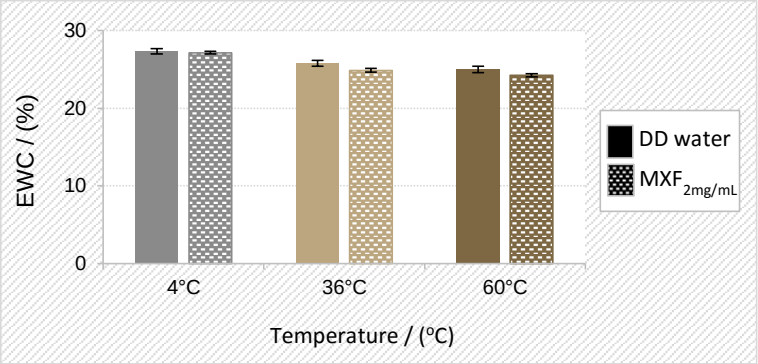

Figure 37. Equilibrium water content (%) of B26Y at 4, 36 and 60^oC, in DD water and in $MXF_{2mg/mL}$ solution. The error bars correspond to $\pm$ mean SD.

Another important issue, is the influence that pH may have during the swelling process. S. Tomić et al. [146] showed that the equilibrium degree of swelling of PHEMA in a lower pH (2.2 – buffer solution) did not change with the increase of temperature, but in a higher pH (7.4 – buffer solution) swelling behaviour present considerable changes along temperature variation (between $0 - 60^oC$) with a maximum value around 40^oC. They explained this behaviour as a consequence of the increased amount of bound fluid in the hydrogels at higher pH. Their results also led them to conclude that the increase in temperature caused an increase in the fluid uptake rate, which is in concordance with our obtained results.

The same authors loaded a modified polymer made of HEMA with gentamicin (pH 7.4, prepared in a buffer solution) and demonstrate that the release was higher, once again, around 40^oC which corresponds to the temperature at which the swelling was found to be maximum [146]. This result is not consistent with our results, since B26Y swelled less but loaded/released more drug with the increase in temperature. The obtained results show that the temperature effect on swelling capacity is not a determinant factor to explain the observed drug release behaviour.

IV-2.2.2.2. Thermotropic Behaviour

The determination of the glass transition temperature (T_g) of IOL material before and after soaking in [MXF] $2\ mg/mL$ at 4 and 60^oC was performed by the acquisition of DSC thermograms. T_g values were determined considering the midpoint of the step in the baseline of the first heating cycle. Thermograms and T_g values are presented in Figure 38 and Table 14, respectively.

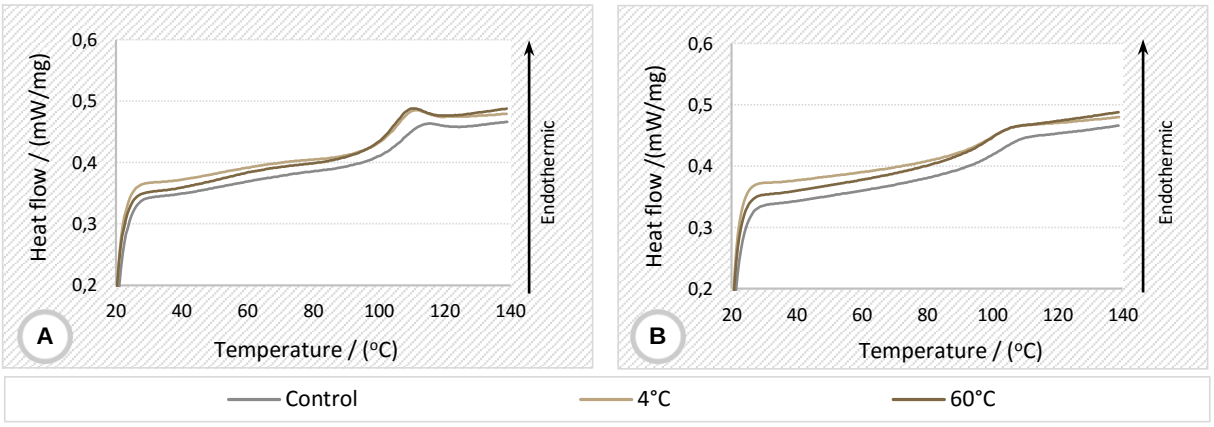

Figure 38. Thermograms obtained by DSC for B26Y before and after loading with MXF (loading temperature 4 and $60^{o}C$). (A) – 1^{st} Heating cycle. (B) – 2^{nd} Heating cycle.

Table 14 . Experimental T_g values obtained by DSC, for B26Y loaded with MXF at 4 and $60^{o}C$.

Solution	Loading T (^{o}C) (during 4 days)	$T_g \pm$ SD (^{o}C) (middle temperature)	
		1^{st} Heating	2^{nd} Heating
DD water (Control)	4	103 ± 2	101 ± 2
$MXF_{2\ mg/mL}$		102 ± 1	98.5 ± 0.6
	60	100.6 ± 0.5	98.3 ± 0.3

The results revealed that, when the polymeric material is placed in a drug solution at 4 or $60^{o}C$, its transition temperature is not affected either by the presence of the drug or by the temperature at which it was exposed. If in any case, the material was eventually affected, this amendment was reversible and so, the results do not present changes in the glass transition temperature (endothermic reaction). In the first heating, the T_g arises along with an enthalpy relaxation peak. This may be the principal cause of the slightly difference in the T_g values between the 1^{st} and 2^{nd} cycles.

G. Liu, et al. [155] present a similar value of T_g for a P(MMA-co-HEMA) material of approximately $105^{o}C$. Also, other authors present T_g values in the range of $100 - 119\ ^{o}C$ for similar copolymers of P(MMA-co-HEMA), confirming the present results [156], [157]. In addition, thermogravimetric analysis (TGA) data found in the literature confirmed that several copolymers of P(MMA-co-HEMA) are thermo-oxidatively stable up to $330^{o}C$ [157].

IV-2.2.2.3. Structural proprieties

ssNMR spectroscopy was performed to analyse whether there have been structural changes in the hydrogel induced by the loading of MXF at different temperatures. Powdered samples of MXF, IOLs materials hydrated in DD water (for 24h at $4^{o}C$) and loaded with MXF (during 4 days with $2\ mg/mL$ at 4 and $60^{o}C$) were all analysed.

Figure 39 shows the tentative spectral assignment of MXF (without and with $\overline{DD}$), whose structural formula is represented in Figure 40.

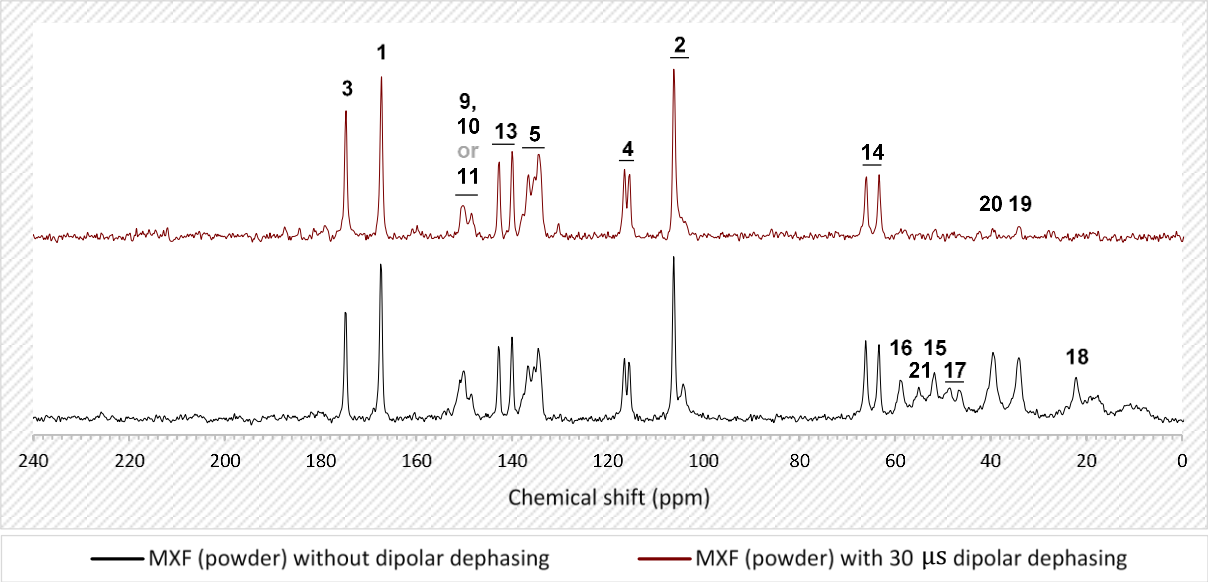

Figure 39. ^{13}C CP/MAS – TOSS spectra, obtained for MXF (powder), without (black) and with 30 μs dipolar dephasing (maroon). The numbers indicate the carbons on the molecule.

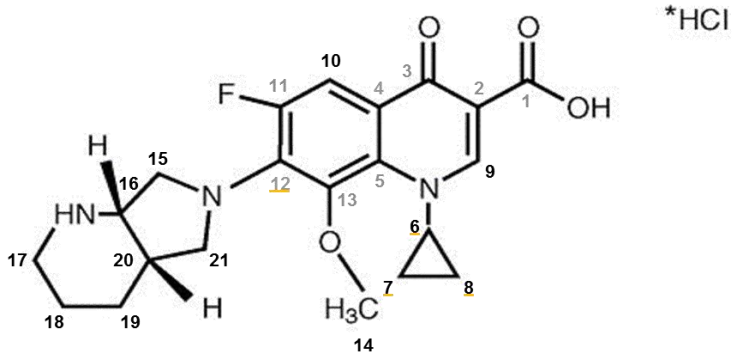

Figure 40. Structural formula of MXF. The numbers indicate the carbons on the molecule. Carbons corresponding to grey numbers are quaternary carbons, and numbers underlined in yellow were not identified by ssNMR (^{13}C CP/MAS – TOSS). Adapted [158].

In the spectra obtained for MXF it is possible to identify almost all the carbons (quaternary and non-quaternary) from MXF molecule. The values from the chemical shifts are presented in Annex XI in Table A7), and compared with the values reported in the literature.

Figure 41 shows the acquired spectra for all the B26Y tested samples. For comparison purposes the spectra of MXF is also presented. The structural formulas of the main components of the polymeric material are presented in Figure 42.

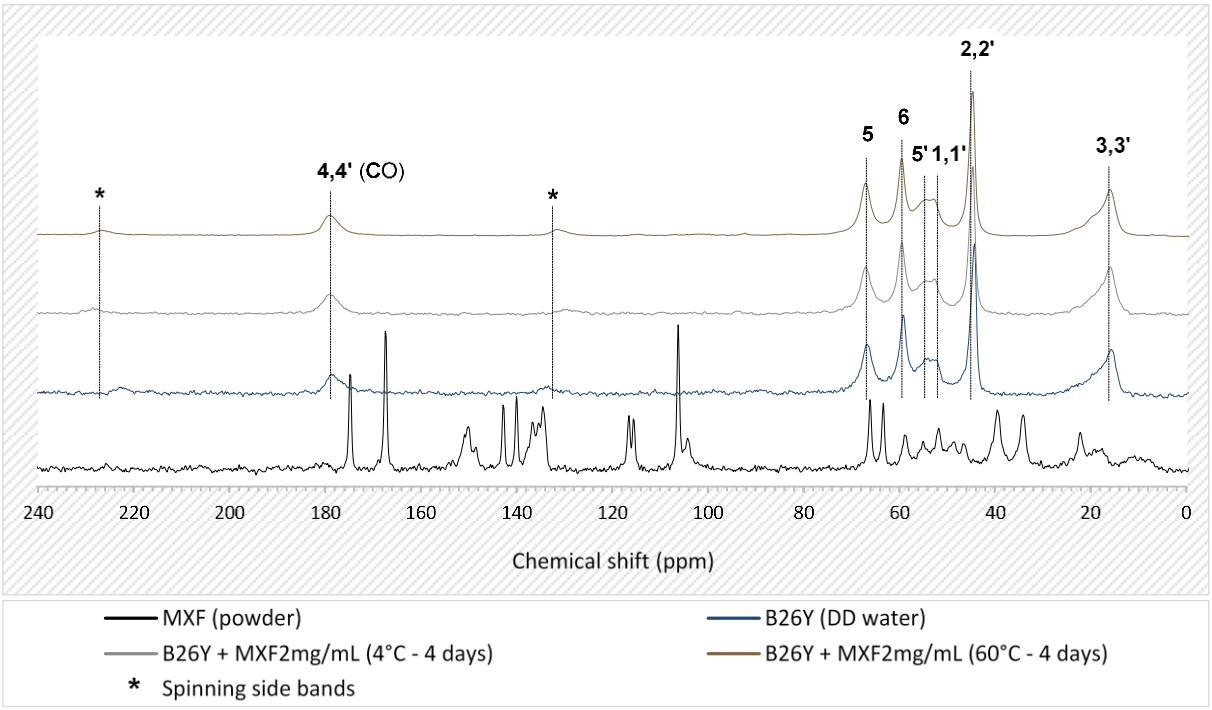

Figure 41. ^{13}C CP/MAS spectra, obtained for B26Y (hydrated in DD water), and B26Y previously loaded for 4 days with [MXF] $2\,mg/mL$ at 4 and $60^{o}C$. The numbers indicate the carbons on the PHEMA and PMMA molecules and black lines are eyelids. The spectra of MXF (powder) is also presented.

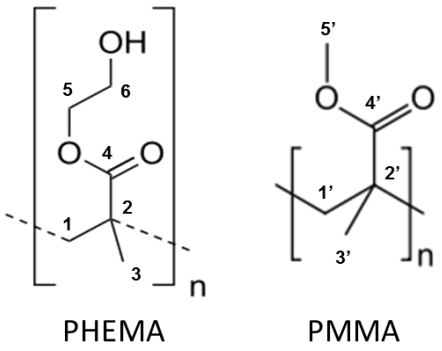

Figure 42. Structural formulas of PHEMA and PMMA. Each polymer is composed by n monomers of HEMA and MMA respectively. The numbers are indicating carbons.

It can be seen that the signs of MXF do not appear in the same regions of the loaded hydrogels spectra, because the concentration of MXF in the hydrogel shall be under the detection limit of NMR. Comparing the hydrogel spectra from IOLs (hydrated in DD water) with IOLs (loaded with MXF), no significant changes in the signs of the polymers are observed.

In the spectra of the polymeric samples a manifold of SSB is also visible (peaks equally spaced from the isotropic peak – CO signal). The values from the chemical shifts of the obtained peaks are also reported in Annex XI, Table A7, and are compared with the values found in the literature.

In order to try to observe the signals of MXF in the materials, to see if it is occurring any interaction between the polymer and the drug, the IOL material was loaded with higher concentrations of MXF and

for a longer time at different temperatures (with $10\ \mathrm{mg/mL}$ at 36 and $60^{o}\mathrm{C}$ during 10 days). The resulting spectra are compared with the previous in Figure 43.

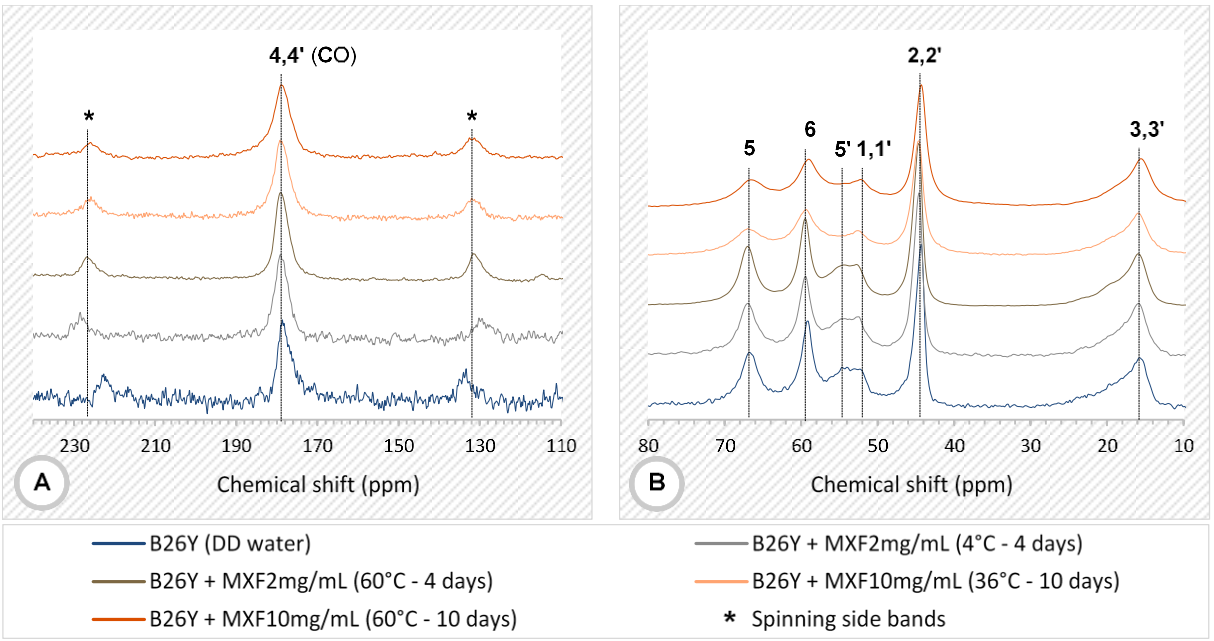

Figure 43. $^{13}\mathrm{C}$ CP/MAS spectra, obtained for B26Y (hydrated in DD water) and for B26Y previously loaded for 4 or 10 days with [MXF] $2\ \mathrm{mg/mL}$ or $10\ \mathrm{mg/mL}$ at 4, 36 or $60^{o}\mathrm{C}$. The numbers indicate the carbons on the PHEMA and PMMA molecules, the black lines are guides for the eye and (A) and (B) represent different areas of chemical shift (x –axis) from the same spectra.

Once again, despite the concentration of MXF being higher, the loaded hydrogels spectra do not show signs of MXF, since it is still under the detection limit of NMR. However, there are peaks in the spectra of the loaded hydrogels that present significant changes when compared with the previously obtained spectra. Thus, a broadening on the signals is well noted, especially on carbons 5 and 6 (of PHEMA) and 5' ($-\mathrm{OCH_3}$ of PMMA). This feature is already visible in the samples loaded at $36^{o}\mathrm{C}$ and more prominent in the samples loaded at $60^{o}\mathrm{C}$. It may be explained by the plasticizing effect of the water, inducing an increased mobility of the chains and consequently reducing the interaction between the chains, turning the process of cross polarization (CP) less efficient, that is, the transference of the magnetic polarization from abundant nuclei (e.g., $^{1}\mathrm{H}$ or $^{19}\mathrm{F}$) to rare nuclei (e.g., $^{13}\mathrm{C}$) during the spectral acquisition is reduced. This observation may be due to the interaction between the drug and the polymer and/or to the effect of temperature on the polymer structure. It may explain the significant improvement in the drug release behaviour (with a more controlled kinetics) when the hydrogels are loaded with MXF at high temperatures.

To clarify this issue and to verify if the plasticizing effect of the water is the only responsible for the sustained released, samples were loaded with the saline solution without drug (NaCl $130\ \mathrm{mM}$) during 10 days at $60^{o}\mathrm{C}$. The result is presented together with the spectrum of the hydrated polymer and of the polymer loaded in the same conditions with $10\ \mathrm{mg/mL}$ of MXF, in Figure 44.

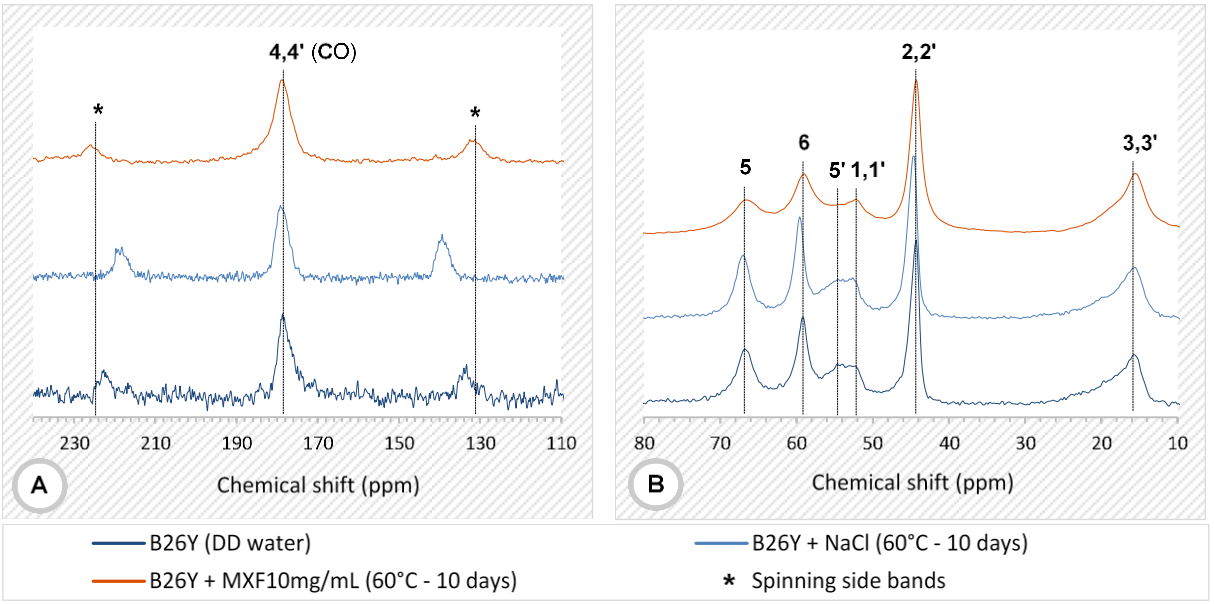

Figure 44. ^{13}C CP/MAS spectra, obtained for B26Y hydrated in DD water and B26Y previously loaded for 10 days with NaCl (drug solvent) and [MXF] 10 mg/mL, both at $60^{o}C$. The numbers indicate the carbons on the PHEMA and PMMA molecules, black lines are guides for the eye and (A) and (B) represent different areas of chemical shift ($x-$axis) from the same spectra.

Comparing with the previous spectrum of the sample loaded in the same conditions but with MXF, the spectrum of the polymer loaded in NaCl does not present enlargement of the peaks neither from the carbons 5 and 6 (of PHEMA) nor from 5' ($-OCH_3$ of PMMA). Therefore, the enlargement of the peaks cannot be explained only by the plasticizing effect of the water, the interaction between the polymeric material and the drug seems to be the dominant effect. It is also noticed that PMMA seems to be more influenced than PHEMA (carbon signal 5' is widest).

IV-2.3. Effect of the release conditions and reversibility of drug release profiles

A new set of experiments was designed, using different loading/release conditions, with the aim of: determine the effect that release protocol has on the release profile; ascertain the reversibility of the loading/release behaviour; and investigate the possibility of a part of the loaded drug be retained within the matrix. Table 15 describes all the loading/release conditions applied for such purposes.

Table 15. Summary of loading/release conditions for the proposed studies.

Release curve names	Loading conditions (during 4 days)		Release conditions (during 78 days)		
	C (mg/mL)	T (^{o}C)	Periodicity of aliquots collection	Aliquot V (mL)	Total n^{o} of aliquots collected
Release A	2	60	Between 1 to 8 hours of the 1st day of release: 1 / h. Between day 1 to 13 of release (days): 1; 2; 3; 4; 5.5; 7; 9; 11; 13. Between day 13 to 78 of release: Every 5 days.	0.3	30
Release B*			Between day 1 to 10 of release: 1 / day. Between day 10 to 78 of release: Every 2 days.	3 (total volume)	44
1st Loading		4	Between 1 to 8 hours of the 1st day of release: 1 / h. Between day 1 to 13 of release (days): 1; 2; 3; 4; 5.5; 7; 9; 11; 13. Between day 13 to 78 of release: Every 5 days.	0.3	30
2nd Loading*					

*Release B and 2nd Loading were performed using exactly the same lenses materials (first in Release B and then in 2nd Loading).

To study the effect of the release conditions, samples were soaked in the same conditions but the protocol of release has modified. The studied curves were named: Release A and Release B. The results are exhibited in Figure 45.

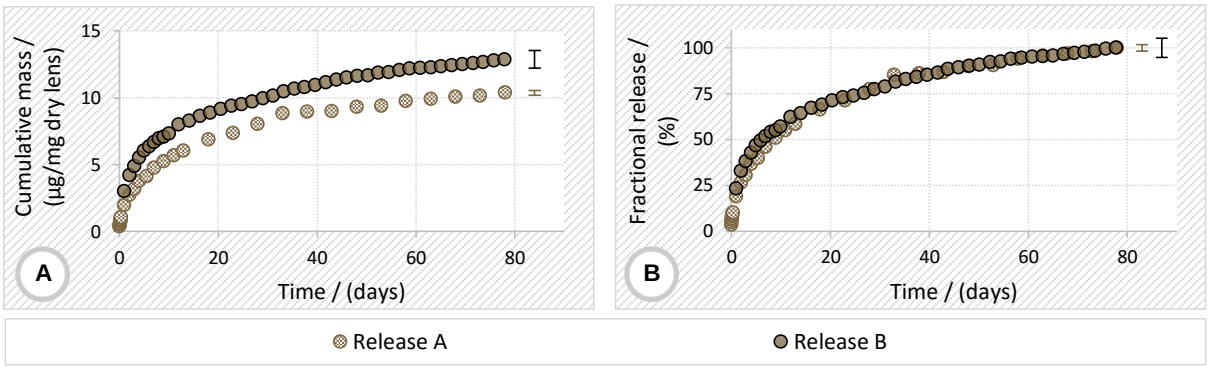

Figure 45. Cumulative release (A) and fractional release (%) (B) profiles of MXF from B26Y, determined by UV−Vis spectrophotometry, using different conditions of release. The error bars correspond to ± mean SD.

The drug release results appear to have been affected by the change in the rates of collection of aliquots during the release assay. However, it seems that only the amount released was influenced, while the kinetic, in terms of percentage released, was maintained. The total mass released was $179{,}15 \pm 5{,}19\ \mu g/lens$ in Release A and $234{,}98 \pm 5{,}10\ \mu g/lens$ in Release B (more 31.16% of drug than in Release A). The total volume of fresh solution that passed through the lenses material during the experiment was $12\ mL$ in the release A and $132\ mL$ in the release B. This means that a more efficient "washing" was done in Release B and the driving force was increased, leading to a higher amount of drug released.

Several studies in the literature report the effect that the release conditions may have in the release behaviour. The most important parameters that may influence the release are the volume, the mixing rate and the temperature of the assay. A. Tieppo et al. [159] demonstrate that the experimental conditions chosen to study the release behaviour, have a considerable effect on the release profiles. They showed that the amount of drug released in large volumes with mixing was 3 to 12 times greater than the released amounts in small volumes with no forced mixing. They also observed that an increase in temperature and mixing rate increases the fractional mass released by 1.2 and 1.4 times, respectively. Due these influences, they recommend the utilization of a dynamic, continuous flow system with low volumetric flow to perform the assays.

To evaluate the reversibility of the loading/release behaviour, samples were loaded and submitted to release studies under identical conditions, but one set of samples was new, and the other one reused samples used in Release B), i.e., the first set of materials was not previously submitted to any procedure but the second set was previously soaked at $60^{o}C$ for 4 days and used after finishing the release study. Before use this second set of samples, the materials were "washed" in $250\ mL$ of DD water, placed in a shaker at $36^{o}C$ at $400\ rpm$ for $48\ h$, to remove any traces of the drug and then dried for 7 days at $36^{o}C$ before starting the new drug loading/release assay. The release curves obtained with the two types of samples were named 1^{st} Loading (new) and 2^{nd} Loading (reused) and are presented in Figure 46.

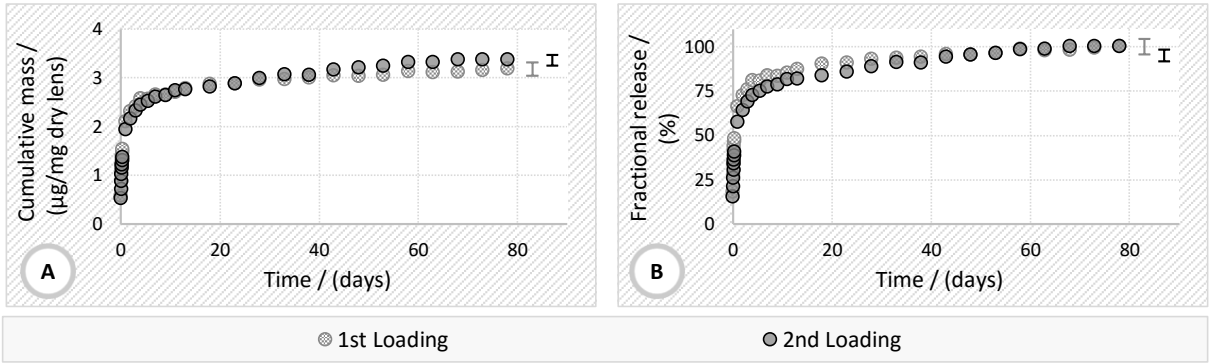

Figure 46. Cumulative release (A) and fractional release (%) (B) profiles of MXF from B26Y, determined by UV−Vis spectrophotometry for new (1^{st} Loading) and reused (2^{nd} Loading) samples. The error bars correspond to $\pm$ mean SD.

Identical release profiles were observed for both experimental conditions. This demonstrates that the loading/release behaviour was reversible, and hence, the interactions between the polymer and the drug, when disks are loaded at $60^{o}C$ may also be reversible. The total amount of mass from each release was $65{,}39 \pm 4{,}41\ \mu g/lens$ in 1^{st} Loading and $61{,}37 \pm 2{,}54\ \mu g/lens$ in 2^{nd} Loading.

Lastly, to infer about the possibility of a part of the drug have remained inside the material, the drug uptake (determined from depletion measurements) and the drug release from the samples used in Release B and "2^{nd} Loading were compared. The values obtained are given in Table 17.

Table 16. Experimental values of MXF uptake through loading solutions and MXF released.

Release curve names	MXF uptake (µg/mg dry lens)	MXF released (µg/mg dry lens)
*Release B	12 ± 1	12.9 ± 0.7
*2^{nd} Loading	3.0 ± 0.3	3.4 ± 0.1

The analysis of the results shows that in both, "Release B" and "2^{nd} Loading", all the drug (or the majority of the drug) entered to the disk was released. Once more, this confirms that the interactions between the polymer and the drug are more likely to be reversible.

IV-3. Effect of storage of IOLs materials loaded with MXF

This section aims to explore the effect of storage on IOLs materials pre-loaded with MXF. It is intended to assess the drug release behaviour and the activity of the drug released, after IOLs materials have been soaked in the drug solution at high temperatures, SH sterilized and kept in the drug solution for different periods.

Knowing in advance that any ophthalmic solution exists on the market without other excipients, and to ascertain if these excipients could have some effect in the release behaviour under the studied procedures, MXF was used in its pure form (MXF hydrochloride solution) and compared to its commercial form, VGMX ophthalmic solution $5\ mg/ml$, free of preservatives, for the whole process. The same drug concentration was used in both cases. Considering what was mentioned before about the

effect of the pH of the solutions, in this section, to limit the possibility of having one more variable, the solvent used was HBSS (pH 7.3 – buffer solution).

IV-3.1. Drug release studies

Lenses materials were previously soaked for 4 days at 60 and $80^{o}C$ with $1\ mL$ of MXF solution (commercial or prepared in the lab), and sterilized by SH in drug solution. Then, the disks were stored, for periods of 1, 2 and 3 months, in their loading solutions, protected from light and at room temperature. UV–Vis spectrophotometry was used to determine the amount of MXF released. The release profiles of IOLs loaded at $60^{o}C$ are presented in Figure 47 and at $80^{o}C$ in Figure 48. For comparison purposes, the profiles obtained with non-stored samples, both non-sterilized and SH sterilized, are also included.

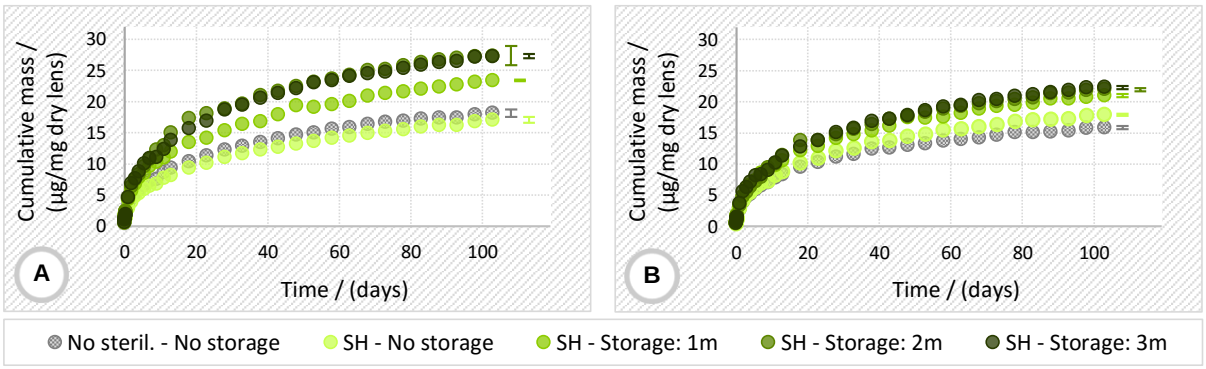

Figure 47. Cumulative release profiles of MXF from B26Y samples loaded at $60^{o}C$ and stored in their loading solution of MFX (A) or VGMX (B) for different periods. The quantifications were determined by UV–Vis spectrophotometry. The error bars correspond to $\pm$ mean SD.

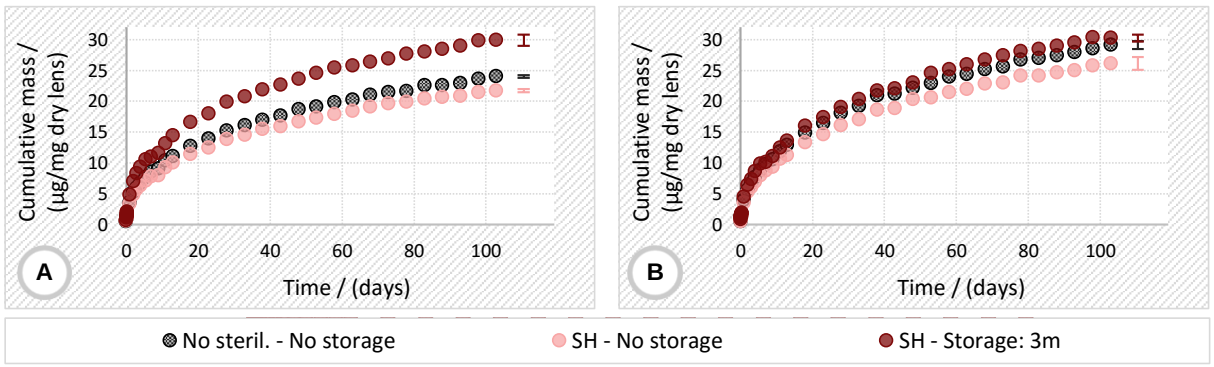

Figure 48. Cumulative release profiles of MXF from B26Y samples loaded at $80^{o}C$ and stored in their loading solution of MFX (A) or VGMX (B) for different periods. The quantifications were determined by UV–Vis spectrophotometry. The error bars correspond to $\pm$ mean SD.

For the first time in this work, the cumulative effect of loading the drug at high temperature and sterilize by SH is assessed. Focusing on the curves of non-stored samples, it can be seen that, after performing loadings at higher temperatures, sterilization has a minor or neglectable effect on the profiles. As concluded before, the rate of release was enhanced by the increase in temperature. For loadings at $60^{o}C$, no significant differences were found on the release profiles from samples soaked in pure MXF solution or in VGMX, but at $80^{o}C$, the released amount was slightly higher when samples were soaked in VGMX.

Concerning the effect of storing time, generally, for longer storage times, IOLs materials released more and the kinetic was slightly improved. This was more evident for MXF in its pure form then for VGMX. When soaked at $60^{o}C$, both formulations led to the equilibrium after 2 months (note that, the corresponding curves overlap). Although, different times of storage have not been tested when loaded at $80^{o}C$, since the value of the cumulative mass released after 100 days for 3 months of storage is higher than for the samples loaded at $60^{o}C$ (both for MFX and VGMX) it may be concluded that the equilibrium point between the drug and the material increase with temperature (this does not mean that equilibrium have been reached at $80^{o}C$).

Moreover, from the obtained results, VGMX seems to be a viable option for loading and storage this lens if proved it doesn't affect the materials proprieties.

HPLC was used to evaluate the possibility of drugs degradation. The results, available in Annex X, Tables A5 and A6, sowed that the drugs were not degraded even after 3 months of storage.

The diffusional exponent values determined with Korsmeyer–Peppas model (in Annex VIII, Table A3 were between $0.45 < n < 0.89$ denoting a non-Fickian drug diffusion or anomalous drug transport, as was already expected for loadings preformed at high temperatures.

IV-3.2. Determination of the activity of released drugs

To evaluate the stability of the drug released after 3 months of storage of the disks loaded at $60^{o}C$ and $80^{o}C$ with MXF and VGMX solutions and SH sterilized, microbiological assays were performed with the objective of determining the drugs activity against SA and SE. For this purpose, the solutions collected at day 3 and 7 were quantified by HPLC. Then, using the agar diffusion method the antimicrobial activity (%) was calculated with Equations 5 and 7. The results (in Annex XII, Figure A16) showed that in all cases the drug was still active, in their maximum performance.

IV-3.3. Estimation of the *in vivo* efficacy of drug loaded lenses

A mathematical model that considers the physiological conditions of the anterior chamber of the eye, in particular the rate of renovation and the volume of AH present in the eye at each instant, was applied to estimate the MXF concentration in the AH over time, after implantation of a drug loaded IOL. The model was adapted to the proposed by R. Galante et al. [160]. It assumes that the amount of drug delivered by a drug loaded lens to the AH (M_t), during a given time interval (Δt) can be estimated by:

$$M_t = \dot{q} \times m_l \times \Delta t \qquad \textbf{Equation 15}$$

where m_l is the dry mass of the lens and $\dot{q}$ is the fraction of drug released at each minute. The lenses mass used, were the mean weight obtained experimentally for each set of lenses used in the experimental release (approx. $20\ mg$). Using the software TableCurve $2D$, the equation that better describes the cumulative release data was found (by fitting the experimental data) and then by calculating the derivative of that expression, $\dot{q}$ was obtained.

Assuming a renewal rate of the AH of $2.4 \pm 0.6\ \mu l/min$ [161], and a total volume (V_t) of $248 \pm 12\ \mu L$ [162], the volume fraction of renovated fluid in each minute, R_r corresponds to $0{,}0096$, i.e. $0{,}96\%$.

Thus, the drug concentration in the aqueous chamber, $[\mathrm{Drug}]_t$, at a given time, t (min) after the lens implantation can be estimated using the following equation:

$$[\mathrm{Drug}]_t = \left(\frac{M_t}{V_t}\right) + (1 - R_r) \times [\mathrm{Drug}]_{t-1} \qquad \textbf{Equation 16}$$

The model was applied to all the data obtained in the study of the effect of storage. The obtained results for the predicted MXF concentrations in the AH are represented in Figure 49 for samples soaked in pure MXF solution and in Figure 50 for samples soaked in VGMX solution. Table 17 resumes the estimated times, during which the concentration of the drug in the AH shall be above the MIC. Two values of MIC were considered (0.5 $\mu g/mL$ and 1 $\mu g/mL$) in agreement with what was determined in section IV-1.

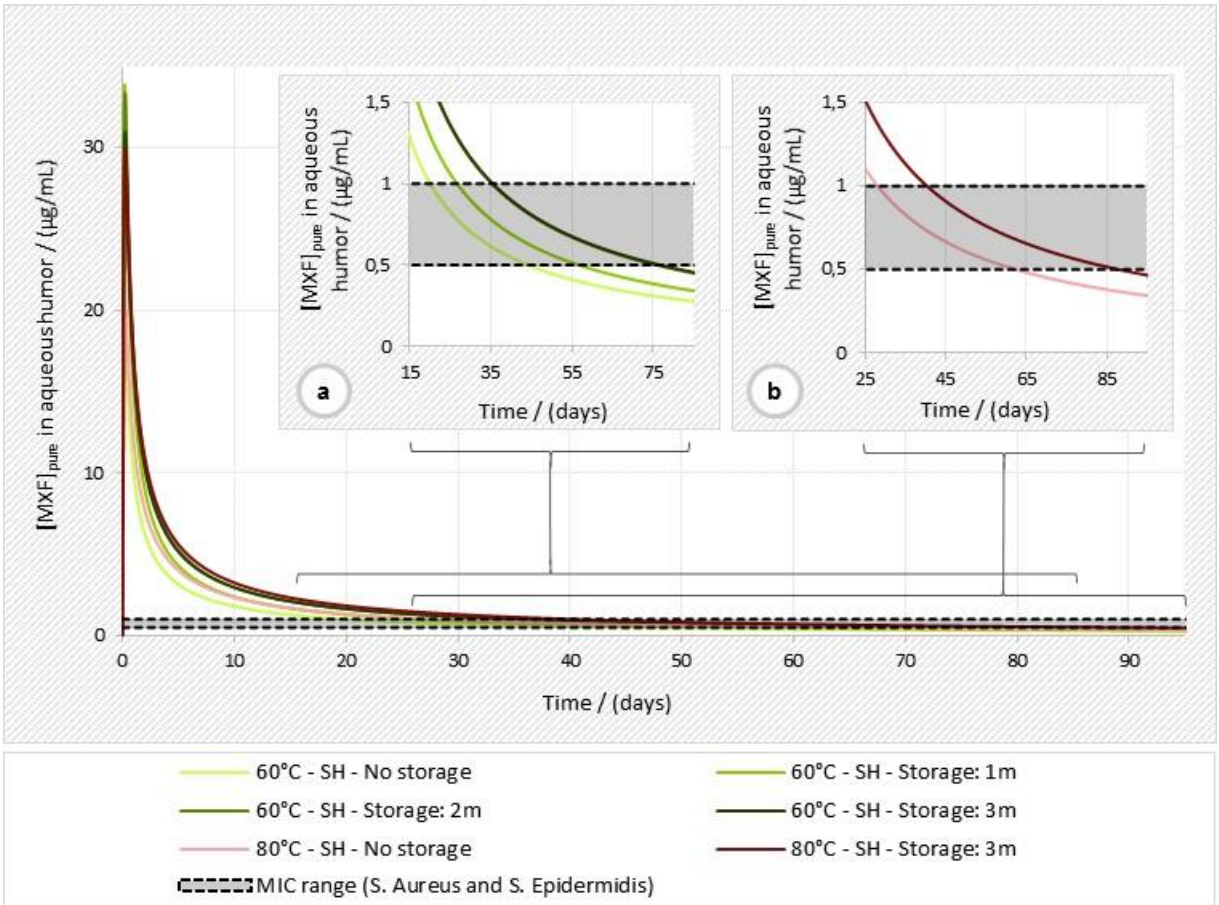

Figure 49. Prediction of [MXF] in the AH, resulting from the drug release of disks loaded at $60^{o}C$ (a) and $80^{o}C$ (b), sterilized by SH and stored in MXF solution.

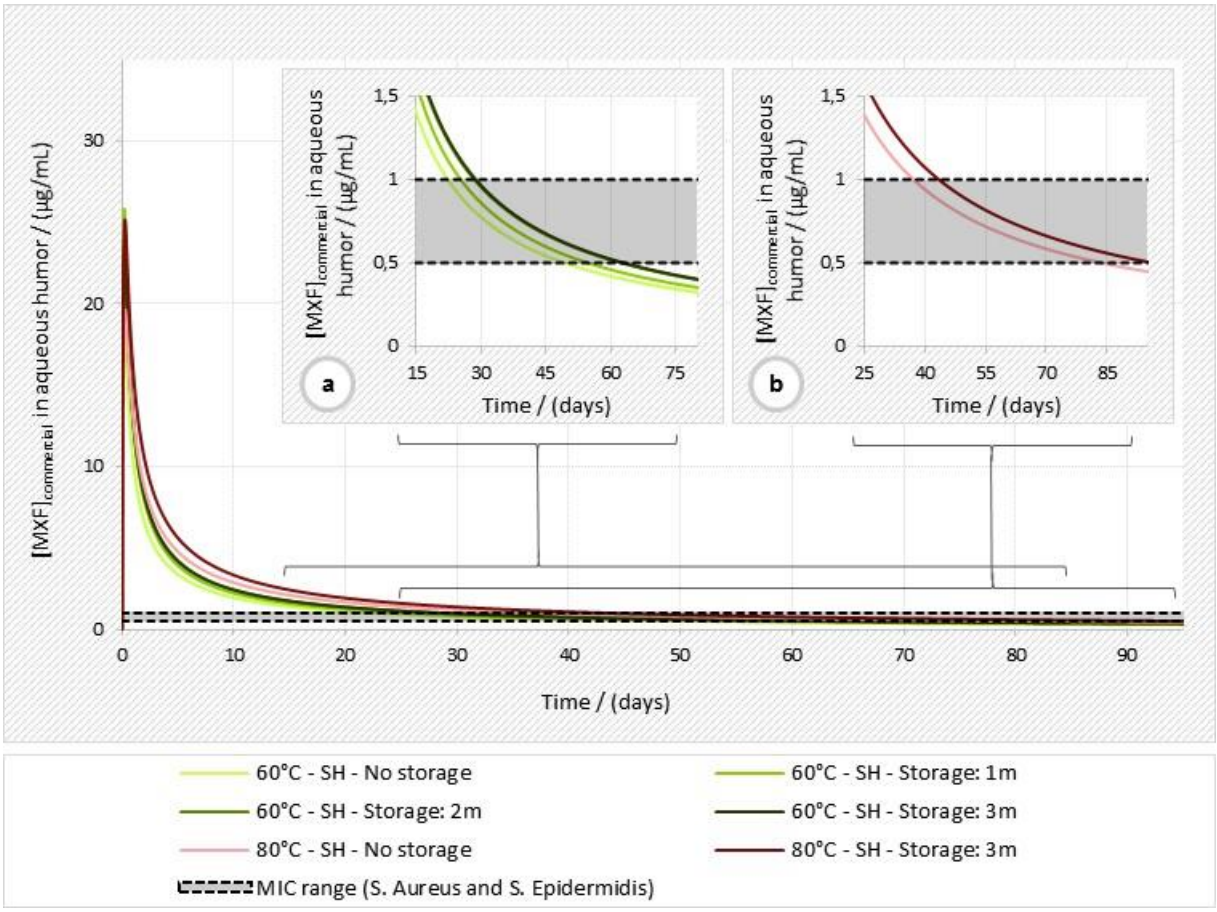

Figure 50. Prediction of [MXF] in the AH, resulting from the drug release of disks loaded at $60^{o}C$ (a) and $80^{o}C$ (b), sterilized by SH and stored in VGMX solution.

Table 17. Summary of the efficiency time estimated for the loaded lenses.

Drug solution	Loading T (ºC) (during 4 days)	Sterilization conditions (method, duration and moment)	Storage (months)	Nº of days with [MXF] > MIC	
				0.5 μg/mL	1 μg/mL
MXF	60ºC	SH 30 min After loading	No storage	44	20
			1	57	27
			2	76	35
			3	77	35
	80ºC		No storage	63	28
			3	88	40
VGMX	60ºC		No storage	49	22
			1	55	25
			2	62	28
			3	63	29
	80ºC		No storage	84	37
			3	96	44

The results show that the loaded lenses shall be efficient at least 20 days. In some cases, the concentrations remain above the MIC up to $80 - 90$ days. This means that the loading conditions may need to be adjusted, so that the release only occurs during the therapeutic period set ($1 - 2$ weeks) and does not bring the risk of inducing bacteria resistance to the antibiotic.

There are few pharmacokinetic data in literature, concerning the effect of drug loaded IOLs implantation.

G. Kleinmann, et al., evaluated the performance and safety of a hydrophilic acrylic IOL implanted in rabbit eyes, pre-soaked for 24h with MXF (at $5\ \text{mg/mL}$) [163]. Clinical examinations were performed $24\ \text{h}$ postoperatively, and AH samples were collected at 4, 8, and 12 hours after IOL implantation. None eye showed signs of clinical toxicity and the determined antibiotic mean concentrations were $9.78 \pm 2.69\ \mu\text{g/mL}$, $4.55 \pm 0.90\ \mu\text{g/mL}$ and $2.66 \pm 0.28\ \mu\text{g/mL}$ correspondingly. In our work, an accentuated decrease of the predicted concentration of MXF in AH was also observed in the first hours, after an initial burst. However, the values of [MXF] in AH that we predict using the model are quite superior (although bellow the toxicity limit which shall be $\geq 140\ \mu\text{g/mL}$ [164]). In fact, they cannot be directly compared with those obtained by Kleinmann, et al., since the polymeric matrix is not exactly the same and the conditions of preparation of the lenses (e.g. loading time, loading temperature, sterilization and storage) are distinct. Howsoever, it shall be stressed that it is important to get a sustained release that ensures [MXF] in AH higher than the MIC for a long period, since besides early acute endophthalmitis which manifests within the first 2 days after surgery, subacute endophthalmitis, which presents a much higher prevalence may occur till the 30^{th} day after surgery [165]. After the 1^{st} month, prolonged and persistent inflammation marked chiefly by new connective tissue formation (chronic endophthalmitis), may also be observed.

It is important to note that the applied model is a simplistic approach that does not take into account other clearance mechanisms of the drug or the effect of the AH composition. The way the fitting of the experimental data is done may origin significant differences in the time of efficiency of the lenses (time during which the predicted [MXF] in AH > MIC), due to the low slope of the curves in this zone. More, the variations in the values considered for the MIC also have significant repercussions in the time of efficiency of the lenses. The model gives a rough idea of what shall happen *in vivo*, but the best way to check the lens behaviour would be through clinical trials on animals. Antibiotic resistance tests shall also be carried out to validate the safety of the lenses before proceed to higher stage tests.

V. CONCLUSIONS AND FUTURE WORK

V-1. Conclusions

The main conclusion from the results obtained with the stability studies and antimicrobial assays of the studied drugs is that the effects of sterilization depend, not only on the method, but also on the type of drug preparation. For all studied drugs there was no degradation when they were sterilized by SH (in solution) or with all doses of GR (in powder). However, all drugs degraded with higher doses of GR (15 and 25 kGy) when they were sterilized in solution. Generally, anti-inflammatories were more degraded by GR than antibiotics when in solution, being DFN the most affected. Moreover, KTL and MXF were better resistant to GR when combined, especially for higher doses of GR. Considering that MXF+KTL solution was more concentrated then MXF and KTL solutions, the number of particles competing during radiolysis is higher, thus the percentage of particles affected by radiolysis in the mixture decreased when comparing with MXF and KTL solutions. Also, the addition of mannitol as a radio-protective excipient did not present the expected effect of protection. A major concern with the results of GR sterilization is that the identification and the determination of the side effects of the radiolytic products resulting from the decomposition of the drug solutions was not achieved. Lastly, the sterility tests indicated that only SH was able to ensure the sterility state, while the results for GR were not fully conclusive.

Regarding the effects of sterilization on the properties of the ophthalmic lenses materials, it was found that the increase in the radiation dose affects some of the CLs properties, decreasing the transmittance below the threshold established for the CLs (for 15 and 25 kGy of GR), decreasing the EWC and slightly decreasing the hydrophilicity. In the case of B26Y only a partial degradation of the violet light filtering chromophore and a slightly increase in the hydrophilicity was noted with the increase of the radiation dose. The main conclusion about the effects of sterilization on the materials properties is that SH is the more appropriate method for the sterilization of both materials, but also GR (5 kGy) for both materials and all doses for IOLs materials (without the UV-A blocking and the violet light filtering chromophore) may be used. Moreover, within the study of both materials proprieties, the swelling profiles demonstrate that the water uptake was faster at high temperatures and the EWC was higher at low temperatures. Finally, the sterility tests made for both materials sterilized with SH and GR (5 kGy) revealed that both lenses were sterile. Other modifications in the lenses materials matrix may also had occurred however they were not detected by the studied properties.

From the drug release experiments carried out with both materials, it is possible to conclude that the effects of the sterilization methods (SH and 5 kGy of GR) on the drug release behaviour were similar for different drugs, in the same sterilization conditions and for each lens material. In relation to IOLs material, GR slightly decreased the release of the studied drugs, while SH improved the release profile, not only in the amount released but also in the kinetics of release. Referring to CLs material, GR led to a lower release of the drug, while SH did not affect the drug release. Application of the Korsmeyer–Peppas model to the release profiles led to the conclusion that drug release was controlled by non-Fickian drug diffusion with the exception of MXF and for MXF+KTL releases from B26Y which

demonstrated a Fickian behaviour. For both materials sterilized in drug solution with $5\ \mathrm{kGy}$ of GR, the chromatograms of all the drug release solutions revealed degradation peaks.

In regard to the effect of the sterilization on the proprieties of drug loaded IOLs materials only the transmissibility of irradiated lenses loaded with KTL was affected. Summarizing, GR may not be an option for the sterilization of drug loaded materials specially if the degradation products prove to be harmful for the patient ocular tissues. However, SH is a great option for both materials, it didn't cause any harmful effect and improved the quantity of drug released, the release rate and delivered the drugs for a longer period.

It is well known that is not possible to achieve a single sterilization method for all drug delivery systems. Instead, for each system, sterilization studies must be performed.

The MXF loaded IOLs materials were chosen for further investigation of the effects of SH sterilization and of the loading/release conditions on the properties and release profiles, due to the promising results presented for the release of drugs from this material when sterilized by SH. The most relevant conclusions obtained from the study of the effects of SH sterilization conditions on the release profiles are:

1. No effect of the moment of sterilization (1^{st} day or 3^{rd} day of the loading period);
2. No effect of the sterilizing period (30, 60 or 90 min);
3. The increase in drug concentration of the loading/sterilization solution increases the quantity released but does not affect the release rate.

For all SH sterilizing conditions, a sustained release was observed for more than 60 days.

Relatively to the loading conditions, we restricted the study only to the effect of temperature. The increase in temperature led to the increase on the amount of drug released and highly improved the drug release kinetics. MXF was not degraded as a consequence of having been exposed to $60^{\mathrm{o}}\mathrm{C}$ and $80^{\mathrm{o}}\mathrm{C}$ during 4 days. Application of the Korsmeyer–Peppas model to the release data showed that when lenses materials are soaked at $4^{\mathrm{o}}\mathrm{C}$, independently of being sterilized, the diffusion mechanism is mostly Fickian. However, for temperature $\geq 36^{\mathrm{o}}\mathrm{C}$, the diffusion turns into a non-Fickian process.

Concerning the properties of IOLs materials loaded at high temperatures:

1. The swelling profiles demonstrate that, even in the presence of the drug, the solution uptake is faster and the EWC decreases with the increase of temperature.
2. The $\mathrm{T_g}$ values obtained for loaded IOLs at 4 or $60^{\mathrm{o}}\mathrm{C}$ with MXF, were not affected either by the presence of the drug or by the temperature at which the material was exposed.
3. From the NMR studies the main conclusions were that the sustained release of MXF from materials loaded at high temperature results from the plasticizing effect of the water and, mainly, from the interactions between MXF and the polymeric matrix, specially with the PMMA component. The results from the reversibility studies of loading/release behaviour suggest that these interactions are reversible.

Finally, the modifications of the release conditions led to conclude that the increase in the frequency of aliquots collection and consequently, in the volume used to perform the release, increased the amount released but did not affect the kinetics in percentage terms.

Analysis of the influence of the time of storage on the drug release profiles was done using the IOLs materials loaded in different conditions. For longer storage times, IOLs materials release more and the release kinetic was lightly improved. This was more evident for MXF in its pure form then for VGMX. When soaked at $60^{o}C$, both formulations reached the equilibrium after 2 months. VGMX seems to be also a viable option for loading and storage the IOLs, if proved that it does not affect the materials properties. Moreover, for loadings performed at high temperatures, sterilization had a minor or neglectable effect on the profiles. No degradation of the released drug was observed being active in their maximum performance after 3 months of storage.

From the estimation of the *in vivo* efficacy of drug loaded IOLs materials, it was concluded that the drugs may be released, in some cases during $80 - 90$ days above the MIC. Considering that the MXF therapeutic period after cataract surgery is $1 - 2$ weeks, this means that the loading conditions may need to be adjusted by changing temperature, loading time and concentration of loading solution. Furthermore, we must stress that the model applied to estimate the *in vivo* efficacy is a simplistic approach which does not take into account other clearance mechanisms of the drug in the eye, and that the predicted values will depend on the fitting to the experimental data.

V-2. Future work

Concerning drug sterilization, possible strategies to reduce the degradation caused by GR are: addition of other radio-protective excipients, reduction of the temperature of irradiation (cryo-irradiation) and/or minimization of the water content to limit the activity of the free radicals and also opt for super saturated solutions for drugs that need to be sterilized in the solution form.

To better understand what happens to the drug loaded materials upon sterilization, mechanical properties should be investigated.

Other methods of sterilization are necessary to be explored for CLs material, such as dry heat, ethylene oxide, electron beam, supercritical CO_2, H_2O_2 or O_3.

Toxicological assays are required to analyse the degradation products from the studied drugs, if GR was eventually chosen as sterilization method. In addition, other studies, such as electron paramagnetic resonance (EPR) are recommended to assess the radio stability of the drugs.

Regarding the effects of SH sterilization conditions, only temperature was analysed in this study; it would be interesting to test the effect of different pressures (without temperature) on the drug release behaviour.

Following the study of the effects of loading temperature, pH values should be monitored and controlled to keep within the best range to perform the loading experiments.

To better approach the release behaviour from the real on, release assays should be performed in dynamic conditions, using a microfluidic cell.

Additionally, besides MXF, other drugs, particularly inflammatory drugs should be considered to test with the B26Y material.

Finally, the drug loaded systems with the best performance shall be submitted to bacterial resistance tests (if loaded with antibiotic) and tested in *in vivo* experiments with animals to conclude on their safety and efficiency.

LIST OF REFERENCES

[1] K. Cholkar, S. R. Dasari, D. Pal, and A. K. Mitra, “Eye: anatomy, physiology and barriers to drug delivery,” in *Ocular Transporters and Receptors*, Elsevier, 2013, pp. 1–36.

[2] C. Van De Pol, “Anatomy and Structure of the Eye,” *Helmet Mounted Displays - Sensation, Perception and Cognitive Issues*, 2003. [Online]. Available: http://www.usaarl.army.mil/publications/HMD_Book09/files/Section 13 - Chapter 6 Anatomy and Structure of the Eye.pdf. [Accessed: 04-Sep-2016].

[3] B. G. Short, “Safety Evaluation of Ocular Drug Delivery Formulations: Techniques and Practical Considerations,” *Toxicol. Pathol.*, vol. 36, no. 1, pp. 49–62, 2008.

[4] A. L. Weiner, “Drug Delivery Systems in Ophthalmic Applications,” in *Ocular Therapeutics*, vol. 96, Elsevier, 2008, pp. 7–43.

[5] V. K. Yellepeddi and S. Palakurthi, “Recent Advances in Topical Ocular Drug Delivery,” *J. Ocul. Pharmacol. Ther.*, vol. 32, no. 2, pp. 67–82, 2016.

[6] Y. Ali and K. Lehmussaari, “Industrial perspective in ocular drug delivery,” *Adv. Drug Deliv. Rev.*, vol. 58, no. 11, pp. 1258–1268, 2006.

[7] R. Gaudana, H. K. Ananthula, A. Parenky, and A. K. Mitra, “Ocular Drug Delivery,” *AAPS J.*, vol. 12, no. 3, pp. 348–360, Sep. 2010.

[8] R. B. Nagare, D. S. Bhambere, R. S. Kumar, V. K. Kakad, and S. N. Nagare, “In Situ Gelling System: Smart Carriers for Ophthalmic Drug Delivery,” *Int. J. Pharm. Res. Sch.*, vol. 4, no. 2, pp. 10–23, 2015.

[9] Y. Kapoor and A. Chauhan, “Ophthalmic delivery of Cyclosporine A from Brij-97 microemulsion and surfactant-laden p-HEMA hydrogels.,” *Int. J. Pharm.*, vol. 361, no. 1–2, pp. 222–229, 2008.

[10] B. Mandal, K. S. Alexander, and A. T. Riga, “Sulfacetamide loaded Eudragit® RL100 nanosuspension with potential for ocular delivery.,” *J. Pharm. Pharm. Sci. a Publ. Can. Soc. Pharm. Sci. Société Can. des Sci. Pharm.*, vol. 13, no. 4, pp. 510–523, 2010.

[11] J. I. Lim, M. Niec, and V. Wong, “One year results of a phase 1 study of the safety and tolerability of combination therapy using sustained release intravitreal triamcinolone acetonide and ranibizumab for subfoveal neovascular AMD,” *Br. J. Ophthalmol.*, vol. 99, no. 5, pp. 618–623, 2015.

[12] J. Barar, A. Aghanejad, M. Fathi, and Y. Omidi, “Advanced drug delivery and targeting technologies for the ocular diseases,” *Bioimpacts*, vol. 6, no. 1, pp. 49–67, 2016.

[13] O. Wichterle and D. Lím, “Hydrophilic Gels for Biological Use,” *Nature*, vol. 185, no. 4706, pp. 117–118, 1960.

[14] T. R. R. Singh and D. Jones, “Advances in ophthalmic drug delivery,” *J. Pharm. Pharmacol.*, vol. 66, no. 4, pp. 487–489, 2014.

[15] D. Bozukova, C. Pagnoulle, R. Jérôme, and C. Jérôme, “Polymers in modern ophthalmic implants—Historical background and recent advances,” *Mater. Sci. Eng. R Reports*, vol. 69, no. 6, pp. 63–83, 2010.

[16] X. Hu, L. Hao, H. Wang, X. Yang, G. Zhang, G. Wang, and X. Zhang, “Hydrogel Contact Lens for Extended Delivery of Ophthalmic Drugs,” *Int. J. Polym. Sci.*, vol. 2011, no. 14, pp. 1–9, 2011.

[17] H. P. Filipe, J. Henriques, P. Reis, P. C. Silva, M. J. Quadrado, and A. P. Serro, “Contact lenses as drug controlled release systems: a narrative review,” *Rev. Bras. Oftalmol.*, vol. 75, no. 3, pp. 241–247, 2016.

[18] K. Boyd and E. M. Jimenez, “Catarats,” *American Academy of Ophthalmology*, 2014. [Online]. Available: http://www.aao.org/eye-health/diseases/what-are-cataracts. [Accessed: 12-Aug-2016].

[19] CDER, “Approval Letter (NDA 20-809) on April 5, to Alcon, Inc.” Maryland, Rockville, 1998.

[20] CDER, “Approval Letter (NDA 21–528) on May 30, to Allergan, Inc.” United States, 2003.

[21] CDER, “Approval Letter (NDA 21–598) on April 15, to Alcon, Inc.” Maryland, Rockville, 2003.

[22] J. I. Lim, V. A. Shah, S. Kamjoo, and K. Tripathy, “Endophthalmitis,” *American Academy of Ophthalmology*, 2014. [Online]. Available: http://eyewiki.aao.org/Endophthalmitis. [Accessed: 12-Aug-2016].

[23] M. L. Durand, “Endophthalmitis,” *Clin. Microbiol. Infect.*, vol. 19, no. 3, pp. 227–234, 2013.

[24] C. González-Chomón, A. Concheiro, and C. Alvarez-Lorenzo, “Drug-Eluting Intraocular Lenses,” *Materials (Basel).*, vol. 4, no. 12, pp. 1927–1940, 2011.

[25] “Refractive surgery,” *American Academy of Ophthalmology*, 2015. [Online]. Available: http://www.aao.org/eye-health/treatments/what-is-refractive-surgery. [Accessed: 12-Aug-2016].

[26] K. Boyd, E. M. Jimenez, and D. A. Harrison, “Conjunctivitis,” *American Academy of Ophthalmology*, 2015. [Online]. Available: http://www.aao.org/eye-health/diseases/pink-eye-conjunctivitis. [Accessed: 12-Aug-2016].

[27] K. Boyd and D. A. Harrison, “Keratitis,” *American Academy of Ophthalmology*, 2015. [Online]. Available: http://www.aao.org/eye-health/diseases/what-is-keratitis. [Accessed: 12-Aug-2016].

[28] “Diclofenac sodium salt,” *Sigma-Aldrich*. [Online]. Available: http://www.sigmaaldrich.com/catalog/product/sigma/d6899?lang=en&region=US&gclid=CPX1l82pvs4CFRJZhgodvlIIPQ. [Accessed: 13-Aug-2016].

[29] “Acular LS Label.” Allergan, Inc., United States, 2011.

[30] “Ketorolac Ophthalmic,” *American Society of Health-System Pharmacists, Inc.*, 2016. [Online]. Available: https://medlineplus.gov/druginfo/meds/a601241.html. [Accessed: 12-Aug-2016].

[31] “Vigamox Label.” Alcon, Inc., Fort Worth, United States, 2011.

[32] “Moxifloxacin Ophthalmic,” *American Society of Health-System Pharmacists, Inc.*, 2016. [Online]. Available: https://medlineplus.gov/druginfo/meds/a605016.html. [Accessed: 12-Aug-2016].

[33] D. Miller, “Review of moxifloxacin hydrochloride ophthalmic solution in the treatment of bacterial eye infections,” *Clin. Ophthalmol.*, vol. 2, no. 1, p. 77, 2008.

[34] C. M. Adeyeye and P.-K. Li, “Diclofenac Sodium,” in *Analytical Profiles of Drug Substances*, vol. 19, 1990, pp. 123–144.

[35] “Ketorolac Tromethamine,” *Sigma-Aldrich*. [Online]. Available: http://www.sigmaaldrich.com/catalog/substance/ketorolactromethamine376407410307411?lang=en&region=US. [Accessed: 13-Aug-2016].

[36] D. S. Wishart, C. Knox, A. C. Guo, S. Shrivastava, M. Hassanali, P. Stothard, Z. Chang, and J. Woolsey, “Ketorolac,” *DrugBank database*, 2016. [Online]. Available: http://www.drugbank.ca/drugs/DB00465. [Accessed: 13-Aug-2016].

[37] M. M. H. Al Omari, D. S. Jaafari, K. A. Al-Sou’od, and A. A. Badwan, “Moxifloxacin Hydrochloride,” in *Profiles of drug substances, excipients, and related methodology*, vol. 39, 2014, pp. 299–431.

[38] F. Varanda, M. J. Pratas de Melo, A. I. Caço, R. Dohrn, F. A. Makrydaki, E. Voutsas, D. Tassios, and I. M. Marrucho, “Solubility of Antibiotics in Different Solvents. 1. Hydrochloride Forms of Tetracycline, Moxifloxacin, and Ciprofloxacin,” *Ind. Eng. Chem. Res.*, vol. 45, no. 18, pp. 6368–6374, 2006.

[39] C. R. G. Espiritu, M. E. A. Sy, and T. L. G. Tayengco, “Efficacy and Tolerability of a Combined Moxifloxacin/Dexamethasone Formulation for Topical Prophylaxis in Phacoemulsification: An Open-Label Single-Arm Clinical Trial,” *J. Ophthalmol.*, vol. 2011, pp. 1–5, 2011.

[40] B. A. Schechter, “Ketorolac During the Induction Phase of Cyclosporin-A Therapy,” *J. Ocul. Pharmacol. Ther.*, vol. 22, no. 2, pp. 150–154, 2006.

[41] M. E. Pina, P. Coimbra, P. Ferreira, P. Alves, A. I. Figueiredo, and M. H. Gil, “Polymeric Materials in Ocular Drug Delivery Systems,” in *Handbook of Polymers for Pharmaceutical Technologies*, vol. 2, Hoboken, NJ, USA: John Wiley & Sons, Inc., 2015, pp. 439–458.

[42] M. S. Attia and M. S. A. Abdel-Mottaleb, “Polymer-Doped Nano-Optical Sensors for Pharmaceutical Analysis,” in *Handbook of Polymers for Pharmaceutical Technologies*, Hoboken, NJ, USA: John Wiley & Sons, Inc., 2015, pp. 383–409.

[43] L. Werner, “Glistenings and surface light scattering in intraocular lenses,” *J. Cataract Refract. Surg.*, vol. 36, no. 8, pp. 1398–1420, 2010.

[44] R. Bellucci, “An Introduction to Intraocular Lenses: Material, Optics, Haptics, Design and Aberration,” in *Cataract*, vol. 3, 2013, pp. 38–55.

[45] “Intraocular Lens Materials & Manufacturing Technology 2013.” [Online]. Available: http://benzrd.com/Uploads/2013_benz_manual.pdf. [Accessed: 13-Aug-2016].

[46] “ISO 21348:2007,” *Space environment (natural and artificial) - Process for determining solar irradiances*. [Online]. Available: https://www.iso.org/obp/ui/#iso:std:iso:21348:ed-1:v1:en. [Accessed: 26-Aug-2016].

[47] “Methyl methacrylate,” *PubChem*. [Online]. Available: https://pubchem.ncbi.nlm.nih.gov/compound/6658#section=Vapor-Pressure. [Accessed: 13-Aug-2016].

[48] “Methyl methacrylate,” *Sigma-Aldrich*. [Online]. Available: http://www.sigmaaldrich.com/catalog/product/aldrich/m55909?lang=en&region=US. [Accessed: 13-Aug-2016].

[49] “2-Hydroxyethyl methacrylate,” *PubChem*. [Online]. Available: https://pubchem.ncbi.nlm.nih.gov/compound/13360#section=Top. [Accessed: 13-Aug-2016].

[50] “2-Hydroxyethyl methacrylate,” *Sigma-Aldrich*. [Online]. Available: http://www.sigmaaldrich.com/catalog/product/aldrich/128635?lang=en&region=US. [Accessed: 13-Aug-2016].

[51] “N-Vinyl-2-Pyrrolidone,” *PubChem*. [Online]. Available: https://pubchem.ncbi.nlm.nih.gov/compound/6917#section=3D-Conformer. [Accessed: 13-Aug-2016].

[52] “1-Vinyl-2-pyrrolidinone,” *Sigma-Aldrich*. [Online]. Available: http://www.sigmaaldrich.com/catalog/product/sial/95060?lang=en&region=US. [Accessed: 13-Aug-2016].

[53] K.-H. Hsu, S. Gause, and A. Chauhan, “Review of ophthalmic drug delivery by contact lenses,” *J. Drug Deliv. Sci. Technol.*, vol. 24, no. 2, pp. 123–135, 2014.

[54] N. Efron and C. Maldonado-Codina, “Development of Contact Lenses from a Biomaterial Point of View – Materials, Manufacture, and Clinical Application,” in *Comprehensive Biomaterials*, Elsevier, 2011, pp. 517–541.

[55] “Beer-Lambert Law: Measuring Percent Transmittance of Solutions at Different Concentrations (Teacher’s Guide),” *Ward’s Science*, 2012. [Online]. Available: https://www.wardsci.com/www.wardsci.com/images/BeerLamb_Colorimeter.pdf. [Accessed: 17-Aug-2016].

[56] A. Patel and K. Mequanint, “Hydrogel Biomaterials,” in *Biomedical Engineering - Frontiers and Challenges*, R. Fazel-Rezai, Ed. InTech, 2011, pp. 275–296.

[57] N. Peppas, “Hydrogels in pharmaceutical formulations,” *Eur. J. Pharm. Biopharm.*, vol. 50, no. 1, pp. 27–46, 2000.

[58] S. A. Dergunov and G. A. Mun, “γ-Irradiated chitosan-polyvinyl pyrrolidone hydrogels as pH-sensitive protein delivery system,” *Radiat. Phys. Chem.*, vol. 78, no. 1, pp. 65–68, 2009.

[59] C. E. Soltys-Robitaille, D. M. Ammon, P. L. Valint, and G. L. Grobe III, “The relationship between contact lens surface charge and in-vitro protein deposition levels,” *Biomaterials*, vol. 22, no. 24, pp. 3257–3260, 2001.

[60] P. Paradiso, R. Galante, L. Santos, A. P. Alves de Matos, R. Colaço, A. P. Serro, and B. Saramago, “Comparison of two hydrogel formulations for drug release in ophthalmic lenses,” *J. Biomed. Mater. Res. Part B Appl. Biomater.*, vol. 102, no. 6, pp. 1170–1180, 2014.

[61] J. H. Park and Y. H. Bae, “Hydrogels based on poly(ethylene oxide) and poly(tetramethylene oxide) or poly(dimethyl siloxane): synthesis, characterization, in vitro protein adsorption and platelet adhesion,” *Biomaterials*, vol. 23, no. 8, pp. 1797–1808, 2002.

[62] A. S. Hoffman, “Hydrogels for biomedical applications,” *Adv. Drug Deliv. Rev.*, vol. 54, no. 1, pp. 3–12, 2002.

[63] T. Alfrey, E. F. Gurnee, and W. G. Lloyd, “Diffusion in glassy polymers,” *J. Polym. Sci. Part C Polym. Symp.*, vol. 12, no. 1, pp. 249–261, Mar. 1996.

[64] C. Abela-Formanek, M. Amon, J. Schauersberger, A. Kruger, J. Nepp, and G. Schild, “Results of hydrophilic acrylic, hydrophobic acrylic, and silicone intraocular lenses in uveitic eyes with cataract: comparison to a control group.,” *J. Cataract Refract. Surg.*, vol. 28, no. 7, pp. 1141–1152, 2002.

[65] Q. Huang, G. Pak, M. Cheng, K. Chiu, and G. Q. Wang, “Surface Modification of Intraocular Lenses,” vol. 129, no. 2, pp. 206–214, 2016.

[66] T. Young, “An Essay on the Cohesion of Fluids,” *Philos. Trans. R. Soc. London*, vol. 95, pp. 65–87, 1805.

[67] Y. Yuan and T. R. Lee, “Contact Angle and Wetting Properties,” in *Surface Science Techniques*, vol. 51, no. 1, G. Bracco and B. Holst, Eds. Berlin, Heidelberg: Springer Berlin Heidelberg, 2013, pp. 3–34.

[68] F. J. Montes Ruiz-Cabello, M. A. Rodríguez-Valverde, A. Marmur, and M. A. Cabrerizo-Vílchez, “Comparison of Sessile Drop and Captive Bubble Methods on Rough Homogeneous Surfaces: A Numerical Study,” *Langmuir*, vol. 27, no. 15, pp. 9638–9643, 2011.

[69] C.-C. Peng and A. Chauhan, “Ion transport in silicone hydrogel contact lenses,” *J. Memb. Sci.*, vol. 399–400, pp. 95–105, 2012.

[70] A. R. Ferreira da Silva, V. Compañ, and J. M. González-Méijome, “Reduction in ionic permeability of a silicone hydrogel contact lenses after one month of daily wear,” *Mater. Res. Express*, vol. 2, no. 6, pp. 1–18, 2015.

[71] Y. Qiu and X. Qian, “Methods for increasing the ion permeability of contact lenses,” Patent 20110133350, 2011.

[72] C. Lehman, “Hydrogel intraocular lens and method of forming same,” Patent 20090248150, 2009.

[73] M. T. Sheehan, “Eye modelling for personalised intraocular lens design,” National University of Ireland, 2012.

[74] A. Topete, “Effects of sterilization on drug loaded soft contact lenses,” Instituto Superior Técnico - University of Lisbon, 2015.

[75] B. Hafner and B. Hafner, “Scanning Electron Microscopy Primer,” *Characterization Facility*. University of Minnesota, pp. 1–29, 2007.

[76] T. Ariyafar, A. P. Saffar, P. Tajalli, and H. Tajalli, “Wettability and Surface Morphology Investigation of RGP Eye Contact Lens Irradiated by 193 nm Excimer Laser,” *OALib*, vol. 2, no. 4, pp. 1–8, 2015.

[77] S. Mutlur, “Thermal Analysis of Composites Using DSC,” in *Advanced Topics in Characterization of Composites*, Victoria, BC, Canada: Trafford Publishing, 2004, pp. 11–33.

[78] “Investigation of Polymers with Differential Scanning Calorimetry,” *Humboldt University of Berlin*, 2015. [Online]. Available: http://polymerscience.physik.hu-berlin.de/docs/manuals/DSC.pdf. [Accessed: 19-Aug-2016].

[79] “Calorimetro a scansione differenziale (DSC),” *La calorimetria a scansione differenziale (DSC) - Ingegneria ENG-GHM*. [Online]. Available: http://www.eng-ghm.com/Tesi/Tesi 111-120.pdf. [Accessed: 04-Sep-2016].

[80] D. Pranitha, N. Parthiban, D. Sathis Kumar, S. Ghosh, D. Banji, and Saikiran, “Solid State Nuclear Magnetic Resonance Spectroscopy – a Review,” *Asian J. Pharm. Clin. Res.*, vol. 4, no. 4, pp. 9–14, 2011.

[81] G. J. Leary and R. H. Newman, “Cross Polarization/Magic Angle Spinning Nuclear Magnetic Resonance (CP/MAS NMR) Spectroscopy,” in *Methods in Lignin Chemistry*, S. Y. Lin and C. W. Dence, Eds. Berlin, Heidelberg: Springer Berlin Heidelberg, 1992, pp. 146–161.

[82] N. Dias, “Nuclear Magnetic Resonance study of molecular interaction of ionic liquids with aromatic compounds,” Instituto Superior tecnico - University of Lisbon, 2013.

[83] D. L. Bryce, G. M. Bernard, M. Gee, M. D. Lumsden, K. Eichele, and R. E. Wasylishen, “Practical Aspects of Modern Routine Solid-State Multinuclear Magnetic Resonance Spectroscopy: One-Dimensional Experiments,” *Can. J. Anal. Sci. Spectrosc.*, vol. 46, pp. 46–82, 2001.

[84] T. Glasbey and S. D. Newman, “Methods and systems for contact lens sterilization,” Patent 8109064, 2012.

[85] “The International Pharmacopoeia - 5th Edition,” *World Health Organization*, 2015. [Online]. Available: http://apps.who.int/phint/alt/index.html#d/b.7.5.9. [Accessed: 20-Aug-2016].

[86] “ISO 11607-1:2006,” *Packaging for terminally sterilized medical devices - Part 1: Requirements for materials, sterile barrier systems and packaging systems*. [Online]. Available: https://www.iso.org/obp/ui/#iso:std:iso:11607:-1:ed-1:v1:en. [Accessed: 26-Aug-2016].

[87] “Submission and Review of Sterility Information in Premarket Notification (510(k)) Submissions for Devices Labeled as Sterile,” *FDA*, 2016. [Online]. Available: http://www.fda.gov/downloads/MedicalDevices/.../ucm109897.pdf. [Accessed: 21-Aug-2016].

[88] P. J. Missel, J. C. Lang, D. P. Rodeheaver, R. Jani, M. A. Chowhan, J. Chastain, and T. Dagnon, “Design and Evaluation of Ophthalmic Pharmaceutical Products,” in *Modern Pharmaceutics: Applications and Advances*, Volume 2., A. T. Florence and J. Siepmann, Eds. CRC Press, 2009, pp. 101–189.

[89] D. S. Aldrich, C. M. Bach, W. Brown, W. Chambers, J. Fleitman, D. Hunt, M. R. C. Marques, Y. Mille, A. K. Mitra, S. M. Platzer, T. Tice, and G. W. Tin, “Ophthalmic Preparations,” *U.S. Pharmacopeial Convention*, 2013. [Online]. Available: http://www.usp.org/sites/default/files/usp_pdf/EN/meetings/workshops/ophthalmicpreparations.pdf. [Accessed: 21-Aug-2016].

[90] “Intraocular Lens Guidance Document,” *FDA*. [Online]. Available: http://www.fda.gov/ohrms/dockets/98fr/994052gd.pdf. [Accessed: 21-Aug-2016].

[91] “Application of the device good manufacturing practice regulation to the manufacture of sterile devices,” *FDA*, 1997. [Online]. Available: http://www.fda.gov/downloads/medicaldevices/deviceregulationandguidance/guidancedocuments/ucm081619.pdf. [Accessed: 21-Aug-2016].

[92] B. M. Boca, E. Pretorius, R. Gochin, R. Chapoullie, and Z. Apostolides, “An Overview of the Validation Approach for Moist Heat Sterilization , Part I,” *Pharm. Technol.*, no. September, pp. 62–67, 2002.

[93] P. G. Mazzola, A. M. da S. Martins, and T. C. V. Penna, “Determination of decimal reduction time (D-value) of chemical agents used in hospital disinfection,” *Brazilian J. Microbiol.*, vol. 34, pp. 33–34, 2003.

[94] F. Weithöner, “Autoclaves.” [Online]. Available: http://www.frankshospitalworkshop.com/equipment/documents/autoclaves/equipment/images/vertical_construction_web.jpg. [Accessed: 20-Aug-2016].

[95] F. Hasanain, K. Guenther, W. M. Mullett, and E. Craven, “Gamma Sterilization of Pharmaceuticals--A Review of the Irradiation of Excipients, Active Pharmaceutical Ingredients, and Final Drug Product Formulations,” *PDA J. Pharm. Sci. Technol.*, vol. 68, no. 2, pp. 113–137, 2014.

[96] A. Maquille, J.-L. H. Jiwan, and B. Tilquin, “Radiosterilization of drugs in aqueous solutions may be achieved by the use of radioprotective excipients,” *Int. J. Pharm.*, vol. 349, no. 1–2, pp. 74–82, 2008.

[97] C. M. Mendes, J. C. Almeida, M. L. Botelho, M. C. Cavaco, E. Almeida-Vara, and M. E. Andrade, “The Portuguese gamma irradiation facility,” *Int. J. Radiat. Appl. Instrumentation. Part C. Radiat. Phys. Chem.*, vol. 35, no. 4–6, pp. 576–579, 1990.

[98] E. S. Kastango, “Finished Preparation Release Checks and Tests,” in *Compounding Sterile Preparations*, 3rd ed., E. C. Buchanan and P. J. Schneider, Eds. 2009, pp. 159–170.

[99] “The International Pharmacopoeia - 5th Edition,” *World Health Organization*, 2015. [Online]. Available: http://apps.who.int/phint/alt/index.html#d/b.7.3.2. [Accessed: 22-Aug-2016].

[100] “Esterilidade (2.6.1.),” in *Farmacopeia Portuguesa 9.8*, Lisboa: INFARMED, 2010, pp. 6953–7358.

[101] "Test for sterility," *WHO*, 2012. [Online]. Available: http://www.who.int/medicines/publications/pharmacopoeia/TestForSterility-RevGenMethod_QAS11-413FINALMarch2012.pdf. [Accessed: 22-Aug-2016].

[102] E. M. Tóth, A. K. Borsodi, T. Felföldi, B. Vajna, R. Sipos, and K. Márialigeti, "Cell-and germ-counting methods," in *Practical Microbiology: based on the Hungarian practical notes entitled "Mikrobiológiai Laboratóriumi Gyakorlatok,"* A. Náfrádi, Ed. Budapest: Eötvös Loránd University, 2013, pp. 27–34.

[103] "The International Pharmacopoeia - 5th Edition," *World Health Organization*, 2015. [Online]. Available: http://apps.who.int/phint/alt/index.html#d/b.7.1.14.4. [Accessed: 20-Aug-2016].

[104] "HPLC Analysis and Testing," *ACTA Laboratories*. [Online]. Available: http://www.actalabs.com/ac/HPLC.php. [Accessed: 20-Aug-2016].

[105] "Microbiology Module," *College of Veterinary Medicine, Michigan State University*, 2011. [Online]. Available: http://amrls.cvm.msu.edu/microbiology/detecting-antimicrobial-resistance/test-methods/tools/module-pdf-files/microbiology. [Accessed: 22-Aug-2016].

[106] E. M. Tóth, A. K. Borsodi, T. Felföldi, B. Vajna, R. Sipos, and K. Márialigeti, "Strain culture and cultivation-based techniques," in *Practical Microbiology: based on the Hungarian practical notes entitled "Mikrobiológiai Laboratóriumi Gyakorlatok,"* A. Náfrádi, Ed. Budapest: Eötvös Loránd University, 2013, pp. 36–103.

[107] M. Balouiri, M. Sadiki, and S. K. Ibnsouda, "Methods for in vitro evaluating antimicrobial activity: A review," *J. Pharm. Anal.*, vol. 6, no. 2, pp. 71–79, 2016.

[108] B. L. Sherwal and A. K. Verma, "Epidemiology of ocular infection due to bacteria and fungus - A prospective study," *JK Sci.*, vol. 10, no. 3, pp. 127–131, 2008.

[109] P. A. Asbell, C. M. Sanfilippo, C. M. Pillar, H. H. DeCory, D. F. Sahm, and T. W. Morris, "Antibiotic Resistance Among Ocular Pathogens in the United States," *JAMA Ophthalmol.*, vol. 133, no. 12, pp. 1445–1454, Dec. 2015.

[110] M. B. Abelson, A. Shapiro, and D. Rimmer, "Caring for the Eye's Gatekeepers," *Rev. Ophthalmol.*, vol. 23, no. 4, pp. 66–69, 2016.

[111] "Contaflex - Technical Data Sheet," *Contamac*, 2007. [Online]. Available: http://www.contamac.com/files/Soft Lens Technical Data Sheet.pdf. [Accessed: 23-Aug-2016].

[112] "Support technique (matériaux, outils d'adaptation)," in *Lentilles de Contact sur mesure*, Novacel, pp. 1–29.

[113] "BenzFlex 26 Natural Yellow - Specifications," *Benz Research & Development*. [Online]. Available: http://benzrd.com/benzflex_26_natural_yellow.php. [Accessed: 23-Aug-2016].

[114] Y. C. Lai, D. V. Ruscio, D. P. Vanderbilt, and S. P. Bartels, "Method of purification of polymeric medical device materials using continuous soxhlet extraction," Patent WO2004031275, 2004.

[115] G. Morrison, "Serum Chloride," in *Clinical Methods: The History, Physical, and Laboratory Examinations*, 3rd ed., H. K. Walker, W. D. Hall, and J. W. Hurst, Eds. Boston: Butterworth Publishers, 1990, pp. 890–894.

[116] B. Ben-Nissan, A. H. Choi, D. W. Green, B. A. Latella, J. Chou, and A. Bendavid, "Synthesis and Characterization of Hydroxyapatite Nanocoatings by Sol–Gel Method for Clinical Applications," in *Biological and Biomedical Coatings Handbook: Processing and Characterization*, S. Zhang, Ed. CRC Press, 2011, pp. 37–79.

[117] R. A. Shaalan and T. S. Belal, "Validated Stability-Indicating HPLC-DAD Method for the Simultaneous Determination of Diclofenac Sodium and Diflunisal in Their Combined Dosage Form," *Sci. Pharm.*, vol. 81, no. 3, pp. 713–731, 2013.

[118] S. Naveed and F. Qamar, "UV spectrophotometric assay of Diclofenac sodium available brands," *J. Innov. Pharm. Biol. Sci.*, vol. 1, no. 3, pp. 92–96, 2014.

[119] M. Ashfaq and I. Mariam, "Stability indicating hplc method for simultaneous determination of Moxifloxacin Hydrochloride and Ketorolac Tromethamine in pharmaceutical formulations," *Quim. Nov.*, vol. 35, no. 6, pp. 1216–1221, 2012.

[120] G. Sunil, M. Jambulingam, S. Ananda Thangadurai, D. Kamalakannan, R. Sundaraganapathy, and C. Jothimanivannan, "Development and validation of Ketorolac Tromethamine in eye drop formulation by RP-HPLC method," *Arab. J. Chem.*, 2013.

[121] P. Djurdjevic, A. Ciric, A. Djurdjevic, and M. J. Stankov, "Optimization of separation and determination of moxifloxacin and its related substances by RP-HPLC," *J. Pharm. Biomed. Anal.*, vol. 50, no. 2, pp. 117–126, 2009.

[122] N. Pradhan, H. Rajkhowa, H. Giri, and B. Shrestha, "Simultaneous spectrophotometric estimation of Moxifloxacin Hydrochloride and Doxorubicin Hydrochloride," vol. 7, no. 11, pp. 7–12, 2015.

[123] J. N. Hiremath and B. Vishalakshi, "Effect of Crosslinking on swelling behaviour of IPN hydrogels of Guar Gum and Polyacrylamide," *Der Pharma Chem.*, vol. 4, no. 3, pp. 946–955, 2012.

[124] J. Wang and W. Wu, “Swelling behaviors, tensile properties and thermodynamic studies of water sorption of 2-hydroxyethyl methacrylate/epoxy methacrylate copolymeric hydrogels,” *Eur. Polym. J.*, vol. 41, no. 5, pp. 1143–1151, 2005.

[125] M. Hoorfar and Aw. Neumann, “Axisymmetric Drop Shape Analysis (ADSA),” in *Applied Surface Thermodynamics*, 2nd ed., CRC Press, 2010, pp. 107–174.

[126] A. M. Castillo, L. Patiny, and J. Wist, “Fast and accurate algorithm for the simulation of NMR spectra of large spin systems,” *J. Magn. Reson.*, vol. 209, no. 2, pp. 123–130, 2011.

[127] H. Terryn, A. Maquille, C. Houeelevin, and B. Tilquin, “Irradiation of human insulin in aqueous solution, first step towards radiosterilization,” *Int. J. Pharm.*, vol. 343, no. 1–2, pp. 4–11, 2007.

[128] Q. Liu, X. Luo, Z. Zheng, B. Zheng, J. Zhang, Y. Zhao, X. Yang, J. Wang, and L. Wang, “Factors that have an effect on degradation of diclofenac in aqueous solution by gamma ray irradiation,” *Environ. Sci. Pollut. Res.*, vol. 18, no. 7, pp. 1243–1252, 2011.

[129] M. Silindir and Y. Ozer, “The Effect of Radiation on a Variety of Pharmaceuticals and Materials Containing Polymers,” *PDA J. Pharm. Sci. Technol.*, vol. 66, no. 2, pp. 184–199, 2012.

[130] A. Maquille, J.-L. Habib Jiwan, and B. Tilquin, “Cryo-irradiation as a terminal method for the sterilization of drug aqueous solutions,” *Eur. J. Pharm. Biopharm.*, vol. 69, no. 1, pp. 358–363, 2008.

[131] EMA-CHMP, “Assessment report - Omidria,” *European Medicines Agency*, 2015. [Online]. Available: http://www.ema.europa.eu/docs/en_GB/document_library/EPAR_-_Public_assessment_report/human/003702/WC500192868.pdf. [Accessed: 28-Aug-2016].

[132] J. Roy, M. Islam, A. H. Khan, S. C. Das, M. Akhteruzzaman, A. K. Deb, and A. H. Mahbub Alam, “Diclofenac sodium injection sterilized by autoclave and the occurrence of cyclic reaction producing a small amount of impurity,” *J. Pharm. Sci.*, vol. 90, no. 5, pp. 541–544, 2001.

[133] “Public Assessment Report - Moxifloxacin Hexal 5 mg/ml,” *Heads of Medicines Agencies: MRI Product Index*. [Online]. Available: http://mri.medagencies.org/download/de_h_3817_001_par_4of4.pdf. [Accessed: 28-Aug-2016].

[134] A. Özer, S. Turker, S. Çolak, M. Korkmaz, E. Kiliç, and M. Özalp, “The effects of gamma irradiation on diclofenac sodium, liposome and niosome ingredients for rheumatoid arthritis,” *Interv. Med. Appl. Sci.*, vol. 5, no. 3, pp. 122–130, 2013.

[135] K. G. Parthiban, R. Manivannan, B. S. Kumar, and M. B. Ahasan, “Formulation and evaluation of Ketorolac ocular pH-triggered in-situ gel,” *Int. J. Drug Dev. Res.*, vol. 2, no. 2, pp. 379–387, 2010.

[136] B. K. Singh, D. V. Parwate, I. B. Dassarma, and S. K. Shukla, “Radiation sterilization of fluoroquinolones in solid state: Investigation of effect of gamma radiation and electron beam,” *Appl. Radiat. Isot.*, vol. 68, no. 9, pp. 1627–1635, 2010.

[137] P. Pawar, R. Katara, and D. Majumdar, “Design and evaluation of moxifloxacin hydrochloride ocular inserts,” *Acta Pharm.*, vol. 62, no. 1, pp. 93–104, 2012.

[138] B. A. Schlech and E. Alfonso, “Overview of the Potency of Moxifloxacin Ophthalmic Solution 0.5% (VIGAMOX®),” *Surv. Ophthalmol.*, vol. 50, no. 6, pp. S7–S15, 2005.

[139] D. Paillard, J. Grellet, V. Dubois, M.-C. Saux, and C. Quentin, “Discrepancy between Uptake and Intracellular Activity of Moxifloxacin in a Staphylococcus aureus-Human THP-1 Monocytic Cell Model,” *Antimicrob. Agents Chemother.*, vol. 46, no. 2, pp. 288–293, 2002.

[140] M. C. Callegan and B. Novosad, “Efficacy of Fourth–Generation Fluoroquinolones Against Gram–Positive Species Commonly Involved in Ocular Infections,” *Invest. Ophthalmol. Vis. Sci.*, vol. 47, no. 13, 2006.

[141] P. D. Lister, “Pharmacodynamics of Moxifloxacin and Levofloxacin against Staphylococcus aureus and Staphylococcus epidermidis in an In Vitro Pharmacodynamic Model,” *Clin. Infect. Dis.*, vol. 32, no. Supplement 1, pp. S33–S38, 2001.

[142] M. A. Kassem, “Activity of Moxifloxacin and Gentamicin Singly and Combined with Diclofenac or Ketorolac against Planktonic and Biofilm Cells of Staphylococci Isolated from Ocular Flora,” *Egypt. J. Med. Microbiol.*, vol. 18, no. 1, pp. 119–128, 2009.

[143] V. Vedantham, P. Lalitha, T. Velpandian, S. Ghose, R. Mahalakshmi, and K. Ramasamy, “Vitreous and aqueous penetration of orally administered moxifloxacin in humans,” *Eye*, vol. 20, no. 11, pp. 1273–1278, 2006.

[144] A. L. Cooper, A. C. R. Dean, and C. Hinshelwood, “Factors Affecting the Growth of Bacterial Colonies on Agar Plates,” *Proc. R. Soc. B Biol. Sci.*, vol. 171, no. 1023, pp. 175–199, 1968.

[145] S. Cai and Z. Suo, “Mechanics and chemical thermodynamics of phase transition in temperature-sensitive hydrogels,” *J. Mech. Phys. Solids*, vol. 59, no. 11, pp. 2259–2278, 2011.

[146] S. L. J. Tomić, M. M. Mićić, J. M. Filipović, and E. H. Suljovrujić, “Swelling and thermodynamic studies of temperature responsive 2-hydroxyethyl methacrylate/itaconic acid copolymeric hydrogels prepared via gamma radiation,” *Radiat. Phys. Chem.*, vol. 76, no. 8–9, pp. 1390–1394, 2007.

[147] N. Vishal Gupta and H. G. Shivakumar, “Investigation of Swelling Behavior and Mechanical Properties of a pH-Sensitive Superporous Hydrogel Composite,” *Iran. J. Pharm. Res.*, vol. 11, no. 2, pp. 481–493, 2012.

[148] D. E. Liu, T. J. Dursch Jr., N. O. Taylor, S. Y. Chan, and D. T. Bregante, “Diffusion in Polymers: 418545 - Drug Diffusion with Adsorption in Polyelectrolyte Hydrogels,” in *AIChE Annual Meeting*, 2015.

[149] S. Dash, P. N. Murthy, L. Nath, and P. Chowdhury, “Kinetic modelling on drug release from controlled drug delivery systems,” *Acta Pol. Pharm. Reserch*, vol. 67, no. 3, pp. 217–223, 2010.

[150] L. W. Kleiner, J. C. Wright, and Y. Wang, “Evolution of implantable and insertable drug delivery systems,” *J. Control. Release*, vol. 181, no. 1, pp. 1–10, 2014.

[151] J. Clark, “Temperature Dependent of the pH of pure Water,” *UC Davis ChemWiki*, 2015. [Online]. Available: http://chem.libretexts.org/@api/deki/pages/1293/pdf/Temperature%2bDependent%2bof%2bthe%2bpH%2bof%2bpure%2bWater.pdf?stylesheet=default. [Accessed: 31-Aug-2016].

[152] J. J. Barron, C. Ashton, and L. Geary, “The effects of temperature on pH measurement,” *57th Annual Meeting of the International Society of Electrochemistry*, 2006. [Online]. Available: http://www.reagecon.com/pdf/technicalpapers/Effects_of_Temperature_on_pH_v4-_TSP-01-2.pdf. [Accessed: 31-Aug-2016].

[153] A. B. Moustafa, R. A. Sobh, A. M. Rabie, H. E. Nasr, and M. M. H. Ayoub, “Synthesis and in vitro release of guest drugs-loaded copolymer nanospheres MMA/HEMA via differential microemulsion polymerization,” *J. Appl. Polym. Sci.*, vol. 129, no. 2, pp. 853–865, 2013.

[154] A. H. Hogt, J. Dankert, and J. Feijen, “Adhesion of coagulase-negative staphylococci to methacrylate polymers and copolymers.,” *J. Biomed. Mater. Res.*, vol. 20, no. 4, pp. 533–545, 1986.

[155] G. Liu, D. Xie, Y. Li, Y. Zhang, and F. Huang, “Shape memory properties of poly(methyl methacrylate-co-2-hydroxyethyl methacrylate)/poly(ethylene glycol) complexes,” *Polimery*, vol. 58, no. 4, pp. 304–307, 2013.

[156] B. Acevedo, F. Martinez, and A. F. Olea, “Synthesis, thermal behavior, and aggregation in aqueous solution of poly(methyl Methacrylate)-b-poly(2-hydroxyethyl Methacrylate,” *J. Chil. Chem. Soc.*, vol. 58, no. 4, pp. 2038–2042, 2013.

[157] E. Vargün, M. Sankir, B. Aran, N. D. Sankir, and A. Usanmaz, “Synthesis and Characterization of 2-Hydroxyethyl Methacrylate (HEMA) and Methyl Methacrylate (MMA) Copolymer Used as Biomaterial,” *J. Macromol. Sci. Part A*, vol. 47, no. 3, pp. 235–240, 2010.

[158] “AVELOX I.V. (Moxifloxacin Hydrochloride),” *Drugsite Trust*. [Online]. Available: https://www.drugs.com/drp/images/17/40007101.jpg. [Accessed: 29-Aug-2016].

[159] A. Tieppo, A. C. Boggs, P. Pourjavad, and M. E. Byrne, “Analysis of release kinetics of ocular therapeutics from drug releasing contact lenses: Best methods and practices to advance the field,” *Contact Lens Anterior Eye*, vol. 37, no. 4, pp. 305–313, 2014.

[160] R. Galante, P. Paradiso, M. G. Moutinho, A. I. Fernandes, J. L. G. Mata, A. P. A. Matos, R. Colaço, B. Saramago, and A. P. Serro, “About the effect of eye blinking on drug release from pHEMA-based hydrogels: an in vitro study,” *J. Biomater. Sci. Polym. Ed.*, vol. 26, no. 4, pp. 235–251, 2015.

[161] M. Goel, R. G. Picciani, R. K. Lee, and S. K. Bhattacharya, “Aqueous humor dynamics: a review,” *Open Ophthalmol. J.*, vol. 4, pp. 52–59, 2010.

[162] T. L. Maus and R. F. Brubaker, “Measurement of Aqueous Humor Flow by Fluorophotometry in the Presence of a Dilated Pupil,” *IOVS*, vol. 40, no. 2, pp. 542–546, 1999.

[163] G. Kleinmann, D. J. Apple, J. Chew, B. Hunter, S. Stevens, S. Larson, N. Mamalis, and R. J. Olson, “Hydrophilic acrylic intraocular lens as a drug-delivery system for fourth-generation fluoroquinolones,” *J. Cataract Refract. Surg.*, vol. 32, no. 10, pp. 1717–1721, 2006.

[164] I. Marques, J. Mira, J. Cardoso, H. Pereira, M. Ribeiro, M. Rego, C. Lobo, J. Murta, D. Teixeira, M. Soares, and F. Silva, “Moxifloxacina Intracamerular (0,5% vs 0,25%) vs Cefuroxima Intracamerular Profiláctica na Cirurgia de Catarata - Estudo Comparativo : Resultados Preliminares,” *Oftalmologia*, vol. 36, no. 2, pp. 123–132, 2012.

[165] A. Salvanet-Bouccara and P. Junes, “Endophtalmies,” in *Encycl. Med. Chir.*, Ophtalmologie, 21-250-D-40, 12p., 1995.

[166] M. I. B. Tavares and E. E. C. Monteiro, “Solid State 13C NMR Study of Methyl Methacrylate-Methacrylic Acid Copolymers,” *Ann. Magn. Reson.*, vol. 4, no. 3, pp. 69–72, 2005.

[167] C. F. Huang, S. W. Kuo, F. J. Lin, C. F. Wang, C. J. Hung, and F. C. Chang, “Syntheses and specific interactions of poly(hydroxyethyl methacrylate-b-vinyl pyrrolidone) diblock copolymers and comparisons with their corresponding miscible blend systems,” *Polymer (Guildf).*, vol. 47, no. 20, pp. 7060–7069, 2006.

ANNEXES

ANNEX I. HPLC chromatograms of DFN

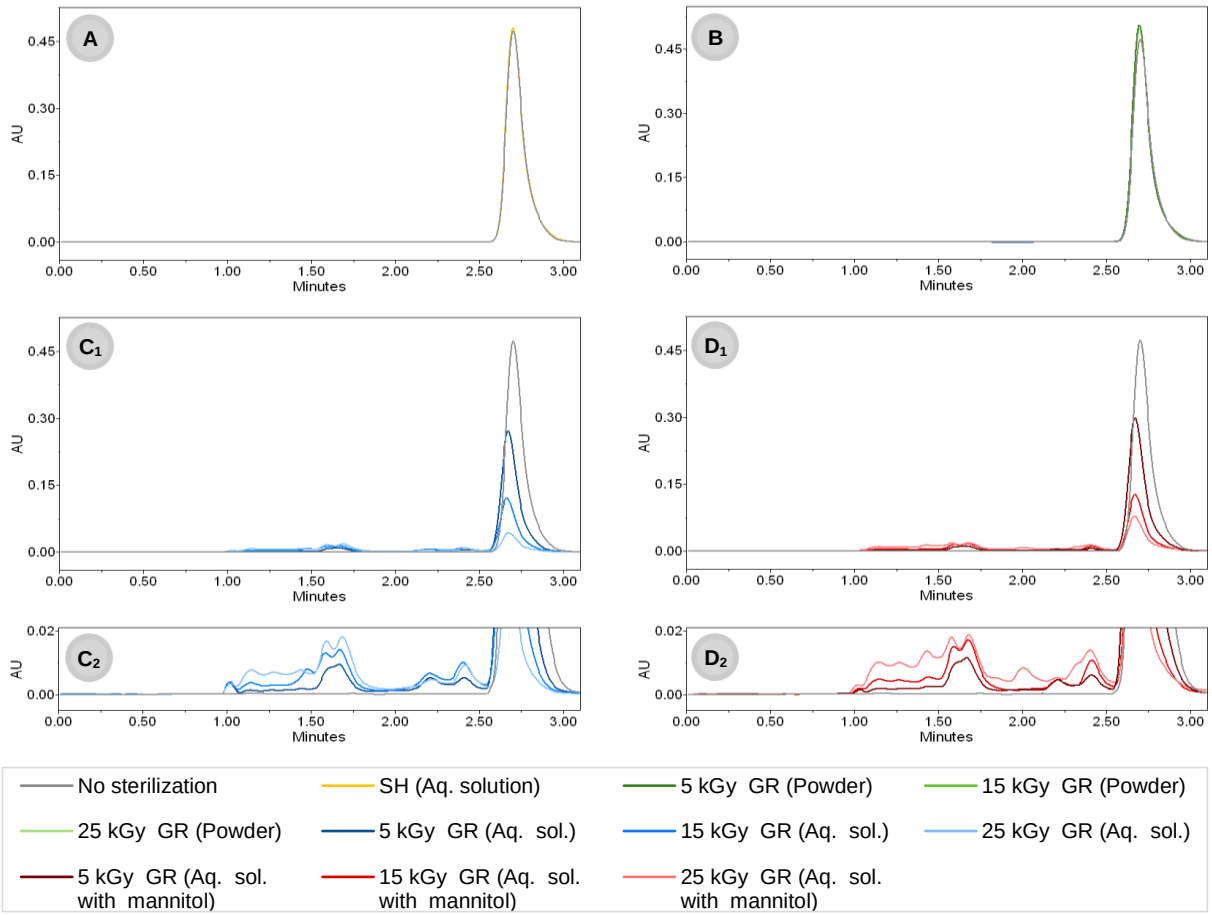

Figure A1. Chromatograms of DFN obtained by HPLC at $276\ \mathrm{nm}$, for all experimental sterilization conditions. C_2 and D_2 are extensions of C_1 and D_1, respectively.

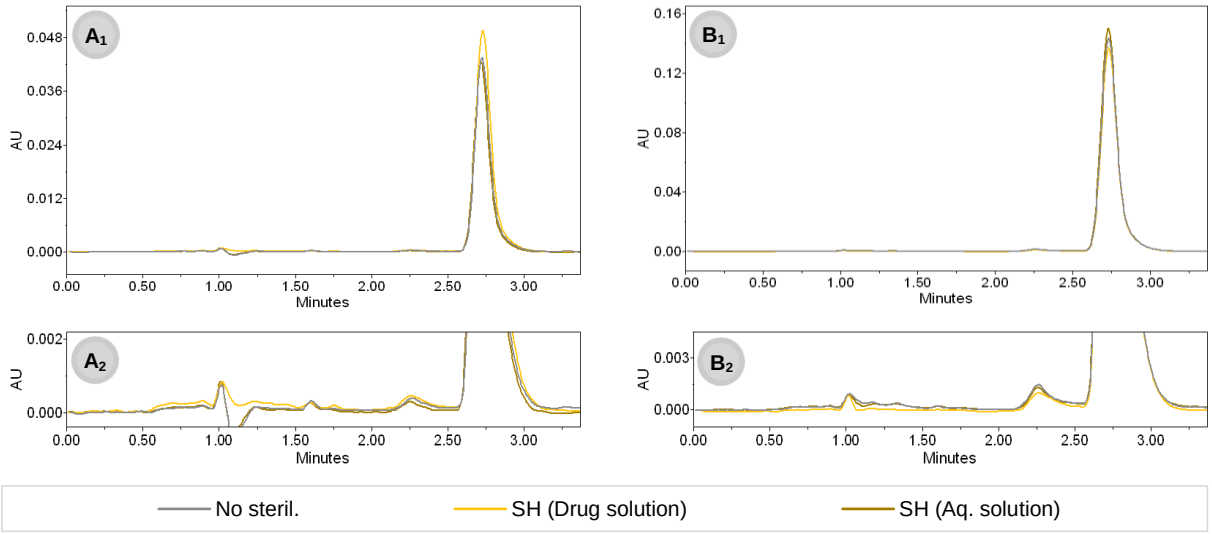

Figure A2. Chromatograms of DFN released solutions from B26Y (A_1 and A_2) and CFL58 (B_1 and B_2), obtained by HPLC at $276\ \mathrm{nm}$. A_2 and B_2 are extensions of A_1 and B_1, respectively.

ANNEX II. HPLC chromatograms of KTL

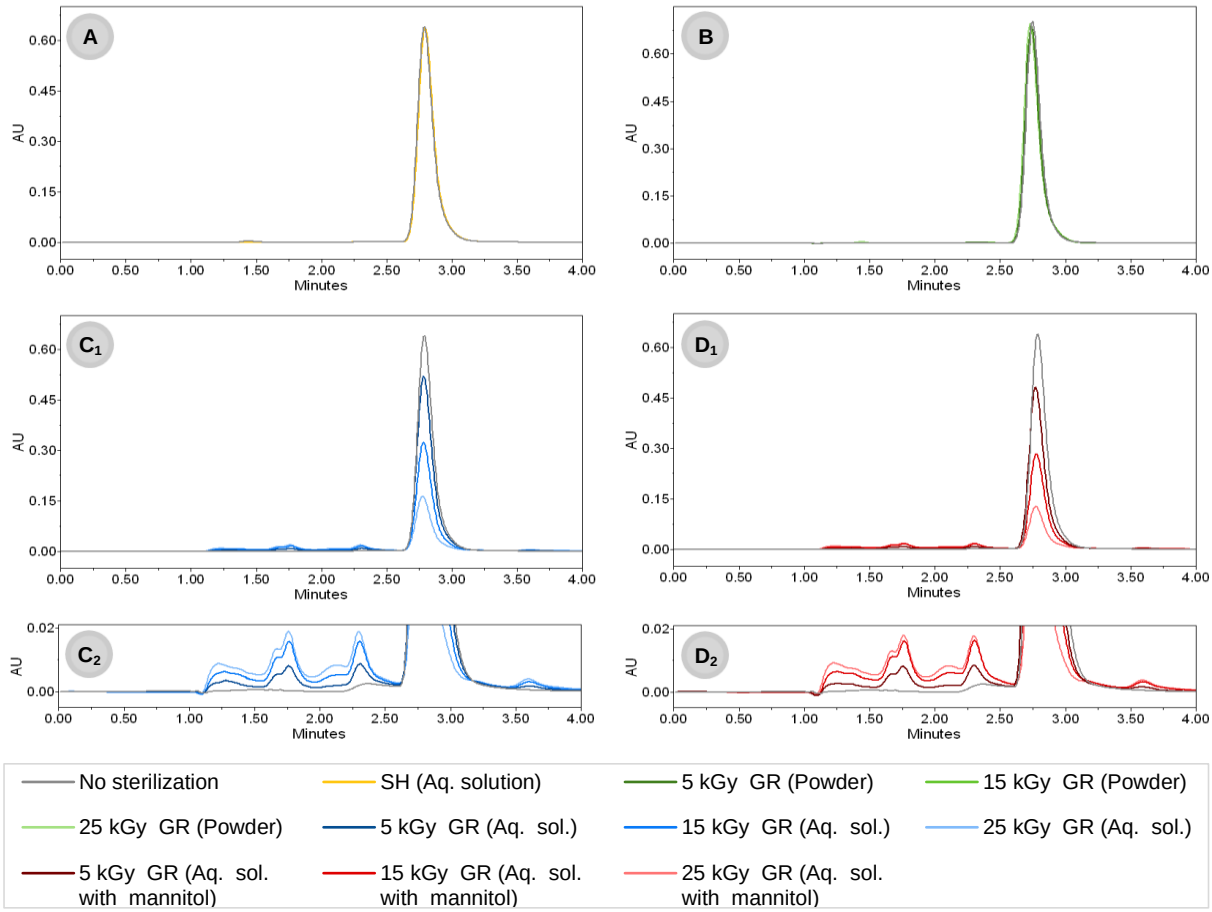

Figure A3. Chromatograms of KTL obtained by HPLC at $315\ \mathrm{nm}$, for all experimental sterilization conditions. C_2 and D_2 are extensions of C_1 and D_1, respectively.

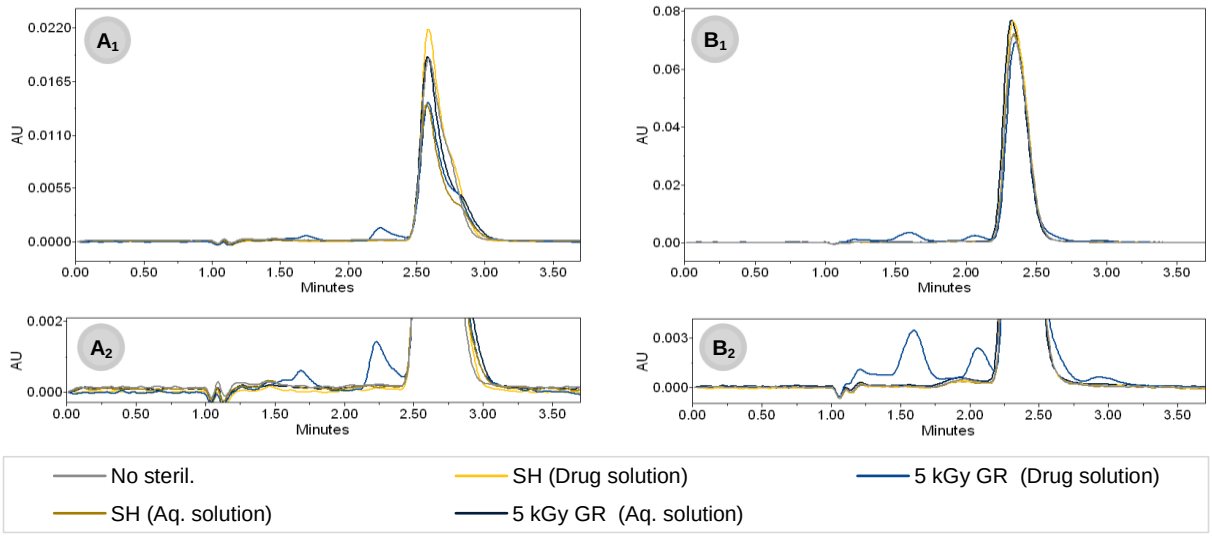

Figure A4. Chromatograms of KTL released solutions from B26Y (A_1 and A_2) and CFL58 (B_1 and B_2), obtained by HPLC at $315\ \mathrm{nm}$. A_2 and B_2 are extensions of A_1 and B_1, respectively.

ANNEX III. HPLC chromatograms of MXF

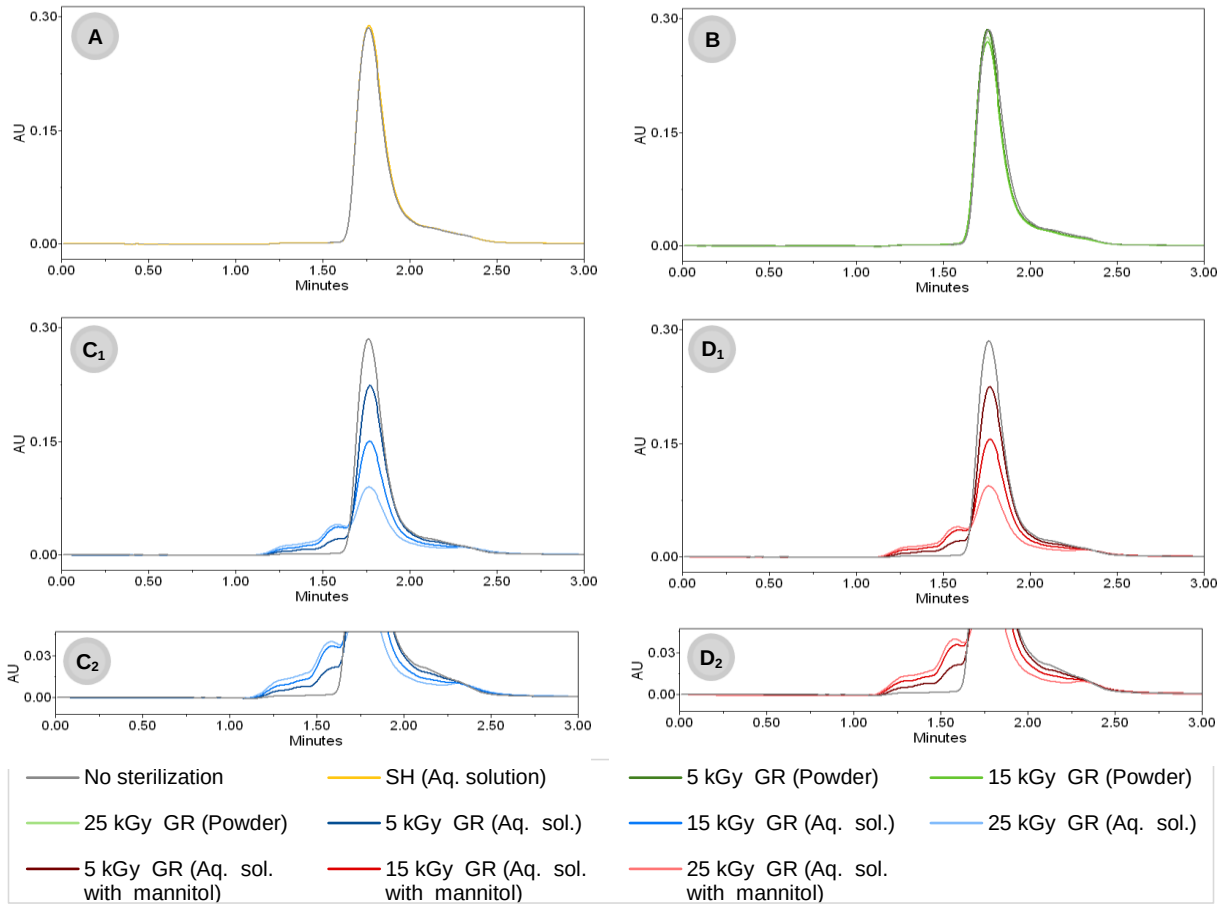

Figure A5. Chromatograms of MXF obtained by HPLC at $290\ \mathrm{nm}$, for all experimental sterilization conditions. C_2 and D_2 are extensions of C_1 and D_1, respectively.

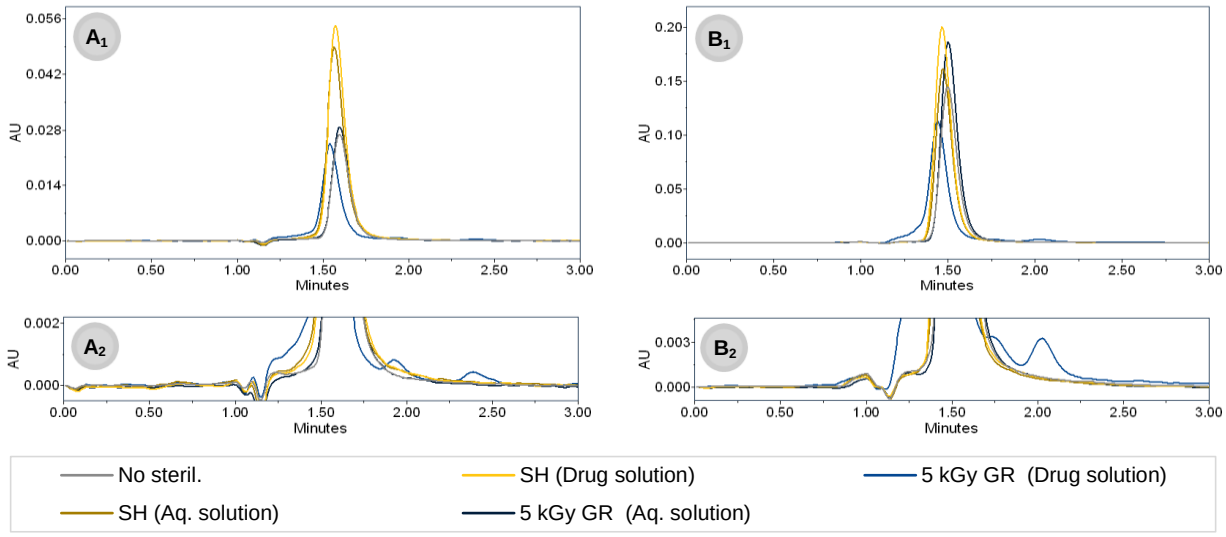

Figure A6. Chromatograms of MXF released solutions from B26Y (A_1 and A_2) and CFL58 (B_1 and B_2), obtained by HPLC at $290\ \mathrm{nm}$. A_2 and B_2 are extensions of A_1 and B_1, respectively.

ANNEX IV. HPLC chromatograms of MXF+KTL

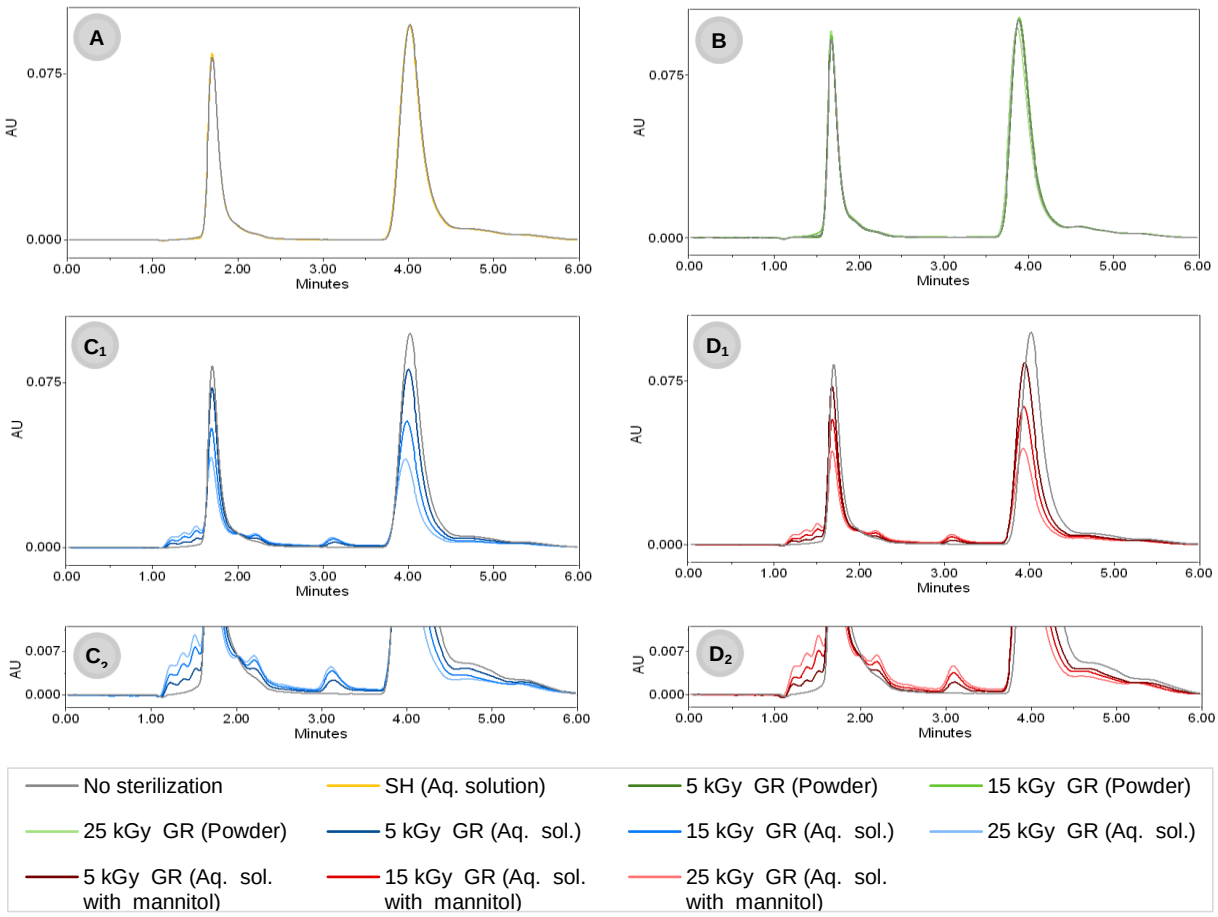

Figure A7. Chromatograms of MXF+KTL obtained by HPLC at $315\ \mathrm{nm}$, for all experimental sterilization conditions. C_2 and D_2 are extensions of C_1 and D_1, respectively.

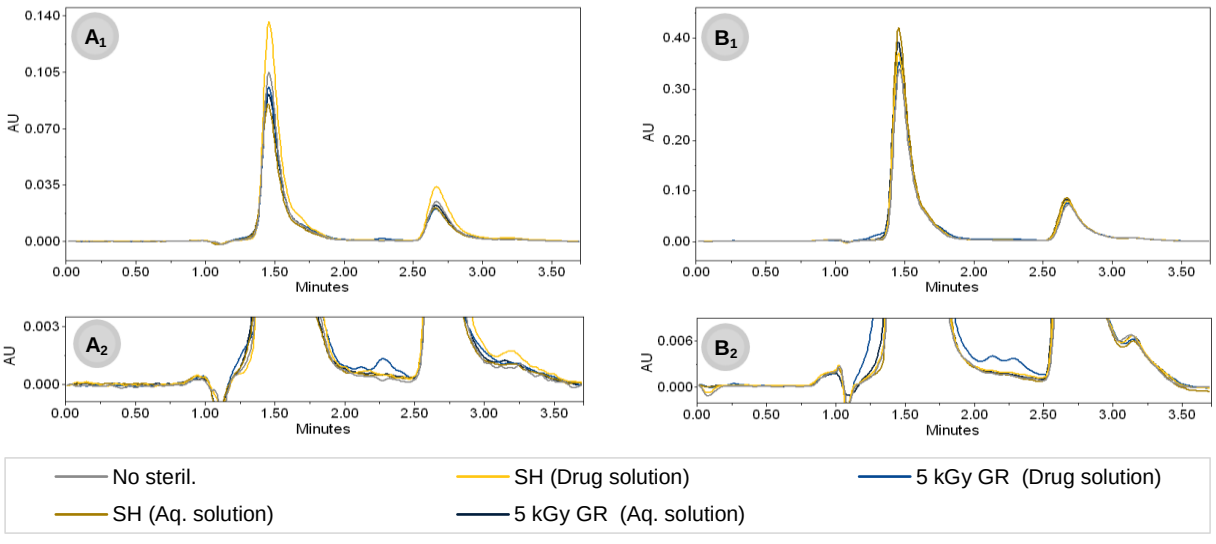

Figure A8. Chromatograms of MXF+KTL released solutions from B26Y (A_1 and A_2) and CFL58 (B_1 and B_2), obtained by HPLC at $315\ \mathrm{nm}$. A_2 and B_2 are extensions of A_1 and B_1, respectively.

ANNEX V. SEM images of the surface of B26Y

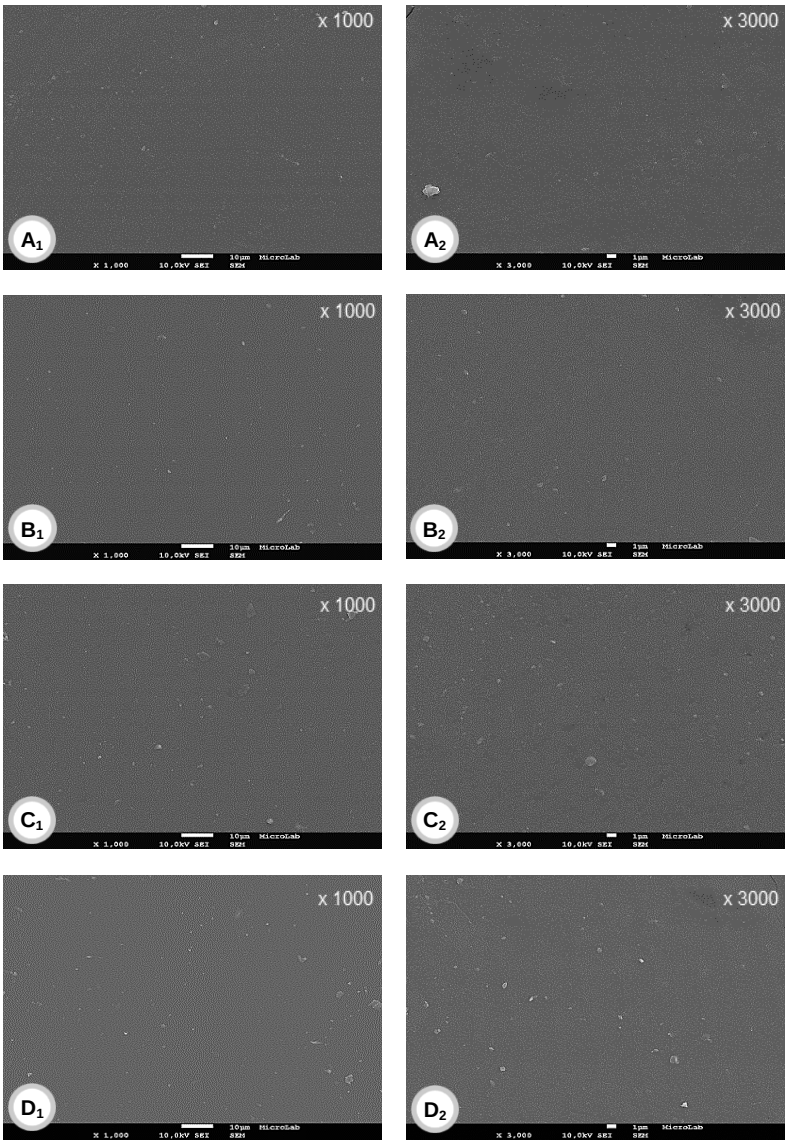

Figure A9. SEM images of the surface of B26Y. Lenses were non-sterilized (A_1 and A_2) or sterilized in aqueous solution by SH (B_1 and B_2) or with 5 kGy (C_1 and C_2) or 25 kGy (D_1 and D_2) of GR. (A_1, B_1, C_1 and D_1) – Magnification of 1000x. (A_2, B_2, C_2 and D_2) – Magnification of 3000x.

ANNEX VI. SEM images of the surface of CFL58

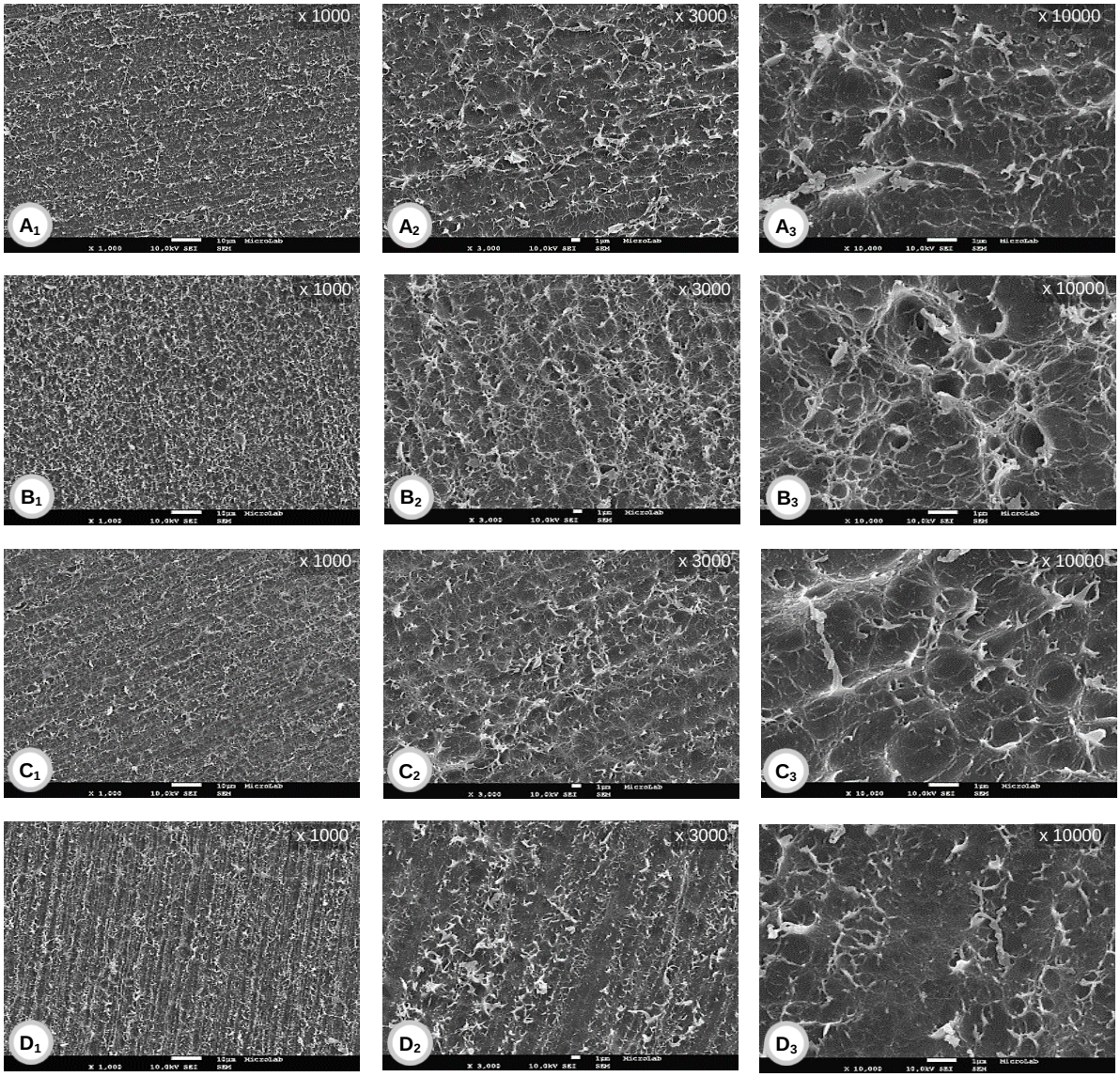

Figure A10. SEM images of the surface of CFL58. Lenses were non-sterilized (A_1, A_2 and A_3) or sterilized in aqueous solution by SH (B_1, B_2 and B_3) or with 5 kGy (C_1, C_2 and C_3) or 25 kGy (D_1, D_2 and D_3) of GR. (A_1, B_1, C_1 and D_1) – Magnification of 1000x. (A_2, B_2, C_2 and D_2) – Magnification of 3000x. (A_3, B_3, C_3 and D_3) – Magnification of 10000x.

ANNEX VII. SEM images of the surface of loaded B26Y

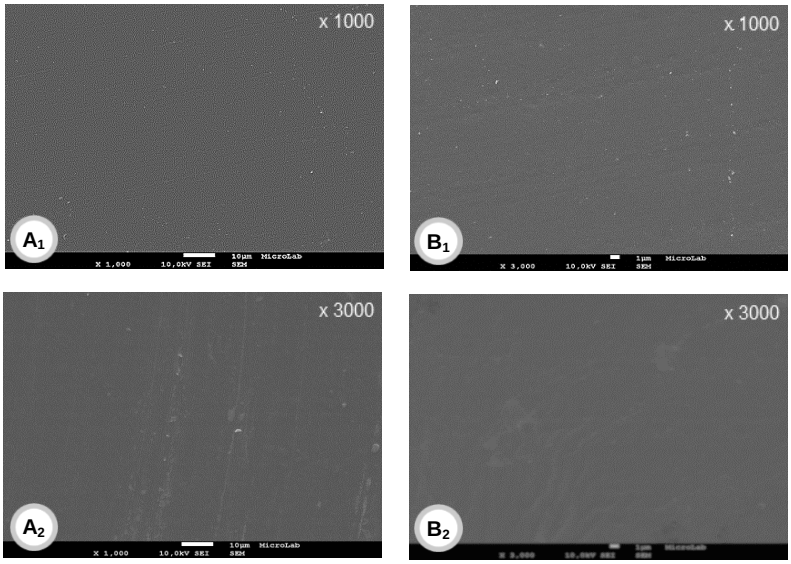

Figure A11. SEM images of the surface of loaded B26Y with DFN. Lenses were non-sterilized (A_1 and A_2) or sterilized in DFN solution by SH (B_1 and B_2). (A_1 and B_1) – Magnification of 1000x. (A_2 and B_2) – Magnification of 3000x.

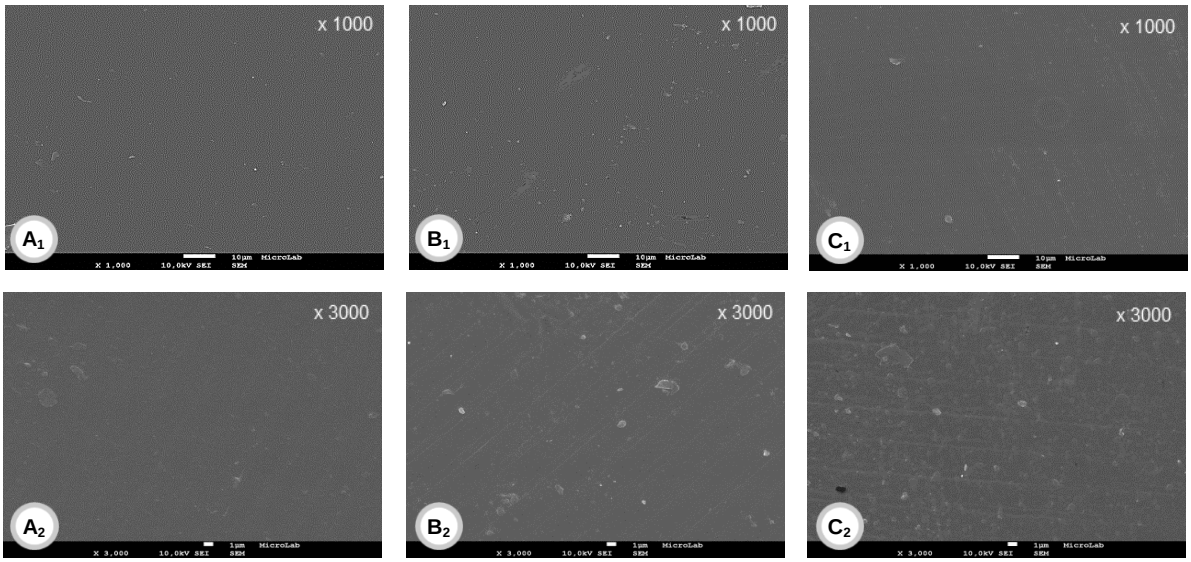

Figure A12. SEM images of the surface of loaded B26Y with KTL. Lenses were non-sterilized (A_1 and A_2) or sterilized in KTL solution by SH (B_1 and B_2) or with 5 kGy of GR (C_1 and C_2). (A_1, B_1 and C_1) – Magnification of 1000x. (A_2, B_2 and C_2) – Magnification of 3000x.

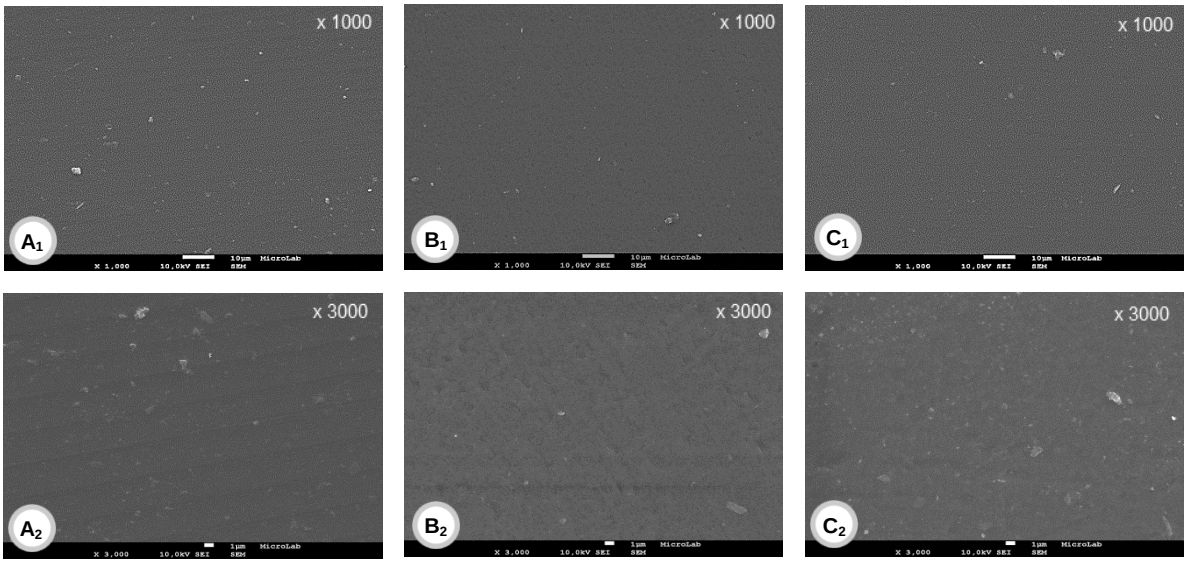

Figure A13. SEM images of the surface of loaded B26Y with MXF. Lenses were non-sterilized (A_1 and A_2) or sterilized in MXF solution by SH (B_1 and B_2) or with 5 kGy of GR (C_1 and C_2). (A_1, B_1 and C_1) – Magnification of 1000x. (A_2, B_2 and C_2) – Magnification of 3000x.

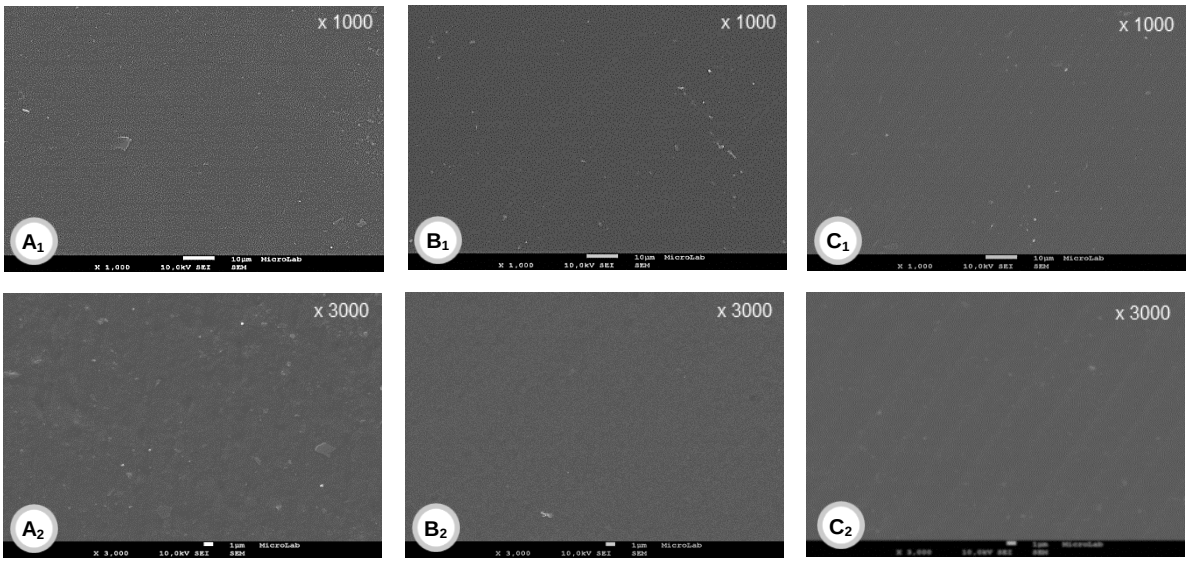

Figure A14. SEM images of the surface of loaded B26Y with MXF+KTL. Lenses were non-sterilized (A_1 and A_2) or sterilized in MXF+KTL solution by SH (B_1 and B_2) or with 5 kGy of GR (C_1 and C_2). (A_1, B_1 and C_1) – Magnification of 1000x. (A_2, B_2 and C_2) – Magnification of 3000x.

ANNEX VIII. Korsmeyer−Peppas kinetic parameters

Table A1. Korsmeyer−Peppas kinetic parameters obtained in the study of the effects of SH and GR sterilization on the release profiles of loaded CLs and IOLs materials.

Samples identification					Korsmeyer−Peppas kinetic parameters					
Drug solution	Sterilization conditions				B26Y			CFL58		
	Method	Solution	Duration (min)	Moment	R^2	n	Drug transport mechanism	R^2	n	Drug transport mechanism
DFN	No sterilization				0.9917	0.5710	Anomalous transport	0.9920	0.5782	Anomalous transport
	SH	Drug sol.	60	*3rd day of loading	0.9877	0.5252		0.9947	0.6005	
		Aq. sol.		**Before loading	0.9956	0.4963		0.9975	0.5357	
KTL	No sterilization				0.9963	0.5658	Anomalous transport	0.9922	0.4612	Anomalous transport
	SH	Drug sol.	60	*3rd day of loading	0.9917	0.6580		0.9997	0.4650	
		Aq. sol.			0.9900	0.5678		0.9967	0.4979	
	GR	Drug sol.		**Before loading	0.9924	0.5941		0.9980	0.5275	
		Aq. sol.			0.9855	0.5706		0.9957	0.5150	
MXF	No sterilization				0.9957	0.4025	Fickian diffusion	0.9995	0.5883	Anomalous transport
	SH	Drug sol.	60	*3rd day of loading	0.9974	0.3906		0.9983	0.6981	
		Aq. sol.			0.9841	0.4275		0.9971	0.7973	
	GR	Drug sol.		**Before loading	0.9927	0.4422		0.9928	0.4987	
		Aq. sol.			0.9860	0.4354		1.0000	0.4865	
KTL (From MOX+KTL solution)	No sterilization				0.9963	0.3465	Fickian diffusion	0.9871	0.4541	Anomalous transport
	SH	Drug sol.	60	*3rd day of loading	0.9929	0.4216		0.9970	0.5702	
		Aq. sol.			0.9785	0.2995		0.9595	0.4682	
	GR	Drug sol.		**Before loading	0.9862	0.3940		0.9865	0.4618	
		Aq. sol.			0.9939	0.3239		0.9974	0.4551	
MXF (From MOX+KTL solution)	No sterilization				0.9989	0.3907	Fickian diffusion	0.9806	0.4677	Anomalous transport
	SH	Drug sol.	60	*3rd day of loading	0.9962	0.4374		0.9942	0.6312	
		Aq. sol.			0.9796	0.3279		0.9851	0.4790	
	GR	Drug sol.		**Before loading	0.9919	0.4365		0.9923	0.4711	
		Aq. sol.			0.9883	0.4017		0.9985	0.4615	

* For samples sterilized in drug solution. ** For samples sterilized in aqueous solution.

Table A2. Korsmeyer−Peppas kinetic parameters obtained in the studies of the effects of SH sterilization and loading temperature on the release profiles of loaded IOLs materials.

Samples identification						Korsmeyer−Peppas kinetic parameters		
Drug solution	Loading conditions (during 4 days)		Sterilization conditions					
	C (mg/mL)	T (°C)	Method	Duration (min)	Moment	R^2	n	Drug transport mechanism
MXF	2	4	No sterilization			0.9901	0.4121	Fickian diffusion
		36				0.9933	0.4593	Anomalous transport
		60				0.9978	0.4955	
		80				0.9962	0.5219	
		4	SH	30	*3rd day of loading	0.9918	0.354	Fickian diffusion
				60		0.9953	0.3611	
				90		0.9929	0.362	
				60	*1st day of loading	0.9934	0.3651	
	5		No sterilization			0.9904	0.3664	Fickian diffusion
			SH	60	*3rd day of loading	0.9943	0.4102	

Table A3. Korsmeyer−Peppas kinetic parameters obtained in the study of the effect of storage on the release profiles of loaded IOLs materials.

Samples identification							Korsmeyer−Peppas kinetic parameters		
Drug solution	Loading conditions (during 4 days)		Sterilization conditions			Storage (months)			
	C (mg/mL)	T (°C)	Method	Duration (min)	Moment		R^2	n	Drug transport mechanism
MXF	5	60	No sterilization			No storage	0.9928	0.5047	Anomalous transport
			SH	30	After loading	No storage	0.9937	0.4941	
						1	0.9991	0.4551	
						2	0.9963	0.5108	
						3	0.9925	0.5725	
		80	No sterilization			No storage	0.9931	0.5247	Anomalous transport
			SH	30	After loading	No storage	0.9927	0.5003	
						3	0.9894	0.5401	
VGMX		60	No sterilization			No storage	0.9920	0.5435	Anomalous transport
			SH	30	After loading	No storage	0.9914	0.5295	
						1	0.9975	0.4748	
						2	0.9969	0.5278	
						3	0.9893	0.5571	
		80	No sterilization			No storage	0.9938	0.5496	Anomalous transport
			SH	30	After loading	No storage	0.9934	0.5369	
						3	0.9910	0.5221	

ANNEX IX. UV−Vis spectra of DFN, KTL, MFX and MXF+KTL

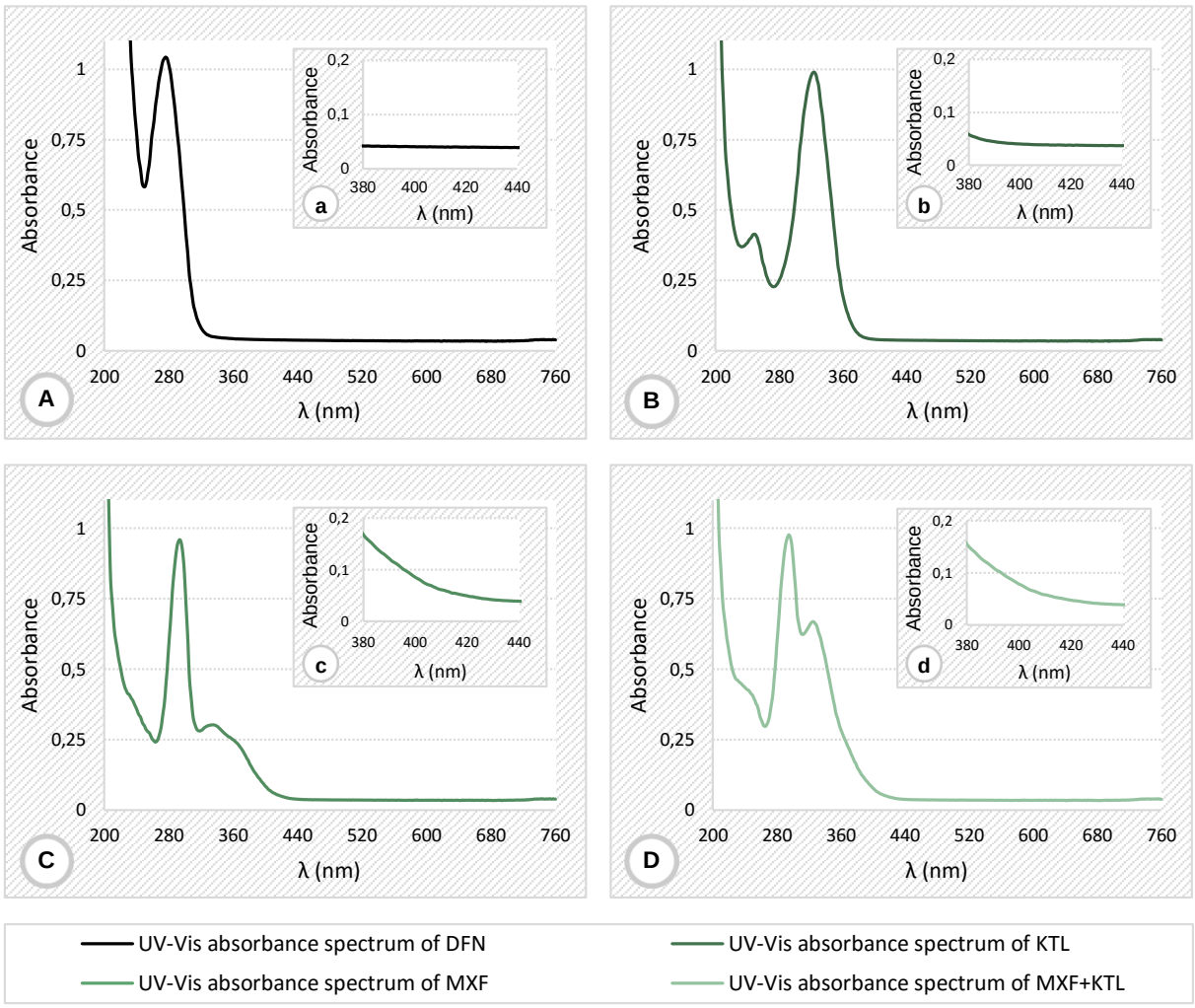

Figure A15. UV−Vis absorbance spectra for, DFN (A), KTL (B), MFX (C) and MXF+KTL (D), determined by spectrophotometry. The a, b, c and d are extensions of A, B, C and D, respectively.

ANNEX X. Quantification of drugs degradation determined by HPLC

Table A4. Quantification of the degradation of MXF solutions exposed to high temperatures.

Samples identification		Relative concentration ± SD (%)
Drug solution	T (ºC) (during 4 days)	
MXF	Freshly made (Control)	100 ± 1
	60	100 ± 3
	80	101 ± 2

Table A5. Quantification of the degradation of MXF solutions exposed to high temperatures and stored for different periods.

Samples identification					Storage (months)	Relative concentration ± SD (%)
Drug solution	T (ºC) (during 4 days)	Sterilization conditions				
		Method	Duration (min)	Moment		
MXF	*Freshly made (Control)					100 ± 4
	60	No sterilization			No storage	101 ± 1
		SH	30	After 4 days with temperature		99 ± 8
					1	102 ± 6
					2	99 ± 3
					3	103 ± 4
	80	No sterilization			No storage	100 ± 3
		SH	30	After 4 days with temperature		100 ± 3
					3	102 ± 6

*Mean of MXF solutions, freshly prepared in the beginning of every month (start,1,2 and 3).

Table A6. Quantification of the degradation of VGMX solutions exposed to high temperatures and stored for different periods.

Samples identification					Storage (months)	Relative concentration ± SD (%)
Drug solution	T (ºC) (during 4 days)	Sterilization conditions				
		Method	Duration (min)	Moment		
VGMX	*Freshly made (Control)					100 ± 1
	60	No sterilization			No storage	102 ± 3
		SH	30	After 4 days with temperature		102 ± 3
					1	100 ± 8
					2	98 ± 2
					3	98 ± 2
	80	No sterilization			No storage	99 ± 4
		SH	30	After 4 days with temperature		101 ± 1
					3	101 ± 1

*Mean of VGMX solutions, freshly prepared in the beginning of every month (start,1,2 and 3).

ANNEX XI. ^{13}C CP/MAS chemical shifts of MXF and B26Y

Table A7. ^{13}C CP/MAS chemical shifts of MXF and B26Y, obtained in this study and reported on the indicated references for MXF and the main components of B26Y (PMMA and PHEMA).

MXF			B26Y			
Carbon number	δ (ppm) obtained experimentally	δ (ppm) from literature [37]	Carbon number	δ (ppm) obtained experimentally	δ (ppm) from literature (PMMA) [166]	δ (ppm) from literature (PHEMA) [167]
3	174.72	175.85	4,4'	178.86 – 178.43	178.1	178.3
1	167.54	165.71	5	66.90	52.2	67.2
9	150.98 150.11	150.13	6	59.28	–	60.2
10		106.49	5'	54.49	52.2	–
11		151.42; 153.41	1,1'	52.53	45.2	45.1
13	142.92	140.33	2,2'	44.25		
	140.09		3,3'	19.85 – 15.49 *	16.7	15.7
12	–	136.56				
5	136.60	134.39				
	135.51					
	134.64					
4	116.56	117.22				
	115.69					
2	106.33	106.32				
	104.37					
14	66.25	61.83				
	63.41					
16	58.84	53.93				
21	55.14	51.97				
15	51.87	54.24				
17	48.60	41.32				
	46.42					
6	–	40.52				
20	39.67	34.51				
19	34.23	17.48				
18	22.24	20.51				
8	–	9.45				
7	–	9.33				

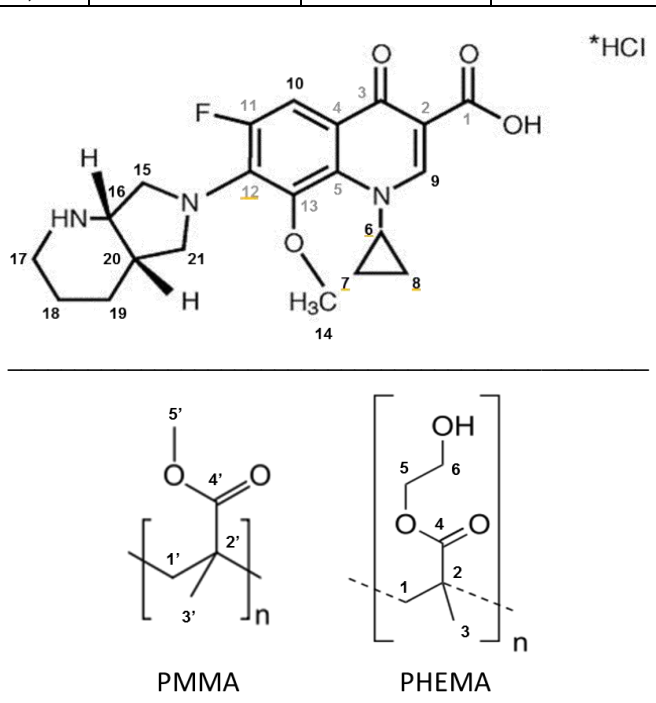

*Broad sign.

ANNEX XII. Antimicrobial activity of MXF and VGMX released solutions

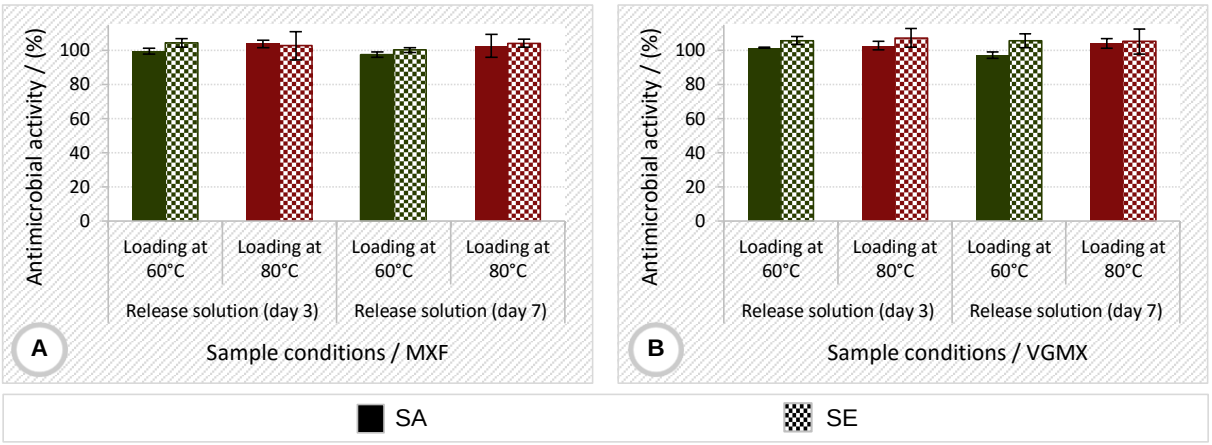

Figure A16. Antimicrobial activity against SA and SE, of MXF (A) and VGMX (B) released solutions from samples loaded at high temperatures for 4 days, sterilized, and stored for 3 months. The error bars correspond to ± mean SD.